Faculdade de Engenharia da Universidade do Porto

Instituto de Ciências Biomédicas Abel Salazar

Functionalization of fibrin-based hydrogel matrices with angiogenic physical cues as a strategy to promote the vascularization of tissue-engineered implants

Joana Catarina Cunha Dias Soares Loureiro

MASTER THESIS

Integrated Masters in Bioengineering

Supervisor: Professor Isabel de Freitas Amaral

September 2016

The research described in this thesis was supported by:

- Santa Casa da Misericórdia de Lisboa – Prémio Melo e Castro (Grant MC-1068-2015);
- Project NORTE-01-0145-FEDER-000008, supported by Norte Portugal Regional Operational Programme (NORTE 2020), under the PORTUGAL 2020 Partnership Agreement, through the European Regional Development Fund (ERDF);
- Fundo Europeu de Desenvolvimento Regional funds through the COMPETE 2020 – Operacional Programme for Competitiveness and Internationalisation (POCI), Portugal 2020, and by Portuguese funds through FCT – Fundação para a Ciência e a Tecnologia/Ministério da Ciência, Tecnologia e Ensino Superior in the framework of the project "Institute for Research and Innovation in Health Sciences" (POCI-01-0145-FEDER-007274).

© Joana Loureiro, 2016

RESUMO

O sucesso dos produtos da Engenharia de Tecidos é intimamente dependente da capacidade de eliminar corretamente os produtos derivados de processos metabólicos e também do suprimento nutritivo e de oxigénio da parte interior das matrizes, após implantação.

A angiogénese – formação de novos capilares sanguíneos a partir de vasos pré-existentes - é um processo morfogénico que, sendo mediado por uma complexa sequência de acontecimentos celulares que levam à neovascularização no local de implantação, se tem vindo a provar como sendo crucial para alcançar tal suprimento nutritivo.

Tendo em conta o conhecimento atual nos mecanismos altamente complexos que motivam a ativação e invasão de células vasculares angiogénicas, um elevado número de estratégias têm sido desenvolvidas no sentido de promover a vascularização de implantes obtidos através da Engenharia de Tecidos. Tais estratégicas incluem a libertação de fatores de crescimento angiogénicos, a transplantação de células, maioritariamente de diferentes tipos de células endoteliais (células endoteliais maturas ou células progenitoras) e o uso de matrizes feitas de biomateriais permissivos à angiogénese. Estratégias terapêuticas com vista a melhorar a densidade de vasos e a restabelecer o fluxo sanguíneo são particularmente ambicionadas após danos no Sistema Nervoso Central (SNC), onde a formação de novos vasos sanguíneos foi relacionada com melhorias na recuperação funcional de vários modelos animais de dano do SNC.

Neste sentido, o objetivo principal desta tese de mestrado era o desenvolvimento de um hidrogel de fibrina capaz de promover a neovascularização de tecidos, quer induzindo a formação de estruturas tubulares por tipos celulares da vasculatura previamente cultivados em hidrogéis de fibrina, ou promovendo a angiogénese *in vivo* através de invasão da vasculatura do hospedeiro. Para tal, hidrogéis de fibrina foram funcionalizados com o péptido T1 (GQKCIVQTTSWSQCSKS), uma sequência de ligação à integrina α6β1, devido ao seu conhecido envolvimento na formação de estruturas tubulares por células endoteliais. Outro ligando da integrina α6β1 (HYD1 peptide - KIKMVISWKG), anteriormente provado pelo nosso grupo como sendo capaz de promover migração celular e a extensão de neurites por células neurais estaminais/progenitoras (derivadas de células estaminais embrionárias) cultivadas em géis tridimensionais de fibrina, foi também explorado. Era esperado que a funcionalização da fibrina com os péptidos T1 e HYD1 resultasse num melhoramento da capacidade da fibrina induzir a neovascularização, nomeadamente através do aumento da proliferação e migração celulares, assim como da formação de estruturas capilares, *in vitro* e da angiogénese, *in vivo.*

Os péptidos foram covalentemente ligados à fibrina usando a ação de reticulação enzimática do fator XIIIa e o efeito da imobilização dos péptidos T1 e HYD1 na capacidade de células endoteliais formarem estruturas capilares quando cultivadas em géis tridimensionais funcionalizados foi avaliado usando um ensaio angiogénico *in vitro* (*microcarrier-based angiogenesis assay*) e microscopia de fluorescência high throughput. Como primeira abordagem, uma linha celular de células da microvasculatura humana do pulmão (HPMEC-ST1.6R), com conhecida capacidade de formar estruturas capilares nos géis tridimensionais de fibrina, foi usada. Os resultados mostraram que a concentração mais elevada de péptido T1

testada (40 µM) aumentou o *sprouting* das células endoteliais, nomeadamente levando a um aumento de 1.4 vezes na área de *sprouting* e no número de *sprouts* por *microcarrier* e um aumento de 1.5 vezes no comprimento máximo de *sprout*, ainda que estas diferenças não tenham sido consideradas estatisticamente significativas, à exceção do número de *sprouts* por *microcarrier*. Por contrário, a imobilização do péptido HYD1 não foi efetiva na indução do *sprouting* das células endoteliais, independentemente da concentração de péptido testadas.

De seguida, uma linha celular de células endoteliais da microvasculatura humana do cérebro (hCMEC/D3), descritas como sendo capazes de formar estruturas tubulares quando colocadas em cima de Matrigel, foi usada. À semelhança dos resultados já descritos, a adição de 40 µM de péptido T1 resultaram num *sprouting* significativamente maior relativamente à área de *sprouting* e ao número de *sprouts* por *microcarrier*, levando em média a um aumento de 1.4 vezes em todos os parâmetros considerados. Novamente, a funcionalização com o péptido HYD1 foi incapaz de promover o sprouting das células endoteliais, dentro da gama de concentrações testadas. A capacidade pro-angiogénica dos géis funcionalizados com o péptido T1 (40 µM de péptido) foi significativamente melhorada na presença do indutor angiogénico solúvel VEGF. Especificamente, a adição de VEGF (25 ng/mL) ao meio de cultura, levou a um aumento para o dobro no que diz respeito à área de sprouting, um aumento de 1.9 vezes no número de *sprouts* por *microcarrier* e um aumento de 1.5 vezes no comprimento máximo de *sprouting*. Mais ainda, também a percentagem de *beads* com *sprouts* aumentou de uma média de 70% na fibrina não funcionalizada para 94.6% nos géis funcionalizados com o péptido T1. A contribuição da integrina α6β1 no *sprouting* das células endoteliais nos géis funcionalizados com o péptido T1 foi avaliado através da incubação com anticorpos de bloqueio funcional. Os resultados evidenciaram que o *sprouting* suscitado pela imobilização do péptido T1 é parcialmente mediado pela integrina α6β1. Não foram encontradas diferenças estatisticamente significativas mas uma redução considerável foi observada quer no número de *sprouts* por *microcarrier* quer no comprimento máximo de *sprouting*. A imobilização do péptido T1 não afetou a viabilidade e proliferação celular, conforme demonstrado pela análise de células vivas e mortas por citometria de fluxo e pela atividade metabólica celular, respetivamente. Os géis funcionalizados foram caracterizados em termos de propriedades mecânicas e os resultados mostraram que não há diferenças significativas nas propriedades viscoelásticas da fibrina após a imobilização do péptido. Estes resultados são concordantes com o descrito na literatura, reportando disrupção mínima da estrutura da fibrina durante a incorporação de pequenos péptidos usando a mesma estratégia de reticulação enzimática.

Em seguida, para avaliar o efeito dos géis de fibrina funcionalizados numa fonte de células endoteliais clinicamente relevante, células derivadas do sangue do cordão umbilical, foram cultivadas em géis de fibrina funcionalizados com 40 µM e 60 µM de péptido T1 e a sua capacidade de formar estruturas capilares foi avaliada. Enquanto que a concentração mais baixa testada falhou em promover o *sprouting* de células endoteliais, a concentração de 60 µM foi bem sucedida, levando a um aumento significativo de 1.7 vezes no número de *sprouts* por *microcarrier* e de 1.8 vezes no comprimento máximo de *sprouting*. Estes resultados sugerem que a concentração de ligando requerida para um aumento do *sprouting* das células endoteliais é dependente do tipo celular usado, e possivelmente relacionado com os níveis de expressão de integrinas.

Finalmente, e dado que os resultados *in vitro* foram promissores, realizaram-se três ensaios CAM independentes com o objetivo de avaliar, *in vivo*, o potencial angiogénico da fibrina funcionalizada com o péptido T1. Para este efeito foi utilizada uma concentração de 50

μM de péptido T1, a qual levou a um aumento significativo de 20% no número de novos vasos, e comprovando deste modo o potencial angiogénico dos hidrogéis desenvolvidos. Para além deste facto, verificou-se uma redução significativa da reação inflamatória para a fibrina funcionalizada, a qual sugere um possível efeito anti-inflamatório dos hidrogéis funcionalizados. A confirmar-se, o efeito anti-inflamatório dos géis funcionalizados com o péptido T1 aliado às suas propriedades angiogénicas pode tornar o gel desenvolvido particularmente interessante para aplicação em lesões do sistema nervoso central e em doenças neurodegenerativas.

Em resumo, os resultados obtidos indicam que os géis funcionalizados com o péptido T1, para além de poderem ser potencialmente úteis para o desenvolvimento de matrizes pré-vascularizadas, podem também ter interesse para promoverem localmente a angiogénese, nomeadamente em situações clínicas tais como lesões da espinal medula, úlceras diabéticas e isquemia.

PALAVRAS-CHAVE: Biomateriais, Hidrogéis de Fibrina, Péptidos angiogénicos, Células endoteliais, Regeneração do Sistema Nervoso Central, Ensaio de angiogénese com *microcarriers*, Ensaio da membrana corioalantóica

ABSTRACT

The success of tissue-engineered constructs after implantation is closely dependent on the ability to correctly dispose metabolic by-products and supply the inner part of the cell-matrix constructs with adequate levels of nutrients and oxygen, following implantation.

Angiogenesis, the formation of new capillary blood vessels from pre-existing vessels, is a morphogenic process that, being mediated by a complex sequence of events leading to neovascularization at the implant site, has been proven to be crucial for achieving this nourishment.

Keeping in mind the present knowledge on the highly complex mechanisms motivating the activation and invasion of angiogenic vascular cells, a number of strategies are being developed to promote vascularization of tissue-engineered implants. Such strategies involve the delivery of angiogenic growth factors, cell transplantation, most often of different types of endothelial cells (mature ECs or progenitor cells), and the use of biomaterial-based matrices permissive to angiogenesis. Therapeutic approaches improving vessel density and restoring blood flow are particularly desirable following injury in the Central Nervous System (CNS), where the formation of new blood vessels has been correlated with improvements in functional recovery in a number of animal models of CNS injury.

In this sense, the main goal of this master thesis was the development of a fibrin-based hydrogel capable of promoting the neovascularization of bioengineered tissues, either by inducing tubule formation by vascular cell types such as mature ECs or endothelial progenitor cells previously seeded in fibrin, or by promoting angiogenesis *in vivo* by invading host's vasculature. For this purpose, fibrin hydrogels were functionalized with the integrin α6β1 binding sequence of the angiogenic inducer CYR61 (T1 peptide - GQKCIVQTTSWSQCSKS), due to its reported involvement in tubule formation by endothelial cells. Another integrin α6β1 ligand (HYD1 peptide - KIKMVISWKG), previously shown by our group to promote cell migration and neurite extension of embryonic stem cell-derived neural stem/progenitor cells cultured within 3-D fibrin gels, was also explored. Tethering of T1/HYD1 peptides to fibrin was expected to improve fibrin ability to induce neovascularization, namely by promoting proliferation, migration and capillary-like structure formation, *in vitro*, as well as angiogenesis, *in vivo*.

Peptides were covalently bound to fibrin using the enzymatic cross-linking action of transglutaminase factor XIIIa and the effect of immobilized T1/HYD1 on EC ability to form capillary-like structures within 3D functionalized gels was evaluated using a microcarrier-based angiogenesis assay and high throughput fluorescence microscopy. As a first approach, a cell line of human microvascular ECs from the lung (HPMEC-ST1.6R), with reported ability to form capillary-like structures within 3-D fibrin gels, was used. Results showed for the highest concentration of T1 peptide tested (40 μM) an increased EC sprouting (1.4-fold increase in the sprouting area and number of sprouts per microcarrier and a 1.5-fold increase in the maximal sprouting length) although statistically significant differences were only found for the number of sprouts per microcarrier. In contrast, tethering of HYD1 peptide was not effective in inducing EC sprouting, regardless the input peptide concentration tested.

Subsequently, a cell line of human brain microvascular EC (hCMEC/D3), described to be capable of tubule formation of top of Matrigel, was used. Further supporting the previous results, the modification with 40 μM of T1 peptide resulted, in average, in 1.4-fold increase in every EC

sprouting parameter evaluated, with statistically significant differences being observed for the sprouting area and number of sprouts per microcarrier. Once again, the functionalization with HYD1 peptide was unable to promote EC sprouting, within the range of input peptide concentrations tested. The pro-angiogenic ability of T1-functionalized fibrin gels (40 μM of peptide in the polymerizing gel) was significantly enhanced in the presence of the soluble angiogenic inducer vascular endothelial growth factor (VEGF). Specifically, the addition of 25 ng/mL of VEGF to the culture medium, led to a 2-fold increase of the sprouting area, a 1.9-fold increase in the number of sprouts per bead and a 1.5-fold increase in the maximal sprouting length. Also, the percentage of beads with sprouts increased from an average of 70% in unmodified fibrin to 94.6% in T1-functionalized fibrin. The contribution of α6β1 integrin to EC sprouting in T1-functionalized gels was assessed using functional blocking antibodies. Incubation with monoclonal antibodies against α6 or β1 integrin subunits partially inhibited the number of sprouts per bead and the maximal sprouting length. Even though significant differences were not attained, these results suggest that the EC sprouting elicited by immobilized T1 peptide was partially mediated by integrin α6β1. Immobilized T1 peptide did not affect cell viability or proliferation, as shown by flow cytometry analysis of LIVE/DEAD cells and cell metabolic activity, respectively. Further characterization of T1-functionalized gels in terms of mechanical properties showed no significant changes in fibrin viscoelastic properties after peptide binding, in agreement with previous findings reporting minor disruption of fibrin structure during peptide incorporation using the same enzymatic cross-linking approach.

Following, to get insight into the effect of T1-functionalized fibrin hydrogels on a clinically relevant source of endothelial cells, outgrowth endothelial cells (OEC), derived from the umbilical cord blood were cultured within T1-functionalized fibrin hydrogels (40 or 60 μM of peptide in the polymerizing gel) and their ability to form capillary-like structures was evaluated. While 40 μM of T1 peptide failed to promote EC sprouting, an input peptide concentration of 60 μM was successful in enhancing EC sprouting, leading to significantly higher number of sprouts per bead (1.7-fold increase), as well as maximal sprouting length (1.8-fold increase). These findings suggest that the ligand concentration required for EC sprouting enhancement in fibrin is cell type dependent, and possibly related to integrin expression levels.

Finally, in order to evaluate the *in vivo* angiogenic potential of T1-functionalized fibrin, the Chorioallantoic Membrane (CAM) assay was performed. Fibrin hydrogels with an intermediate input peptide concentration (50 μM) were used for this purpose. Results from three independent CAM assays evidenced a reproducible and significant increase in the number of newly formed vessels, namely of about 20%, therefore pointing out the angiogenic potential of T1-functionalized fibrin gels. Interestingly, CAMs receiving T1-functionalized fibrin showed a significant reduction of the inflammatory reaction when compared to that elicited by unmodified fibrin. The possible anti-inflammatory effect of T1-functionalized fibrin combined with its angiogenic properties makes it potential interesting for application in the injured CNS as well as in neurodegenerative disorders.

Taken together, these results suggest that T1-functionalized fibrin gels, apart being potentially useful for the development of prevascularized matrices, may also be of interest to induce locally angiogenesis in clinical situations such as spinal cord injuries, diabetic skin ulcers and ischemia.

KEY-WORDS: Biomaterials, Fibrin hydrogels, Angiogenic physical cues, Endothelial cells, Regeneration of the Central nervous system, Microcarrier-based *in vitro* angiogenic assay, Chorioallantoic Membrane (CAM) assay.

ACKNOWLEDGEMENTS/AGRADECIMENTOS

Por saber que terminar um ciclo - seja ele mais ou menos duro - nunca é tão gratificante se não for acompanhado por pessoas gigantes, não podia deixar de agradecer àquelas que foram as minhas pessoas gigantes ao longo destes anos.

Em primeiro lugar, um muito obrigada à minha orientadora, Isabel Amaral, por me ter dado a oportunidade de trabalhar com ela e me ter dado tanto a conhecer e a aprender. Muito obrigada também por todas as palavras de força e de motivação nos momentos mais críticos.

A todo o grupo nBTT, o meu muito obrigada por me terem recebido tão bem e por me terem feito sentir mais em casa durante estes meses, nunca negando qualquer ajuda e nunca poupando em sorrisos e boa disposição. Um agradecimento particular ao Prof. Dr. Paulo Aguiar, por todo o apoio na análise de imagem. Um agradecimento também especial à Ana Rita Bento por me ter aturado em todas as (muitas) vezes que recorri a ela por algum motivo, e um agradecimento também especial ao meu conterrâneo Luís Leitão, por toda boa disposição e disponibilidade, mas sobretudo por ter demonstrado partilhar da mesma panca que eu.

À Ana Luísa Torres, um muito obrigada por toda a disponibilidade e por me ter ajudado também sempre que precisei ao longo da realização deste trabalho. Um obrigada também ao grupo do Prof. Dr. Bruno Sarmento por me terem disponibilizado as células que possibilitaram grande parte do trabalho. À Marta Teixeira Pinto do IPATIMUP um gigante obrigada por todo o apoio nos ensaios *in vivo* e por todas as palavras de motivação.

Às minhas miúdas - Rita, Joana, Sara e Eva - muito obrigada por tudo! Por terem estado lá para mim sempre que precisei e por me terem feito, tantas vezes, perceber que nada é o fim do mundo e que tudo é possível mesmo quando não parece. Obrigada por terem acompanhado todo este percurso tão de perto e por me terem deixado acompanhar o vosso. Estes meses no 214.S3 não teriam sido os mesmos sem vocês. Aos restantes MIBs que partilharam comigo esta invasão ao i3s, obrigada por todas as horas de almoço, todas as pausas para café e todos os momentos de descarga conjunta de tensão acumulada.

À Rita, à Joana e à Lili, obrigada por aturarem as minhas mudanças drásticas de humor e por me suportarem e me darem força em qualquer dos meus extremos. Teria sido tudo muito mais difícil se chegasse a casa todos os dias e vocês não estivessem lá.

Às minhas chicks Rita, Lisa e Clara, obrigada por me deixarem ser eu mesma quando estamos juntas e por me terem ajudado a construir grande parte das memórias que levo destes anos.

Ao meu Gang, obrigada por terem partilhado comigo os primeiros anos de faculdade e lembrem-se: “o primeiro amor nunca se esquece”.

Aos meus aplicadíssimos, obrigada por serem um porto seguro para a minha sanidade, mesmo partilhando da minha loucura. Um agradecimento especial à minha companheira Filipa Duarte, por me compreender e acompanhar sempre.

Aos meus de sempre: vocês sabem que não há palavras para tudo o que nos une. Crescemos juntos e assim continuaremos, longe ou perto! Obrigada por estarem sempre lá.

Ao Hugo, um obrigada gigante, por teres (re)aparecido na altura certa e por me fazeres tão feliz.

À minha família, a quem devo tudo: obrigada por me terem mostrado, durante toda a minha vida, como é amar e ser amado sem limites.

E finalmente aos meus pais, as minhas pessoas preferidas: obrigada por terem tornado tudo isto possível, por me terem ajudado a lidar com cada problema e com cada obstáculo e por me terem ensinado tão bem quais os valores mais importantes. Espero continuar a deixar-vos orgulhosos!

“Sometimes we feel that what we are doing is just another drop in the ocean and we forget that the ocean would be smaller without that single drop.”

Mother Teresa

TABLE OF CONTENTS

CHAPTER 4 – Final remarks and Future perspectives

SUPPLEMENTARY DATA

LIST OF FIGURES

LIST OF TABLES

ABBREVIATIONS

BBB Blood Brain Barrier

BSB Blood-Spinal cord Barrier

BI Brain Injury

CAM Chorioallantoic Membrane

CNS Central Nervous System

CYR61 Cysteine-rich Angiogenic Inducer 61

DAPI 4',6-diamidino-2-phenylindole

EC Endothelial Cell

ECM Extracellular Matrix

EGF Epidermal Growth Factor

EPC Endothelial Progenitor Cell

Fb Fibrinogen

FBS Fetal Bovine Serum

FGF Fibroblast Growth Factor

G' Shear Elastic Modulus

G'' Shear Viscous Modulus

G* Complex Modulus

HBMEC Human Brain Microvascular Endothelial Cell

hCMEC/D3 Human Brain Microvascular Endothelial Cell Line

H&E Hematoxylin-eosin

HPMEC Human Pulmonary Microvascular Endothelial Cell

HUVEC Human Umbilical Vein Endothelial Cell

LN Laminin

LVR Linear Viscoelastic Region

MC Microcarrier

NGS Normal Goat Serum

NSPC Neural Stem Progenitor Cel

NVU Neurovascular Unit

OEC Outgrowth Endothelial Cell

PI Propidium Iodide

SCI Spinal Cord Injury

CHAPTER 1

INTRODUCTION

1. CONTEXTUALIZATION

In 2014, around 86,000 people from the European Union (EU) were on the organ transplantation waiting list, with an average of 16 people dying each day, waiting for transplants that cannot take place because of the fact that current demand for organ and tissue transplants far exceeds the supply [1]. Besides, there is a considerably high rate of rejected transplants due to the inefficiency of providing the adequate amount of oxygen and nutrients to the cells [2]. This is due to the fact that the nearby blood vessels are located at a higher distance than 100-200 μm, being such gap inadequate to deliver sufficient oxygen diffusion and nutrients [3].

Thus, since there is an increasing need for organ transplantation, the ability to promote the formation of blood vessels, in a controlled manner, is even more fundamental for its acceptance and success [4]. One of the main critical issues regarding the success of engineered constructs with clinically relevant size is also the demand for nutrients, waste and oxygen transport [5]. Most successes have been attained on avascular or thin tissues, such as the bladder, cartilage or the skin, because, since cells are merely a few hundred micrometers away from the capillaries, the nutrients and oxygen are able to disperse into the implants and sustain cellular survival and viability [6]. This issue becomes more critical in what concerns larger and more complex organs, such as kidney, heart, liver and brain, because those have an enormous mass of cells requiring individualized nourishment through an organized network of capillaries, veins and arteries [7]. Particularly in such situations, the inability to properly dispose the waste and to provide adequate nourishment to the inner part of the cell-matrix constructs in the initial phase after implantation of the engineered tissues and organs is critical for the success of the graft [2].

1.1. Angiogenesis

Therefore, blood vessels development constitutes a crucial process for the formation and maintenance of tissues and organs. It can be classified in three different types – sprouting angiogenesis, vasculogenesis and intussusception [8] – as depicted in **figure 1**.

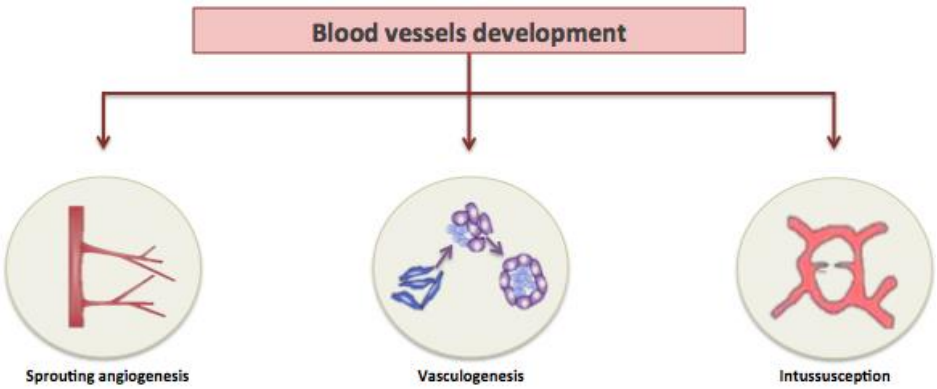

Figure 1: Mechanisms of blood vessels development.

Sprouting angiogenesis refers to the formation of new capillary blood vessels by sprouting from pre-existing vessels. This is an invasive process involving proteolytic agents which degrade the basement membrane, allowing cell migration, removal of blocking matrix proteins and creation of free space in the matrix to allow the formation of a proper lumen by endothelial progenitor cells (EPCs) [9]. Vasculogenesis, in turn, defines the process of differentiation assumed by mesodermal cells in order to originate new blood vessels. Lastly,

intussusception denotes the process in which pre-existing vessels split and raise daughter vessels [8] [10].

Angiogenesis, schematized in **figure 2**, is a morphogenic process mediated by a complex sequence of cellular happenings that lead to neovascularization [11]. After the production and release of angiogenic factors, by diseased or injured tissues, the contact between adjacent ECs is reduced due to the vasodilatation of the parental vessel. Then, the basement membrane of the parental vessel is degraded and the ECs migrate and proliferate in order to form a leading edge of a new capillary and, consequently, the capillary lumen is developed and a tubular-like structure is created. Later, the basement membrane is synthetized and vascular smooth muscle cells and perycites are recruited to stabilize the newly formed blood vessel [7]. At the end of this events sequence, the vascular network is formed and comprised of a layer of ECs separated from the other present cells types through the basement membrane lastly formed [12].

The angiogenic response is dependent on the dynamic balance between stimuli and inhibitors, both acting in the environment of ECs [13]. Interferences in such balance can support the development of new vessels or lead to vessel latency or regression. During tissue remodeling, new blood vessels emerge from the neighbor ones, being angiogenesis a critical regulator of tissue function [14].

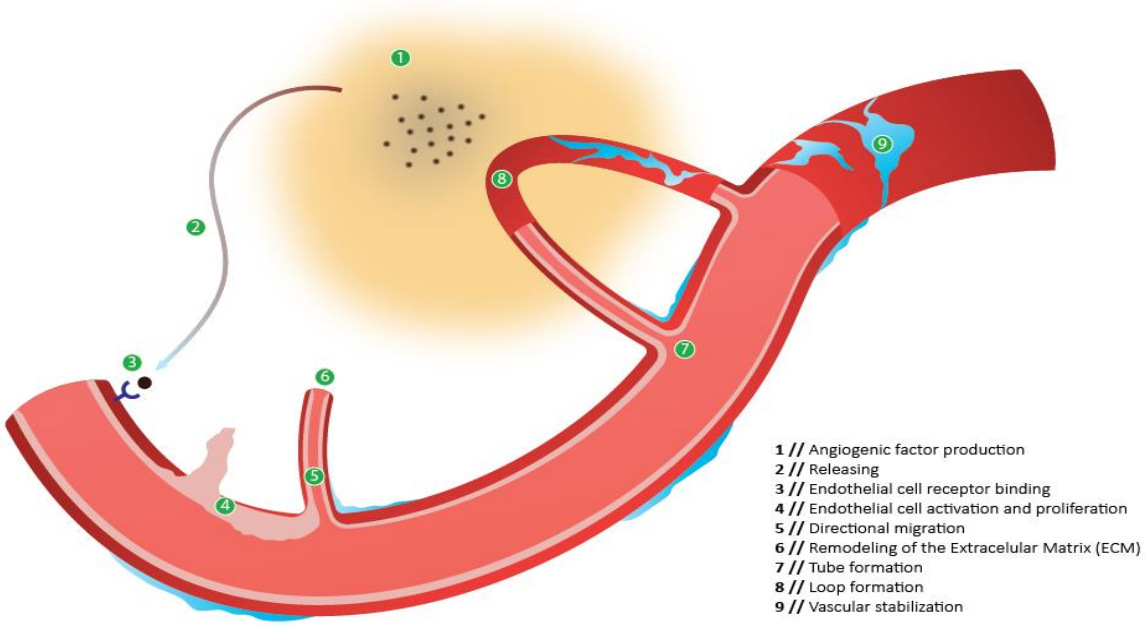

Figure 2: The process of angiogenesis (adapted from Angiogenesis Foundation, 2000)

1.2. Angiogenesis in the Central Nervous System

The Central Nervous System (CNS), consisting of the brain and spinal cord, is one of the most sensitive and critical of any organism. To own a highly specialized vasculature is crucial to answer the demands of this metabolically highly active system and also to defend the most sensitive neurons from toxic agents, such as metabolites and xenobiotics [15]. Therefore, it is essential to understand the mechanisms underlying angiogenesis in this system, since it is seen both as a normal physiological response and a pathological step in disease progression [15].

The vascular and nervous systems share anatomical and developmental principles, since they have the necessity of creating a transferring circuit, respectively, for nutrients and information [16]. At the cellular and molecular levels, there are also similarities between the main elements of each system – vessels and neurons - that use similar cues to guide both ECs and neuronal cells [16]. Apart from the common anatomical, cellular and molecular features, these two systems have developed a close relationship within the CNS itself, connecting to each other at the interface between them – the neurovascular unit (NVU) [17] - composed by ECs, pericytes, glial cells and neurons, tightly connected to control cerebrovascular functions [16].

Several decades ago, Paul Ehrlich suggested the existence of a protective and stabilizing feature, formed by specialized characteristics of brain vessels [17]. When injecting dyes in the vascular system, Ehrlich concluded that they did not penetrate into the brain tissues but were easily absorbed by the peripheral tissues [18] and, thus, the concept of Brain-Blood barrier arose. BBB is now understood as being a physiological and anatomical barrier, located at the level of cerebral capillaries in the frontline defense of the CNS [17], responsible for restricting the permeability of the surrounding blood vessels, regulating the diffusion of ions, peptides, amino acids and other elements from bloodstream to the neural system, while guaranteeing the supply of the required nutrients to the brain for a proper function of the CNS [19]. This barrier is covered with greatly specialized cells, such as astrocytes, pericytes and vascular ECs, strongly interacting with each other due to the angiopoietin (Ang-1)/Tie-2 system [19] and forming the neurovascular unit [17]. The blood-spinal cord barrier (BSB) is the correspondent to the blood-brain barrier, located between the blood flow and the spinal cord, playing a similar protective and regulatory responsibility for the spinal cord parenchyma as BBB in the brain [20]. BBB and BSB are crucial components for the promotion of angiogenesis in the CNS, since their formation and breakdown closely affects the proper balance of vascular permeability required [21].

1.3. Spinal Cord and Brain injuries

Spinal cord and brain injuries affect not only the neural elements but also the vascular ones. Therefore, it is quite important to understand the vascularity of these organs because it is known that the susceptibility of grey and white matter to injury is partially justified by the segmental distribution of blood vessels on those organs [22]. It was already described that the increase of blood vessel density is tightly related to improvement in recovery of several injury models from the CNS [23] [24]. Situations of trauma and stroke give rise to abnormalities in the vasculature and therefore those situations had become the core focus of diverse research groups who are willing to develop engineering strategies capable of establishing a proper angiogenic status after this kind of injury, since the angiogenic extent is closely related to neural regeneration, having an important role in neurologic repair [24].

Angiogenesis occurs after spinal cord trauma in response to the lack of oxygen in restricted tissues. Hypoxic and ischemic conditions are a result of the physical damage to blood vessels and also of the hypoperfusion and vasoconstriction associated with the injury. The degree to which the vascular injury contributes to secondary pathogenesis is determined not only by the early disorder of blood vessels but also on the gradual disturbance of the blood-spinal cord barrier along with the infiltration of inflammatory cells [22].

In case of stroke, one of the main causes of death and disability in the generality of developed countries [25], apart from the activation of brain injury responses, regenerative

responses are also activated, leading to vascular remodeling, angiogenesis and neurogenesis [25].

Different international research groups have concentrating their efforts in the development of strategies for the creation of stable and functional vessels in the CNS after injury [26] and different approaches have been applied both *in vitro* and *in vivo*. This kind of approaches has been proven to support the creation of stable vascular networks capable of contributing to the success of engineered constructs. This way, understanding how angiogenesis is regulated by the diseased microenvironment has a great importance for maintaining the survival and health of implanted tissues for regenerative medicine, as well as identifying ways of controlling angiogenesis as one path to treat neural pathologies.

2. VASCULARIZATION STRATEGIES FOR TISSUE ENGINEERING

There has been a great effort for developing strategies able to create a vascular network throughout the cell-matrix construct capable of supplying the implanted tissue with the nutrients and oxygen required for cell survival in the host organism.

For a proper vascularization of the engineered construct after implantation, there are different strategies that may be followed, namely the angiogenesis approach and the inosculation or anastomosis approach, as depicted in **figure 3**. The first one is focused on the promotion of vascular sprouts growing from the host microvasculature into the implanted engineering construct [27]. In the second approach, a preformed microvascular network is generated within the construct prior to the implantation phase and, after the implantation, the micro vessels will establish interconnections with the host vasculature [27].

These matrices, in order to promote and direct the angiogenic process, the matrices may be combined with soluble factors capable of recruiting EPCs to the implant site or with cellular types that produce angiogenic factors, be colonized with endothelial cells or EPCs to foster the formation of a microvascular network, functionalized with physical ligands to better support adhesion and infiltration of vascular cell types, or be specifically designed to present a structure to able to guide the angiogenesis process.. In the following sub-sections some of these strategies will be presented in further detail.

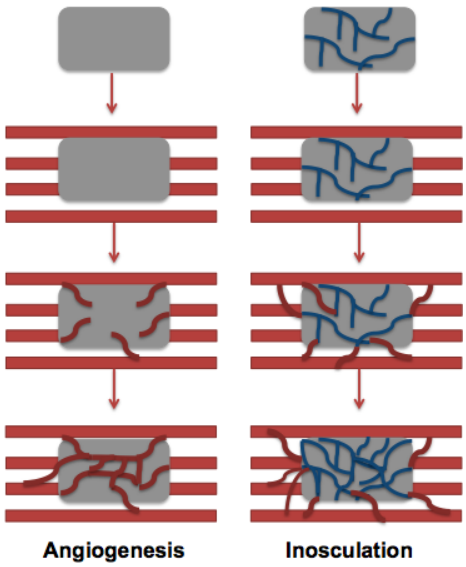

Figure 3: Angiogenesis and Inosculation approaches (based on [27])

2.1. Delivery of angiogenic factors

Strategies focused on the delivery of growth factors delivery are meant to use their signaling properties to stimulate the cells in the area to migrate, proliferate and differentiate. Along the last decades, angiogenesis research has lead to the creation of a considerably extensive list of angiogenic molecules that can stimulate the conversion of EC to the angiogenic phenotype [7].

Vascular endothelial growth factor (VEGF), basic fibroblast growth factor (bFGF) and hepatocyte growth factor (HGF) are part of the group of angiogenic factors that actuate directly on ECs and many studies utilized the local distribution of these factors using controlled drug delivery systems [28] [29]. Moreover, other growth factors were shown to induce angiogenesis *in vivo*, even though they do not induce EC proliferation and migration *in vitro*. These include platelet-derived growth factor (PDGF), transforming growth factor beta (TGF-β) and angiopoietin (ANG).

Several studies have been developed envisaging neovascularization promotion through the injection of these proteins in the blood strem or locally into the target damaged tissue [30] [31]. The delivery of soluble angiogenic factors was shown to improve the chemotaxis of cells. Several *in vitro* and *in vivo* studies using cocktails of growth factors, reported that the delivery of the cocktails had a positive effect on underperfused and incompletely vascularized areas with additional blood flow, supplying the cells with nutrients and oxygen [32]. However, the rapid clearance of these growth factors from the body and the consequent need of increasing of the administered doses of these factors are important drawbacks of simple growth factor injection, which may lead to uncontrolled and unpredictable effects at distant locations, such as bleeding, tumor growth, atherosclerosis and restenosis [33] [34].

Taken all this into consideration, there is a clear need of studying and understanding the kinetics of growth factors and their life-time, in order to calculate the optimal administration dose and define the adequate route of administration [35, 36] [36]. Furthermore, even though growth factors have the ability to stimulate vessels formation, these newly formed vessels have to mature in order to maintain the stability, what may lead to the conclusion that the simple administration of angiogenic factors may not be sufficient to stably form the vessels.

To overcome the previously mentioned problems of systemic injection of angiogenic factors, one of the classical approaches has become the decoration or supplementation of synthetic or natural scaffolds with pro-angiogenic factors such as the ones previously referred in this section [3]. This decoration mimics the *in vivo* ambiance, as these growth factors are associated with the ECM to stabilize its conformation and avoid proteolytic degradation [37].

Therefore, the prolonged delivery of these factors from scaffold materials has been adopted, since the scaffolds allow the distribution to a specific microenvironment and the minimization of the side effects in non-target regions [38] as well as a reduction of the toxicity effects associated with the bolus administration of the growth factors [39].

The ability of controlling the timing and release of growth factors allows the increase of the control exerted on the degree of vascularization within the tissue construct [40]. To direct the angiogenic process it again becomes crucial to determine and control the release kinetics of the factors from the scaffold. This is fundamental because the time course of vascularization may not be compatible with the maintenance of cellular viability throughout the construct and, therefore, it is necessary to provide the scaffolds with known cues, with also known temporal

expression profiles, that further contribute with physiologically relevant properties that increase the sought control [3].

2.1.1. VEGF

VEGF contains potent division activity specific to vascular ECs and has a crucial role in the promotion of vascularization facing several conditions, both normal and pathological [41]. This growth factor, together with its receptors, mediates many crucial angiogenic processes depicted in **figure 4**.

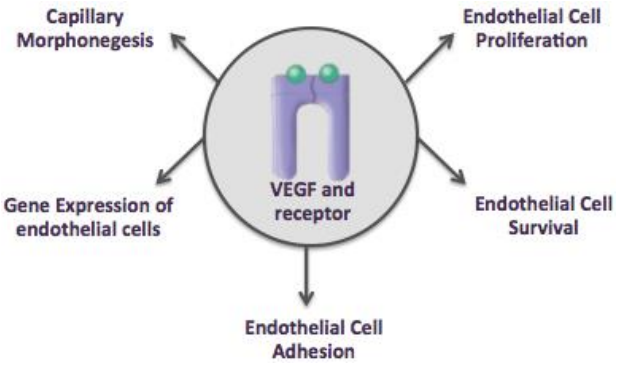

Figure 4: Processes mediated by VEGF and its receptors.

One of the mechanisms that make VEGF able to promote the angiogenesis is the up-regulation of integrins expression and activation [41], being integrins divalent cation-dependent heterodimeric membrane glycoproteins, comprised by α and β subunits non-covalently associated, which promote cell attachment and migration on the nearby ECM [42].

During the last decades many research groups have focus on the understanding of the molecular mechanisms underlying the regulation of angiogenesis and many investigations implicate integrins as regulators of ECs migration and survival during such events [42]. Different experimental approaches have led to several theories of the roles of distinct integrins in angiogenesis, including αv integrins and α2β1 integrin [42]. Tae-Hee Lee *et al* analyzed the effect of VEGF on integrin expression and activation in human brain microvascular endothelial cells. VEGF was found to activate α6β1 integrin and to upregulate their expression. Down-regulation of α6 integrin expression inhibited cell adhesion and migration as well as capillary morphogenesis. Blocking of α6β1 integrin led to the inhibition of VEGF-induced adhesion and migration and also suppressed *in vivo* angiogenesis. Therefore, this study points out that VEGF can modulate angiogenesis through increasing α6 integrin expression and activation [41].

2.2. Cell-based therapies for angiogenesis promotion

Diverse strategies that intend to induce vascularization of tissues are based in cells transplantation, being the most frequent transplanted cell types the mature ECs and the EPCs [43, 44]. Co-cultures with ECs have been used as an opening point for vascularization [45]. Co-culturing methods have been extensively used for *in vitro* vascularization of several tissues, mostly the thicker ones, with ECs being introduced into the tissues through three-dimensional multicellular spheroids or simply by cultures mixing [46] [47]. Borges et al transferred human dermal microvascular endothelial cells (HDMVECs) spheroids and preadipocytes to the chorioallantoic membrane (CAM) using a fibrin matrix and results show the formation of a capillary network consisting of transplanted HDMVECs [47].

Wenger et al developed, in 2005, a three-dimensional spheroidal co-culturing system that consisted on human umbilical vein ECs (HUVECs) and human primary fibroblasts (hFBs) with the goal of improving angiogenesis in tissue engineering applications [46]. Morphological evaluation of these co-spheroids revealed a characteristic temporal and spatial organization and the level of apoptosis of ECs was considerably decreased upon cultivation with fibroblasts, in the presence or absence of growth factors such as VEGF, when compared with the apoptosis level seen in plain HUVEC spheroids [46]. Moreover, an *in vitro* angiogenic assay was performed with collagen- embedded spheroids in order to evaluate the effect of human fibroblasts on the ability of ECs to form sprouts. It was noticed that in HUVEC/hFB co-spheroids, the cumulative sprout length was considerably reduced when compared to the observed sprouting for plain HUVEC spheroids embedded in a collagen matrix containing hFBs in suspension culture. To investigate the reason responsible for this reduction, a transwell co-cultivation system was used to cultivate the cells. This system, preventing the close contact between the cell types being considered while allowing free diffusion of soluble molecules, led to an absence of inhibitory effect of fibroblasts on HUVEC sprouting. It was concluded that the inhibition of the sprouting was not mediated by soluble factors but due to the formation of heterotypic cell contacts between the two cellular types [46]. Therefore, this co-spheroid model is suitable for supplying a preformed capillary network *ex vivo*, which might be useful for the angiogenic improvement *in vivo* tissue engineering applications.

Besides the referred spheroid cultures, simple co-cultures of ECs, fibroblasts and other cellular types have been used to grow diverse vascularized tissues. Through these simple co-culture strategies in a biopolymer gel (e.g. Collagen) or a porous polymer scaffolds, spontaneous formation of tubular structures was observed [3].

The combination of EC layers and other cell types layers within natural hydrogels is also a good strategy for the formation of a vascular network in an engineered tissue *in vitro*. Griffith and his group developed an *in vitro* three- dimensional angiogenesis model capable of forming the foundation of a strategy to vascularize an engineered construct previously to the implantation stage. Their model was composed of microcarrier beads covered with HUVECs and a fibroblast monolayer entrenched in a fibrin matrix. This group along this investigation project attained some important assumptions, concluding that the oxygen diffusion, which leads to a high failure rate of constructs implantation, is not a limiting factor *in vitro*, therefore allowing the creation of prevascularized tissue constructs on the order of centimetres in thickness.

Moreover, the researchers included fibroblasts on their model since they noticed that the soluble factors produced by these cells are quite useful for stabilizing the capillary network and considerably sensitive to the diffusion distance. Mimicking the architecture of a wound healing,

for instance, it is believed that this model can be useful for the design of thicker engineered tissues beyond the diffusion threshold that presently is a limiting factor in the field of tissue engineering [48].

2.3. Biomaterial-based supporting matrices permissive to angiogenesis

Supporting matrices have several crucial roles in what concerns to the promotion of vascularization in tissue engineering, both because they provide the support and stability required by cells to regenerate a considered damaged area and also because they contribute to the maintenance of cells proliferation and differentiation through the delivery of several types of signaling factors.

Several biomaterials are being studied and tested in order to promote vascularization of tissues newly formed in different organs. The main concern in this field of investigation is to develop scaffolds able to create an environment that closely mimics the conditions of the natural tissue to be replaced, providing the necessary soluble and non-soluble signals, which will then influence the cells in different manners, enhancing their migration, proliferation and differentiation. Besides, there are other questions that must be considered during the scaffolds development, namely their controlled biodegradation rate [49], which should match the tissue regeneration kinetics to avoid undesired reactions and their adequate porosity to promote cellular colonization and ingrowth from the host. In addition, the biocompatibility of the scaffolds and their proper mechanical integrity are also crucial conditions in order to escape immunological reactions from the host and early scaffold deterioration, respectively. The microstructure of the matrix also affects the angiogenic response. Hamidreza Mehdizadeh *et al* developed 3-D models with well-defined pore architectures to address this issue. The simulation results indicate that large pores (275-400 μm) with higher connectivity and porosity support rapid and extensive angiogenesis [50].

2.3.1. Angiogenic physical cues

Following, different used angiogenic cues are presented, as well as their respective purposes and mediation agents. Nevertheless, the perceived biological outcomes cannot be attributed to the physical parameters themselves, but to the network characteristics of the matrix used, namely hydrogels, as a whole [51]. An overview of angiogenic physical cues that have been explored along the last years in the field of Tissue Engineering is presented in **Table 1.**

Table 1: Angiogenic Physical Cues

Physical cue	Base matrix	Cellular type	Animal Model	References
PA22-2 (SIKVAV-containing peptide)	Matrigel	B16F10 murine melanoma cells	Mouse	[52] [53]
	Matrigel	ECs	Murine and chicken	[12]
Ephrin-A1	PEGDA hydrogel	ECs	-	[54]
Scl2-2 protein	PEG	ECs	-	[55]
QK peptide	Matrigel	ECs from bovine aorta	-	[56]
	PEGDA hydrogel	HUVECs	Mouse	[57]
	Elastin-like polypeptide (ELP) hydrogel	HUVECs	-	[58]
GYIGSRG	Alginate composite hydrogel	-	Rat	[59]
YIGSR	Matrigel	ECs	CAM assay	[60]
YIGSR + RGD	PEG-based hydrogel	MVECs	-	[61]
Heparin-binding domains	Collagen gel	HUVECs	Lewis rats	[62]
A13 peptide	Matrigel	HUVEC	Rat	[63]

2.3.2. Incorporation of gradients of soluble/physical cues for cell guidance

In order to improve the cell guidance control, efforts have been made concerning the development of tissue engineering scaffolds that present well-defined patterns, both spatially and temporarily, since these patterns play a fundamental role in several physiological processes, both in the embryogenesis and in the adult phase [64] [65].

To study the cell response to such controlled signal spatial distribution, some approaches have been proposed, including electrochemical potential gradients, photolithography techniques, photo-initiated coupling reactions, gradient pumping and microstamping. Moreover, 3-D signal gradients have also been obtained though manipulation of laminar streams of fluids in microchannels, creating complex gradients with soluble or immobilized bioactive molecules [65].

Recently, a considerable amount of experimental data has demonstrated that the inclusion of immobile or mobile biological cues within material scaffolds results in a noteworthy enhancement of tissue morphogenesis [65]. Even though this is known, there are still some challenges to be surpassed, namely the most appropriate form, i.e. if it is best to have the cues bound or unbound, the effective dose and the most suitable spatial distribution [65].

There are three major known mechanisms that direct cells along a gradient of attractive gradient cues, being them the haptotaxis, the chemotaxis and the mechanotaxis [64]. The first of the three is defined as being the directed movement of cells along the direction of a gradient of ligands immobilized in the matrix. The chemotaxis regards the response of the cells as a migration along a concentration gradient of unbound chemo-attractants. Lastly, mechanotaxis is induced by mechanical forces there are exerted through the materials.

2.4. Combined strategies for promotion of the angiogenic process

Besides the development of independent cell-based or biomaterial-based strategies, some efforts have also been directed towards the development of combinatorial and synergetic approaches involving several principals**.** The development of biomaterials that incorporate biomolecules or cells is one example of this.

2.4.1. Fibrin as a biomaterial-based strategy

2.4.1.1. Fibrin structure

Being currently one of the most used biomaterials in a wide diversity of applications, fibrin has proved to have an efficient role in situations such as hemostasis and wound repair, through materials such as fibrin glues and wound dressings, and also in the creation of cell instructive platforms largely used for differentiation and delivery of cells, as well as induction of angiogenesis [66]. This way, it is quite relevant to go further in what concerns this biomaterial, in order to understand the processes that underlie its formation and maximize the applicability of fibrin matrices.

It is not easy to define the ideal fibrin matrix, but it has to be permissive to cell infiltration and regeneration and, simultaneously, exhibit mechanical properties directed to the specific application of the matrix. Such mechanical properties are largely defined by the molecular scale organization of the fibers, which can be modified and adjusted through different processes. A simple way to vary the polymerization dynamics of fibrin is to merely adjust the concentration of fibrinogen and thrombin and/or modify the calcium ions or salt concentrations. As all these

compounds concentrations have been shown to modulate the clot's physical properties [67], they will also have implications in the behavior of cells that are in contact with such matrices, different concentrations resulting in different proliferation, migration and differentiation rates. It is also interesting the fact that the simple incorporation of cells into the gels results in different stiffness rates of the gel [68].

One of the most prominent players on fibrin polymerization is fibrinogen, whose structure is shown on **figure 5**. Fibrinogen is a 340-kDa dimeric glycoprotein, with each dimer being composed by three different chains. Each set of chains get together at the central region of fibrinogen and are linked by disulfide bonds at their N-terminal regions. On **figure 5**, fibrinogen Aα chains are represented in blue, Bβ chains appear in green and γ chains are symbolized in red. The orange connections represent the interchain disulfide bridges, which have the role of connecting the six-polypeptide chains in the central domain, while the yellow rings depict the stabilizers of the coiled-coil regions of this structure.

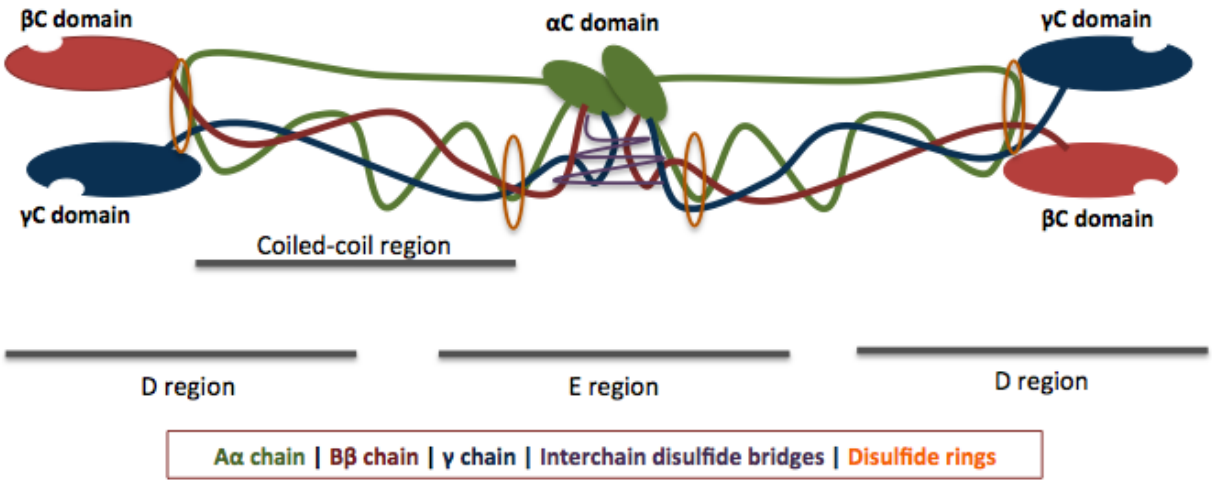

Figure 5: Fibrinogen structure. Aα chains are shown in green, Bβ chains are shown in red and γ chains are depicted in blue. The purple bridges connecting the six-polypeptide chains in the central domain are called interchain disulfide bridges. Lastly, stabilizing disulfide rings of the coiled-coil regions are shown in orange. Adpated from [66].

In order to trigger fibrin polymerization, another essential player is the thrombin, responsible for the cleavage of two sets of fibrin peptides, respectively named A and B and composed by 15 and 16 amino acids, from the central domain of fibrinogen, which circulates in the bloodstream until being cleaved. Along with such enzymatic cleavage, the exposition of peptide sequences is attained at the N-terminal of both alpha and beta chains, which are thus available for interacting with holes a and b from the C terminal of gamma and beta chains, respectively. Such process is depicted on **figure 6** [66]. The crosslinking of fibrin clots by Factor XIIIa notably raises clot stability through the increase of the clot stiffness and resistance to deformation, adding to the decrease of the vulnerability to degradation. The clot stability is thus reflected on the mechanical stability of fibrin clots having an impact in biomaterials design.

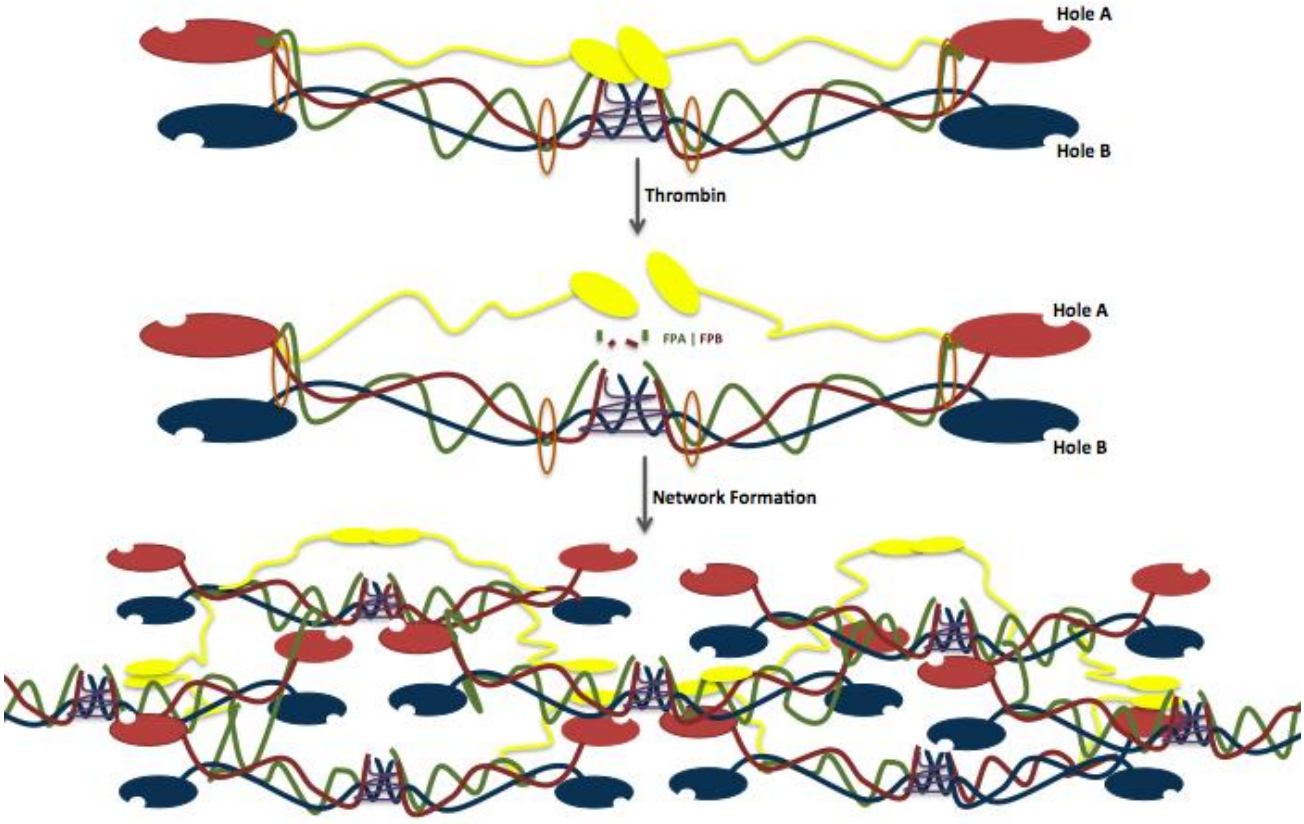

Figure 6: Fibrin polymerization process. Aα chains are shown in green, Bβ chains are shown in red and γ chains are depicted in blue. αC domains are shown in yellow. Adapted from [66].

Fibrin is thus designed to quickly assemble under physiological conditions, unlike nearly all-native cellular matrices and many synthetic ones [69]. Moreover, its softness and large compliance seems to be essential for the efficiency as a matrix for cells that are used to reside in very soft tissues, such as neurons and endothelial cells [14].

2.4.1.2. Fibrin functionalization through the enzymatic cross-linking activity of transglutaminase factor XIIIa

Contrarily to a synthetic matrix, fibrin is not just a passive and unresponsive matrix. Fibrin, by itself, contains numerous bioactive motifs, containing several binding sites for cells, ECM proteins and growth factor. Moreover, fibrin contains binding sequences for several integrins, such as αvβ3, used by endothelial cells for interaction with fibrin. In contrast, motifs interacting with integrin α6β1 receptors are absent [66]. Moreover, fibrin allows the specific binding and functionalization with several domains and growth factors, thus enhancing its specificity and bioactivity [69]. Peptide adhesion domains covalently immobilized within 3-D fibrin hydrogels can also significantly enhance the bioactivity of fibrin.

Schense *et al* described a method that allows the incorporation of exogenous peptides into fibrin matrices by exploiting the enzymology of coagulation process [70]. During coagulation, the physicochemically assembled fibrin network is covalently crosslinked by the activity of Factor XIIIa, which consists on the activated form of factor XIII that circulates in the blood along with fibrinogen until being both cleaved by thrombin. Factor XIIIa, then covalently crosslinks specific glutamine residues within the fibrin network to lysine residues, therefore stabilizing the recently formed fibrin gel [71] [72]. A set of bi-domain peptides containing the

bioactive sequence of interest in one of the domains and a substrate for factor XIIIa in the other, have ben successfully immobilized into fibrin using the cross-linking action of the transglutaminase factor XIIIa. A schematic view of this approach is depicted in **figure 7**.

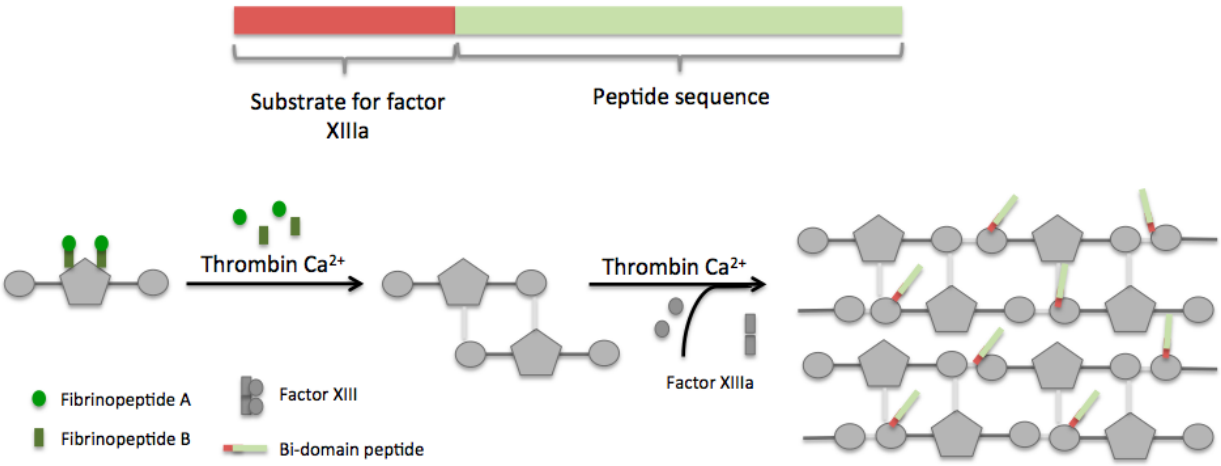

Figure 7: Schematic illustration of covalent incorporation of bioactive peptide sequences into fibrin hydrogels using the enzymatic cross-linking action of transglutaminase factor Xiiia**.** Adapted from: [64]

This approach has been explored in our lab for the tethering of several α6β1 ligands to fibrin, among them T1 peptide (GQKCIVQTTSWSQCSKS) and HYD1 peptide (KIKMVISWKG). The T1 sequence, isolated form the third domain of the angiogenic induced CYR61, was proven to be the critical sequence for CYR61 binding to α6β1 integrin [73]. The interaction of CYR61 (or CCN1) with α6β1 integrin was shown to mediate adhesion and tubule formation by unactivated endothelial cells (in the absence of VEGF), as well as adhesion of fibroblasts and smooth muscle cells [73]. HYD1, in its turn, is a synthetic peptide with reported ability to mediate cell adhesion and spreading mediated by α6β1 and α3β1 integrins [74].

HYD1 or T1-functionalized fibrin hydrogels were evaluated in terms of ability to promote migration of embryonic stem (ES)-derived neural stem progenitor cells (ES-NSPCs) as well as neurite extension from rat sensory neurons. Both the Immobilization of T1 and HYD1 showed to efficiently promote outward migration from ES-NSPC neurospheres mediated through α6β1 and α3β1 integrins, as well as neurite extension [74].

3. ASSESSMENT METHODS OF ANGIOGENIC PROCESSES

Many biomaterials for implantation have been developed and examined for their suitability to support the growth of cells. In order to be successful, a transplanted material must support both the growth of the cells making up the organ or tissue being replaced *in vivo* and the growth of ECs willing to develop an efficiently functioning vasculature to source the cells with oxygen and nutrients [75]. Therefore, the development of promotion strategies for blood vessels formation is not the only critical factor regarding research on angiogenesis. To assess and evaluate the angiogenesis capability of the existing or developing strategies is also crucial and there are several *in vitro* and *in vivo* angiogenesis assays that allow it. Fully developed models enable the development of vascularized engineered tissues for disease treatment, while simultaneously allow the performance of tests relating anti-angiogenic drugs for cancer therapy [44].

Nevertheless, the choice of the suitable assay constitutes a major technical challenge in the studies of angiogenesis and generally it is necessary to combine several assays in order to accurately study and identify the events responsible for the angiogenesis process [76]. Rakesh Jain stated, in 1997, that performing an optimal angiogenesis assay should be cost-effective, rapid, easy-to-use, reproducible and reliable, as well as involve [77]:

a) Knowledge relating the release rate and the spatial and temporal distribution of angiogenic factors and inhibitors, in order to generate the dose/response curves;
b) The definition of a quantitative measure of the structure of the newly formed vasculature;
c) The establishment of a quantitative measure for the functional characteristics of the new vasculature;
d) The existence of a clear distinction between the newly formed structures and the pre-existing ones;
e) The avoidance of tissue damaging, since it may lead to the formation of unwanted blood vessels;
f) The confirmation of the *in vitro* results through the performance of *in vivo* assays.

In **tables 1 and 2** below, a brief description of both *in vitro* and *in vivo* assays for evaluation of angiogenic properties is presented.

Table 1: *In vitro* assays for angiogenesis evaluation.

Assay	Leading principle	Evaluated parameters	Reference
	CELL CULTURE ASSAYS		
Cord and tube formation	Cell seeding and attachment to a gel matrix, followed by a quick assessment of angiogenesis, due to the ability of ECs to form 3-D structures that originate the tubular bodies.	Tubular structures formation	[78] [76]
Cell proliferation	Measurement of cell proliferation at baseline in the presence of angiogenic factors.	Cell proliferation	[79]
Gelatin zymography	Use of a quantifiable polyacrylamide gel-based electrophoretic approach to detect the activity of gelatinases.	Metalloproteinases expression	[75] [80]
Sprout formation	Seeding of cells on top of a gel or embedment of the cells within the gel.	Cell organization and formation of cellular processes	[44] [76] [77] [81]

Microcarrier-based angiogenesis assay	Cell colonization of microcarriers and subsequent embedment within hydrogels.	Quantitative analysis of the cellular processes protruding from the microcarriers	[81]
Microfluidic systems	Attempt to cover the exiting gap between *in vitro* and *in vivo* angiogenesis assays. High ability to tailor structural and biological aspects of the environment and important capability to tune the spatial and temporal control of the applied stimuli.	Migration area and sprouts formation	[82]
	ORGAN CULTURE ASSAYS		
Aortic ring assay	Culture of rings from mouse aortas in 3-D gels. Addition and evaluation of the effects of angiogenic promoting and inhibiting factors.	Neovessel outgrowth	[83] [76]
Chick aortic arch assay	Modification made from the aortic ring assay. Similar rings are obtained from aortic arches of chick embryos. Placement of the rings on a gel and evaluation of the development of the cells and formation of vessel-like structures.	Neovessel outgrowth	[76]

Table 2: *In vivo* assays for evaluation of angiogenesis.

Assay	Leading principle	Evaluated parameters	Reference
Sponge implantation assay	Characterization of fundamental compound in blood vessels and respective roles under physiological and pathological conditions.	Cell migration and proliferation	[84] [85]
Matrigel plug assay	Detection of new blood vessel formation in the transplanted gel plugs in nude mice. Precise	Blood vessel formation	[76]

	visualization of the angiogenic process.		
Wound-healing assay	Evaluation of the impact of several culture conditions through the spotting of changes on the wound area.	Wound area	[76]
Zebrafish assay	Measurement of the angiogenesis extent via fluorescent imaging, due to the intrinsic fluorescent properties of zebrafish embryos.	Angiogenesis extent	[76] [86]
CAM assay	Placement of compounds of interest onto the CAM and monitoring of local angiogenesis through boundaries establishment.	Blood vessel formation and biomaterials degradation	[76] [87]
Dorsal air sac model and chamber assay	Implantation of a chamber across dorsal skin of mice, through which test substances are introduced.	Local angiogenesis	[79] [88]

Even though *in vivo* tests tend to be more time-consuming and harder to perform and to quantify than the *in vitro* ones, it is important to invest on them because there are important characteristics, such as the response to test reagents, that no *in vitro* model can entirely attain [76]. In its turn, *in vitro* methods of evaluation are of great importance because results can be obtained in a short period of time, even though it is recommended to perform each test multiple times to obtain a maximum reliability of the results [76]. Moreover, the *in vitro* tests are important to overcome some limitations of the *in vivo* ones, such as the high expenses associated to animal experiments and the difficulties encountered when isolating specific phenomena *in vivo* [44].

AIM OF THE THESIS

The objective of this master thesis was the development of a fibrin-based hydrogel capable of promoting neovascularization of bioengineered tissues, both by inducing tubule formation by endothelial or endothelial progenitor cells previously seeded in fibrin and by promoting angiogenesis *in vivo* by invasion of the host's vasculature.

To achieve this objective, fibrin hydrogels were functionalized with the integrin α6β1 binding sequence of the angiogenic inducer CYR61 (T1 peptide - GQKCIVQTTSWSQCSKS), due to its reported involvement in tubule formation by endothelial cells. Another ligand for integrin α6β1 receptor (HYD1 peptide - KIKMVISWKG), previously shown by our group to promote cell migration and neurite extension of neural precursors cultured within 3-D fibrin gels, was also explored.

Moreover, as VEGF is described to increase the expression of α6β1 integrin, the effect of fibrin hydrogels tethered with α6β1 integrin ligands in the presence of this soluble angiogenic inducer was also assessed.

Tethering of T1 and HYD1 peptides was expected to improve fibrin ability to induce neovascularization, namely by promoting cell proliferation, migration and capillary-like structures formation, *in vitro*, as well as angiogenesis, *in vivo.*

CHAPTER 2
MATERIALS AND METHODS

1. CELL CULTURE

1.1. Culture of human pulmonary microvascular endothelial cells (HPMEC-ST1.6R cell line)

As a first approach, a cell line of human pulmonary microvascular ECs (HPMEC-ST1.6R), with reported ability to form capillary-like structures within 3-D fibrin gels, including by our group, was used [89] [90].

Cells were routinely expanded at a cell seeding density of 1×10^4 cells/cm^2 on 25-cm^2 or 75-cm^2 regular plastic culture flasks were coated with a pre-warmed 0.2% (w/v) gelatin solution (Sigma-Aldrich) diluted from a 1% (w/v) solution and incubated at 37ºC for a period of, at least, 30 minutes. The cells were cultured in M199 culture medium (Sigma-Aldrich), supplemented with 20% (v/v) FBS (Sigma-Aldrich), 1% (v/v) P/S (Gibco), 2mM Glutamax (Gibco), 50 µg/mL Geneticin (Gibco) and 50 µg/mL ECGS/Sodium heparin (Becton Dickinson/Sigma-Aldrich). Genetinic and ECGS/Sodium heparin were freshly added every time the medium is changed. Finally, the cells were seeded in the coated flasks at a cell seeding density of 25×10^4 cells/mL.

The medium was changed on the first day after thawing to remove DMSO and, from then on, every other day until being passed. For passing, 0.25% Trypsin, 1mM EDTA (Gibco) was used to make the detachment and a centrifugation cycle of 1200 r.p.m, 4ºC for 5 minutes was performed. Whenever needed, cells were frozen using the culture medium with 10% DMSO (Sigma-Aldrich).

1.2. Culture of human brain microvascular endothelial cells (HCMEC/D3 cell line)

Afterwards, a cell line of human brain microvascular endothelial cells (hCMEC/D3), derived from human temporal lobe microvessels isolated from tissue that was excised during surgery for control of epilepsy, was used [91]. Although the culture of hCMEC/D3 within 3-D hydrogels was not previously reported, these cells are described to be able of tubule formation on top of Matrigel [92]. Cells were kindly provided by Professor Bruno Sarmento (i3S, Porto).

Cells were routinely cultured using the same cell seeding density as that referred for HPMEC-ST1.6R cells, on culture flasks previously coated with 0.2 % (w/v) gelatin, in EndoGro-MV culture medium (Merck Millipore), whose components are described in **table 3**.

Table 3: EndoGRO-MV culture medium supplements

Component	Concentration
EndoGRO Basal Medium	
EndoGRO-LS Supplement	0.2 %
rh EGF	5 ng/mL
L-Glutamine	10 mM
Hydrocortisone Hemisuccinate	1 µg/mL
Heparin Sulfate	0.75 U/mL
Ascorbic Acid	50 µg/mL
FBS	5%
FGF	5 ng/mL

The culture medium was supplemented with 1% (v/v) P/S and EGF and FGF freshly added and the medium was refreshed every other day. Cell passaging was identical to that described for HPMEC-ST1.6R cells, although trypsin was diluted in 1mM EDTA (1:5), to be less aggressive to the cells. The freezing method was also the same followed with the HPMEC.

1.3. Culture of outgrowth endothelial cells (OECs)

Outgrowth endothelial cells (OECs) from human umbilical cord blood were provided by Professor Cristina Barrias (i3S, Porto). Human umbilical cord blood was obtained from the UC Davis Umbilical Cord Blood Collection Program (UCBCP) and isolated within 12 hours (h) after cord blood collection, following protocols approved by the UC Davis Stem Cell Research Oversight Committee and as previously described [93].

Cells were cultured in complete EGM-2 MV cell culture medium (Lonza) containing VEGF and supplemented with 1% (v/v) P/S (Gibco). Cells were used in the experiments between passages 5 and 7.

2. MICROCARRIER (MC)-BASED *IN VITRO* ANGIOGENESIS ASSAY

The use of a microcarrier-based angiogenesis assay allows a reliable quantitative analysis of the number of cellular processes protruding from the microcarriers, previously colonized with the desired cell types, into the gel, thus consenting an appropriate evaluation of the effects of the cells themselves or of any functionalization made to the gel on the angiogenic process *in vitro* [94].

In the experiments within the framework of this master thesis, the Cytodex®-3 microcarrier beads (dextran beads coated with denatured porcine-skin collagen, 60-87 μm in diameter when dehydrated, Sigma-Aldrich) were used.

2.1. MC sterilization

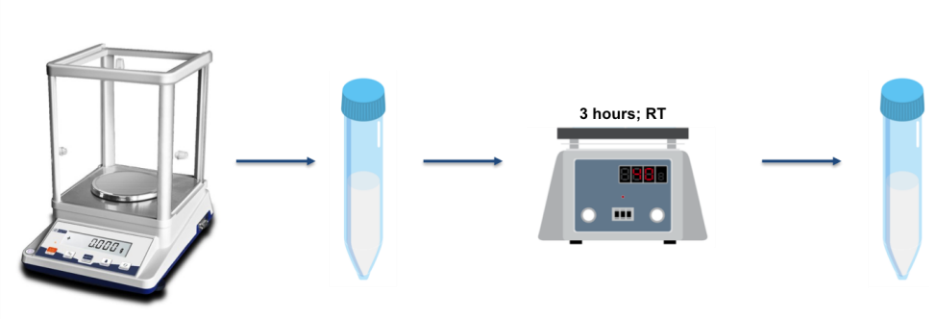

Figure 8: Schematic illustration of the protocol followed to sterilize the microcarriers.

Prior to the colonization of the microcarriers by cells, 8.4 mg of dehydrated microcarriers were dissolved in 5 mL of PBS 1×, in order to obtain a MC stock suspension at 1.68 mg/mL. After three hours of incubation in PBS, at RT under stirring (using a tilting shaker), the supernatant was discarded and the MCs were resuspended in 5 mL of PBS 1×. Lastly, the MCs were sterilized by autoclave according to the recommendations of the supplier (110ºC; 30 minutes), a sterilization method that do not compromise MCs integrity [81].

2.2. MC equilibrium in culture medium

Before placing the microcarriers in contact with the endothelial cells, the MCs were allowed to settle down, the supernatant was discarded and the MCs were resuspended in 1 mL of pre-warmed EC complete culture medium. This procedure was repeated, immediately afterwards, using 0.5 mL of the same medium.

2.3. MCs colonization with endothelial cells

To attain a homogeneous and reproducible colonization of the MCs by the different EC types, the stirring process (Petri dishes placed on a rotary orbital shaker or spinner flasks placed on a magnetic stirrer), the stirring time (1.5 days and 2 days) and the cell seeding density (1.5×10^6 and 3×10^6 cells/mL) were optimized (**Appendix A**). After this optimization step, the following conditions were used for MCs colonization.

A cell suspension containing 1.5×10^6 or 3×10^6 cells/mL for HPMEC/hCMEC/d3 and OECs, respectively, was initially prepared and further centrifuged (1200 r.p.m.; 4ºC; 5 minutes). The cells were subsequently resuspended in the MC suspension and the whole suspension was transferred to a partially closed FACS tube. This was then incubated at 37°C for 4 hours, being the FACS tube inverted every 20 minutes, to assure an homogeneous EC adhesion to the MCs. At the end of this period, the cell/MC suspension was transferred to a new falcon tube and the cell-seeded MCs were rinsed with 2.5 mL of EC complete culture medium. The cell-seeded MCs were finally resuspended in 6 mL of complete culture medium and transferred to three petri dishes placed on a rotary orbital shaker, under slow agitation (60 r.p.m.; **Figure 9**). The cell-seeded MCs were kept at 37ºC in a CO_2 incubator for one day and a half.

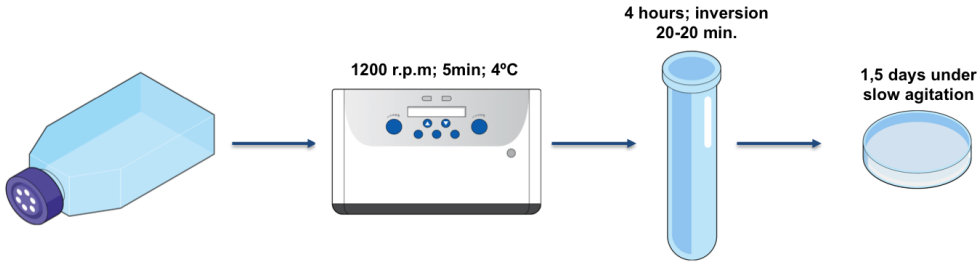

Figure 9: Schematic representation of the steps followed to achieve a homogeneous and reproducible microcarrier colonization by ECs.

2.4. Embedment of MCs colonized with endothelial cells in fibrin hydrogels

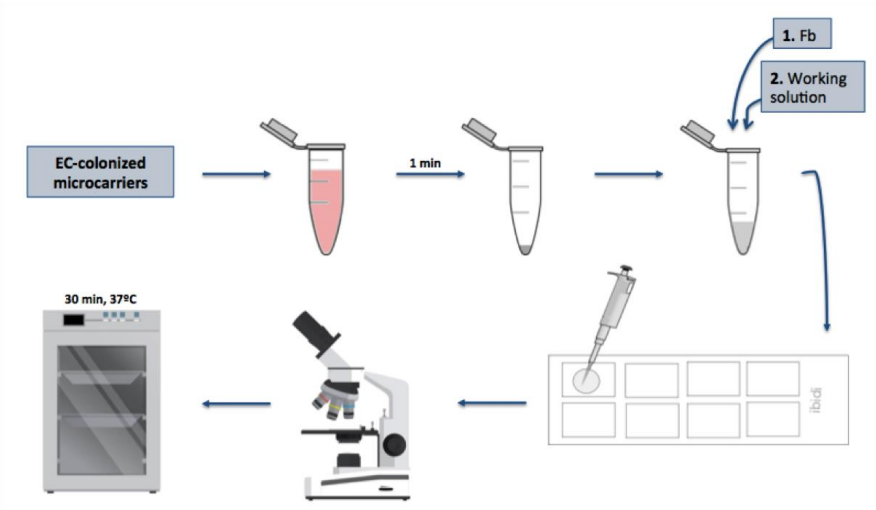

Figure 10: Schematic representation of the protocol followed for the preparation of the fibrin hydrogels.

2.4.1. Preparation of unmodified fibrin hydrogels

Plasminogen-free fibrinogen (Sigma-Aldrich) was obtained from pooled human plasma containing factor XIII, the unactive form of the transglutaminase factor XIIIa. The purification of the fibrinogen was attained through an overnight dialysis process against tris-buffered saline (TBS, 137 mM NaCl; 2.7 mM KCl; 33 mM Trizma base), with the pH adjusted to 7.4. Purified fibrinogen solution was concentrated using 15 mL Vivaspin tubes (Merck Millipore) and its concentration determined spectrophotometrically at 280 and 320 nm, applying an extinction coefficient of 1.51 mL mg^{-1} cm^{-1} [95]. Fibrinogen solution was then sterilized by filtration using a low protein-binding filter and its concentration was adjusted to 12 mg/mL with TBS.

Unmodified fibrin-gels with the following composition in the polymerizing gel were prepared: 6 mg/mL fibrinogen, 2 NIH U/mL bovine thrombin (Sigma-Aldrich), 2.5 mM calcium chloride (Merck) and 10 µg/mL aprotinin (Sigma-Aldrich). The fibrinogen concentration of 6 mg/mL was chosen due to previous works developed in our group, which pointed out such concentration as appropriate for the extension of neuronal and endothelial cell sprouting processes within 3-D fibrin gels [96] [97]. The embedment of the cell-seeded MCs was performed as depicted in **figure 10.** The MCs were initially counted to determine the MC/cell suspension volume required to obtain 50-100 MCs per/fibrin hydrogel. The MC/cell suspension was then transferred to an eppendorf tube containing TBS and the MCs were allowed to settle and, 1 minute later, the supernatant was discarded and the MC/cells resuspended in 25 µL of fibrinogen. Finally, 25 µL of a thrombin working solution constituted by TBS, thrombin, calcium chloride and aprotinin were added to the same eppendorf and, after a quick homogenization, the mixture was transferred to the center of one well of a 8-well ibidi µ-slide chambered coverslip. Polymerizing gels were then incubated at 37ºC for 30 minutes in the CO_2 incubator, to allow cross-linking by factor XIIIa. At the end of this period, 250 µL of complete culture medium containg 5 µg/mL of aprotinin (Sigma-Aldrich), to delay fibrin degradation, were added to the wells. The culture medium was replaced three times during 8 hours and after 48 hours of culture. When referred, VEGF (Prepotech) was added to the medium at a final concentration of 25 ng/mL.

2.4.2. Preparation of functionalized fibrin hydrogels

Bi-domain peptides containing the sequence of interest (T1 or HYD1) at the carboxyl terminus and factor XIIIa substrate from the NH2-terminal sequence of α2-plasmin inhibitor (residues NQEQVSPL) at the amino terminus, were synthesized at GenScript with a C-terminal amide (purity greater than 95%). T1 and HYD1 bi-domain peptides were reconstituted through the addition of sterile ultrapure water to 0.5 mg vials, so that a final concentration of 1 mM was achieved. Peptides were aliquoted (30 and 40 µL aliquots) into sterile low-binding eppendorfs (Sigma-Aldrich) under a nitrogen atmosphere and stored at -80ºC.

Peptides were covalently bound to fibrin using the enzymatic cross-linking action of transglutaminase factor XIIIa [70]. Functionalized hydrogels were prepared as described above. Peptides were added to the thrombin working solution at different concentrations: 20 to 60 uM in the case of T1 and 10 to 20 uM in the case of HYD1. Similarly to unmodified fibrin gels, functionalized gels were allowed to polymerize for 30 minutes at 37ºC, after which complete culture medium supplemented with aprotinin was added. The culture medium was replaced three times during 8 hours, to remove unbound peptide, and after 48 hours of cell culture.

At the end of three days of cell culture, the effect of bi-domain peptides on EC sprouting was assessed.

2.4.3. F-actin/DNA fluorescent staining

After washing the cultures with PBS 1× at RT, cells were fixed with 3.7% paraformaldehyde (Merck Millipore) for 20 minutes, also at RT. Until being immunostained, the cultures were washed and stored in PBS at 4°C.

The first step of the immunostaining was to permeabilize the cells with 0.2% (v/v) Triton X-100 (Sigma-Aldrich) in PBS buffer, under gentle stirring (50 rpm) in an orbital shaker, for 30 minutes. After three washings with PBS 1×, and in order to minimize non-specific adsorption, the samples were incubated for 60 minutes at RT with 1% (w/v) Bovine Serum Albumin (BSA) (Merck Millipore) solution in PBS under gentle stirring. Following, incubation with Alexa Fluor 594-conjugated Phalloidin (Invitrogen) diluted 1:100 in the 1% BSA solution was performed for 60 minutes in the dark and under stirring.

After washings with PBS (3×, 30 minutes each), the samples were incubated with Hoechst 33342 (3 μg/mL in PBS) (Molecular Probes) for 20 minutes at RT under stirring in an orbital shaker.

Lastly, the samples were again washed with PBS 1× and kept in Fluoromount ™ Aqueous Mounting Medium (Sigma-Aldrich) at 4°C in the dark until further analysis in the high throughput fluorescence microscope In Cell Analyzer 2000 imaging system (GE Healthcare).

2.4.4. Integrin functional blocking

To assess the contribution of α6β1 integrin to EC sprouting in functionalized fibrin hydrogels, in parallel, function blocking monoclonal antibodies against α6 and β1 integrin subunits and correspondent isotype controls were added to the culture medium. The antibodies were added 8 hours after fibrin gel polymerization.

To assess the contribution of α6 integrin, the cells were incubated with Rat Anti-human CD49f (clone NKI-GoH3, Abd Serotec) or with the isotype RAT IgG2a negative control (Bio-Rad) at a concentration of 40 μg/mL.

In turn, to assess the contribution of β1 integrin, the cells were incubated with Hamster Anti-Rat CD29 (clone Ha2/5, Pharmingen) and Hamster IgM, λ1 Isotype Control (Pharmingen), both used at the concentration of 10 μg/mL.

3. IMMUNOCYTOCHEMISTRY

3.1. Immunofluorescence staining of α6 integrin subunit

After three days of culture, the plate was removed from the incubator and the cells embedded in the fibrin hydrogel were fixed with 2% paraformaldehyde (Merck Millipore) in culture medium for 30 minutes at RT. After, washings in PBS buffer (3 ×, 5 minutes each), samples were processed for immunostaining. Samples were incubated in the blocking buffer (PBS buffer containing 5% Normal Goat Serum) for 60 minutes at RT, under gentle stirring (around 50 r.p.m.) in an orbital shaker. Subsequently, samples were incubated with the primary antibody (Rat Anti-human CD49f; Abdserotec; 50 μg/mL) diluted in PBS buffer containing 1% NGS (Invitrogen), overnight at 4ºC. After washing with PBS buffer containing 1% NGS (3×, 30 minutes each, under mild agitation) the primary antibody was detected with an Alexa Fluor 594-conjugated goat anti-rat secondary antibody (Invitrogen)– diluted 1:500 in PBS buffer containing 1% NGS. The samples were incubated at 4ºC for 3 hours and then washed in PBS buffer (3×, 30 minutes each, under mild agitation).

Finally, the samples were incubated with DAPI (0.1 µg/mL diluted in PBS; Gibco) for 20 minutes at RT for DNA staining, washed with PBS buffer (3×, 5 minutes each) and mounted in Fluoromount ™ Aqueous Mounting Medium (Sigma-Aldrich).

3.2. Double Immunofluorescence staining of Laminin (LN) and α6 integrin subunit

Samples were fixed as described above. Afterwards, samples were incubated in the blocking buffer (1% BSA and 4% FBS in PBS buffer), for 1 hour at RT under slow agitation in an orbital shaker and then with the primary antibodies – Rat Anti-human CD49f (Abd Serotec; 50 µg/mL) and Rabbit Anti-laminin polyclone antibody (Sigma-Aldrich; 10 µg/mL) diluted in blocking buffer, overnight at 4ºC under slow agitation. After washings in PBS buffer containing 1% BSA and 1% FBS (3 ×, 30 minutes each, under mild agitation), the primary antibodies were detected with donkey 488-conjugated anti-rat and donkey 647-conjugated anti-rabbit secondary antibodies (both Invitrogen) both diluted 1:500 in blocking buffer for 1 hour at RT, under slow agitation. The samples were incubated at 4ºC for 3 hours and then washed using PBS buffer (3 ×, 30 minutes each, under mild agitation).

The samples were finally incubated with DAPI as described above, washed with PBS ad mounted in Fluoromount ™ Aqueous Mounting Medium.

4. CELL METABOLIC ACTIVITY EVALUATION

Cell metabolic activity was quantified to assess cell proliferation of hCMEC/D3 cells seeded in functionalized gels at 2×10^6 cells/mL. For this purpose, a resazurin-based assay was used. Briefly, the cell-fibrin constructs were incubated with 20% (v/v) of resazurin dye (Sigma-Aldrich) for two hours and fifteen minutes. At the end of the incubation period, 100 µL of the supernatant from each well were transferred to a black 96-well plate with clear bottom (Greiner) and the fluorescence readout read at 530 nm excitation and 590 nm emission wavelengths using a spectrophotometer microplate reader (Biotek Synergy MX). Acellular fibrin gels were used as blanks. The cell number was deduced from a polynomial standard curve, in which fluorescence values were plotted against a known number of cells seeded in parallel within unmodified fibrin gels.

5. CELL VIABILITY EVALUATION

5.1. Qualitative analysis

To assess the effect of immobilized peptides on cell viability and cell proliferation, hCMEC/D3 cells were seeded as single cells at different cell seeding densities in fibrin gels (50 µL-drops) formed in the wells of 24-well tissue culture plates. After 30 minutes of gel polymerization at 37ºC, 500 µL of complete EndoGRO-MV culture medium was added to each well, supplemented with 5 µg/mL of aprotinin.

Cell viability in the three dimensional fibrin gels was evaluated through incubation of the gels with Calcein AM and Propidium Iodide (PI) after four days of culture, with a daily routine of change of the culture medium. Calcein AM freely diffuses into the cells, being hydrolyzed by nonspecific esterases into fluorescent products that are taken by the cells with uncompromised plasma membranes. PI is, in turn, used to mark the nonviable cells, entering and staining the cells with damaged membranes.

Quickly, the cells embedded in the fibrin constructs were incubated with 1 µM of Calcein AM (Invitrogen) diluted in pre-warmed PBS, for 20 minutes at 37°C. After removing this solution,

the hydrogels were incubated for more 10 minutes at 37°C, this time with PI (Sigma-Aldrich) diluted in pre-warmed PBS. Lastly, 500 µL of fresh complete EndoGRO-MV culture media (Merck Millipore) were added to each well and the samples were observed under Confocal Laser Scanning Microscopy (CLSM) (Leica Microsystems TCS SP5) as soon as possible (Calcein AM excitation/emission: 488/530 nm; PI excitation/emission: 535/617 nm).

5.2. Quantitative analysis by Flow Cytometry

Quantitative analysis of cell viability was performed by flow cytometry, in four-pooled Fb drops, after cell isolation from the cell-Fb constructs. Briefly, the constructs were washed twice with PBS, and sequentially incubated with 1.25 mg/mL of collagenase type II (Gibco; 1 h at 37°C) and 1× trypsin-EDTA (Gibco; 30 min at 37°C) under stirring (70 rpm). After trypsin inactivation with serum-containing media cells were gently dissociated, centrifuged, and suspended in cell culture medium. The single cell suspensions were then incubated with 67 nM calcein AM (20 min at 37°C) or with 6 µM PI (10 min at 37°C) to label live and dead cells, respectively. Cells were finally washed trice with FACS buffer [2% (v/v) fetal bovine serum (FBS) in PBS], and immediately run on a flow cytometer (FACS CaliburTM, BDBiosciences). Cell debris were excluded by gating on forward and side scatter and fluorescence gates set, using unlabeled cells as negative control.

6. EVALUATION OF THE VISCOELASTIC PROPERTIES OF THE FIBRIN GELS

The effect of fibrin functionalization on fibrin viscoelastic properties was assessed by rheometry using a Kinexus Pro Rheometer (Malvern) and the Rspace for Kinexus software.
The samples consisted in acellular fibrin gels of 50 µL (25 µL of fibrinogen and 25 µL of the respective thrombin working solution). After calibrating the equipment, a gap of 1 mm was defined and the mixed solution was directly and fastly dropped in the chosen plate, in order to avoid both the polymerization of the gel in the pipette's tip and the formation of air bubbles. Afterwards, the upper geometry fell down to the defined gap and the gel was left polymerizing for one hour.

After one hour, the gel was ready to undergo the desired tests. For each condition, the linear viscoelastic region (LVR) was first determined performing strain amplitude sweeps (shear strain: 0.1 to 100%; frequency: 0.1Hz). Frequency sweeps (frequency: 0.01 to 10 Hz; shear strain: 5%) were then performed within the LVR.

Six gels were analyzed per condition and the values of the shear elastic (G'), shear viscous (G'') and complex (G*) modulus were recorded.

7. PROCESS OUTGROWTH AND OCCUPIED AREA QUANTIFICATION

Endothelial cells outgrowth was determined in z-stacks of fluorescent images of samples stained for F-actin and DNA acquired in the IN Cell Analyzer 2000. The IN Cell Analyzer 2000 imaging system (GE Healthcare) is an automated high-throughput microscope that was designed with the purpose of providing the users with the performance and throughput that are desirable both for high content analysis and screening.

Since the goal was to analyze and quantify the sprouting of the cells into the 3-D fibrin gel, images of the lower part of the gels (near the bottom of the well) were not acquired. For

each condition tested, 21 z-stacks, separated by 10 µm and of around 100 fields, were acquired using a magnification of 20×0.75 Pan Apo.

Afterwards, a massive image analysis was done in order to quantify both the maximal extension of the sproutings and the sprouting area, considering every independent bead on each gel. In this regard, Fiji software was a crucial tool, specifically its Freehand Line and Oval Selection functions, used to draw the contours required to calculate the area of the beads and the total area (with the sproutings). Subsequently, the area of each bead was subtracted in order to get the value of the sprouting area alone.

Furthermore, the View 5D plugin, also from Fiji software, was used to quantify the maximal sprouting length protruding from each microcarrier. This plugin allows a 3-D visualization of the z-stack images acquired and allows the determination of the coordinates of each cell. After, selecting the coordinates of a cell on the surface of the bead and the ones of the most distant cell, a conversion was made on Excel in order to get the value of the distance between those two cells.

In order to correctly evaluate the sprouting area and the maximal sprouting length some sensitivity was required. Since a z-step of 10 µm was used, some connections between cells were deleted from the images. Thus, the analysis had to be made considering the orientation of the nuclei. Whenever a nucleus presented a radial orientation in relation to the microcarrier, it was considered in the sprouting. Further, the orientation in relation to the preceding cells had also to be considered in the situations where the sprout was not completely straight. An endothelial sprout was considered as any cell extension leaving the microcarrier in direction to the fibrin matrix, as defined by Grasseli et al [98].

The Fiji tools were used as shown in **figure 11.** As additional parameters, the percentage of beads with sprouts and the number of sprouts per bead were also quantified.

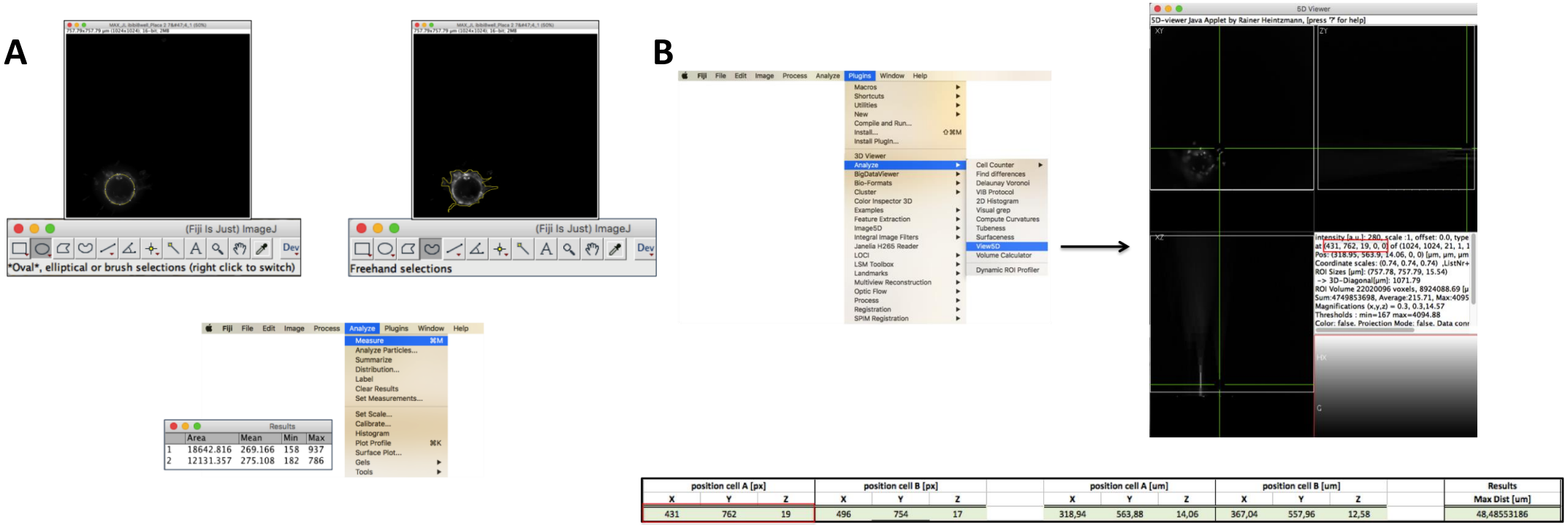

position cell A [px]			position cell B [px]			position cell A [um]			position cell B [um]			Results
X	Y	Z	X	Y	Z	X	Y	Z	X	Y	Z	Max Dist [um]
431	762	19	496	754	17	318,94	563,88	14,06	367,04	557,96	12,58	48,48553186

Figure 11 (A-B): Quantification of the sprouting area (A) and maximal sprouting length (B) using Fiji software

8. *IN VIVO* CHICK CHORIOALLANTOIC MEMBRANE (CAM) ASSAY

In order to validate, *in vivo*, the most promising results obtained through the *in vitro* studies, the chorioallantoic membrane (CAM) assay was performed. CAM is a highly vascularized and specialized tissue of the avian embryo, being vastly used for angiogenic studies. At incubation day 0, fertilized chicken eggs were washed with 70% ethanol and then incubated at 37°C. After three days, 3 mL of albumen were extracted, allowing the developing CAM to grow detached from the top of the egg's shell. A window of about 1.5 cm^2 was opened on the top of the egg, without harming the embryo. To prevent dehydration and infections, the window was closed with transparent adhesive tape, which was removed seven days later to proceed with the placement of the testing hydrogels on the top of the membrane. The hydrogels were made before the removal of the adhesive tape and were left polymerizing for 30 minutes. After the 30 minutes of incubation, unmodified and functionalized fibrin gels were washed trice with EndoGRO-MV basal medium as described above, to eliminate unbound peptide. Incubation day 10 was the time point chosen for the inoculation because, at this time, CAM mitotic rate has stabilized. At incubation day 13, CAM inoculation site was excised, some macroscopic images were acquired and the tissues were prepared for histological processing. Between the 10^{th} and 13^{th} days, the hydrogels were hydrated twice a day with 150 µL of PBS 1×.

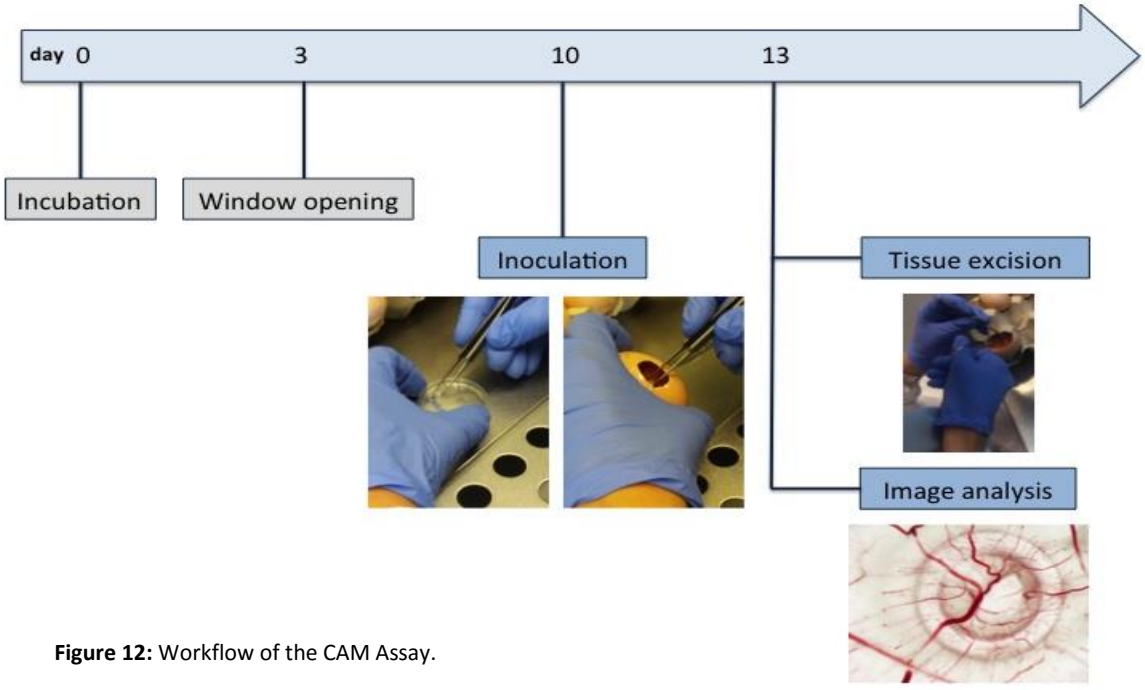

Figure 12: Workflow of the CAM Assay.

9. STATISTICAL ANALYSIS

Statistically significant differences were assessed using the IBM® SPSS® Statistics Software (version 24) was used. Unmodified and functionalized fibrin hydrogels were compared using independent-samples t-test, which automatically performs a Levene's test to assess the equality of variances between the considered groups. Specifically for analysis of CAM results, the paired-samples t-test was used. Results were considered statistically significant whenever p-value was lower than 0,05. The graphs presented along this master thesis were made using GraphPad Prism 7.

CHAPTER 3
RESULTS AND DISCUSSION

1. EFFECT OF IMMOBILIZED α6β1 LIGANDS ON HPMEC BEHAVIOR IN 3-D FIBRIN GELS

1.1. HPMEC-ST1.6R sprouting in functionalized fibrin gels

The pulmonary microvascular endothelial cells are isolated from adult human pulmonary arteries, in which they form a semiselective barrier crucial for gas exchanges and fluidic regulations between the blood flow and the interstitial spaces in the lung [89].

Krump-Konvalinkova and his co-workers generated the microvascular endothelial cell line that was used in this work – HPMEC-ST1.6R - isolating the cells from adult donors and willing to develop a cell line capable of overcoming some of the limitations of the primary cultures, while demonstrating all of the fundamental characteristics of the microvascular endothelial cells [89].

This said, and considering its ability to form sprouts within biological extracellular matrices, including in fibrin, this cell line was used for the preliminary assessment of the angiogenic properties of the functionalized fibrin hydrogels.

Fibrin hydrogels functionalized with the two different peptides (T1 and HYD1) at two different input concentrations each (20 μM and 40 μM for T1 and 10 μM and 20 μM for HYD1), were assessed for their ability to promote EC sprouting. HPMEC sprouting in functionalized fibrin gels was evaluated using the microcarrier-based assay after three days of cell culture, namely in terms of number of sprouts per bead, sprouting area and maximal sprouting length. Results are presented in **Figures 13 and 14.**

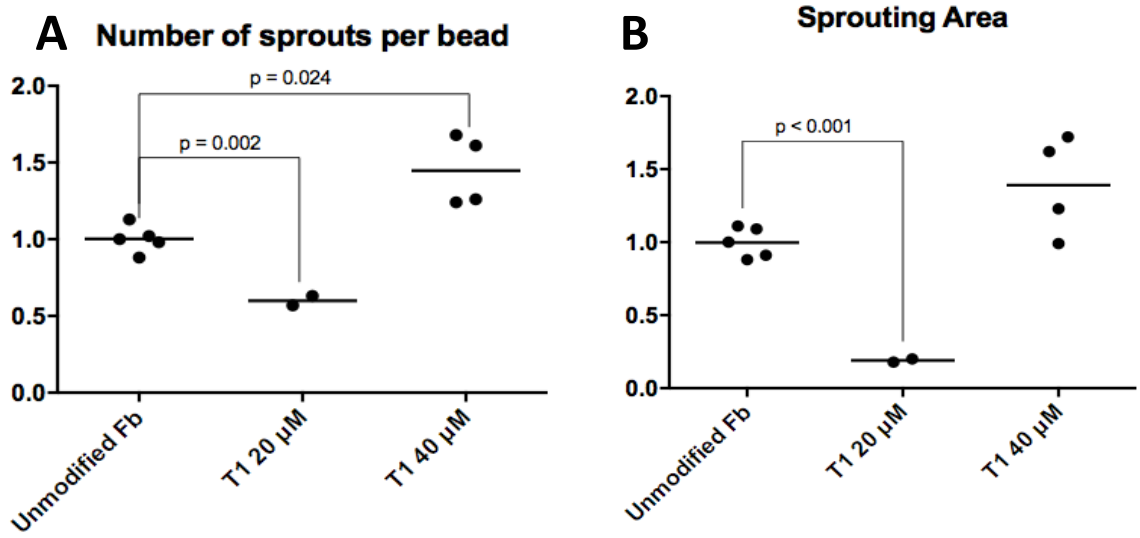

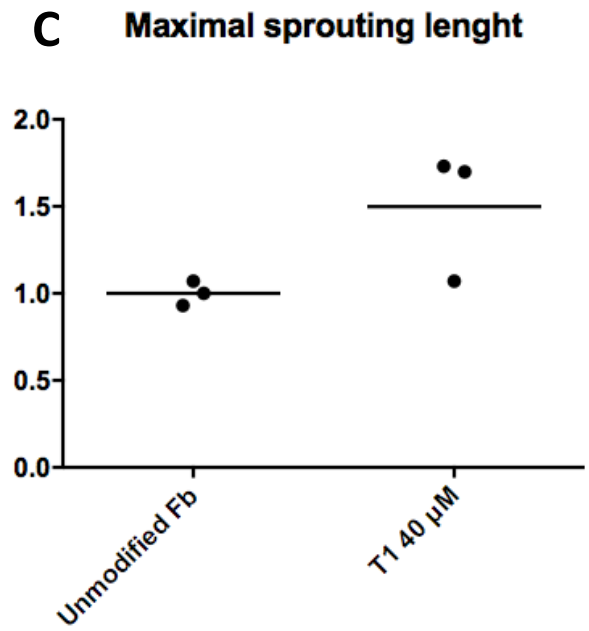

Figure 13 (A-C): EC sprouting of HPMECs into T1-functionalized fibrin hydrogels after 3 days of culture in terms of (A) number of sprouts per bead, (B) sprouting area and (C) maximal sprouting length. The microcarriers embedded in each fibrin gel drop were analyzed and mean values were determined. EC sprouting was normalized to sprouting in unmodified Fb. The percentage of beads with EC sprouts was also determined (Appendix B). Graphs denote results from replicate cultures from two (T1 20 µM) to three independent experiments.

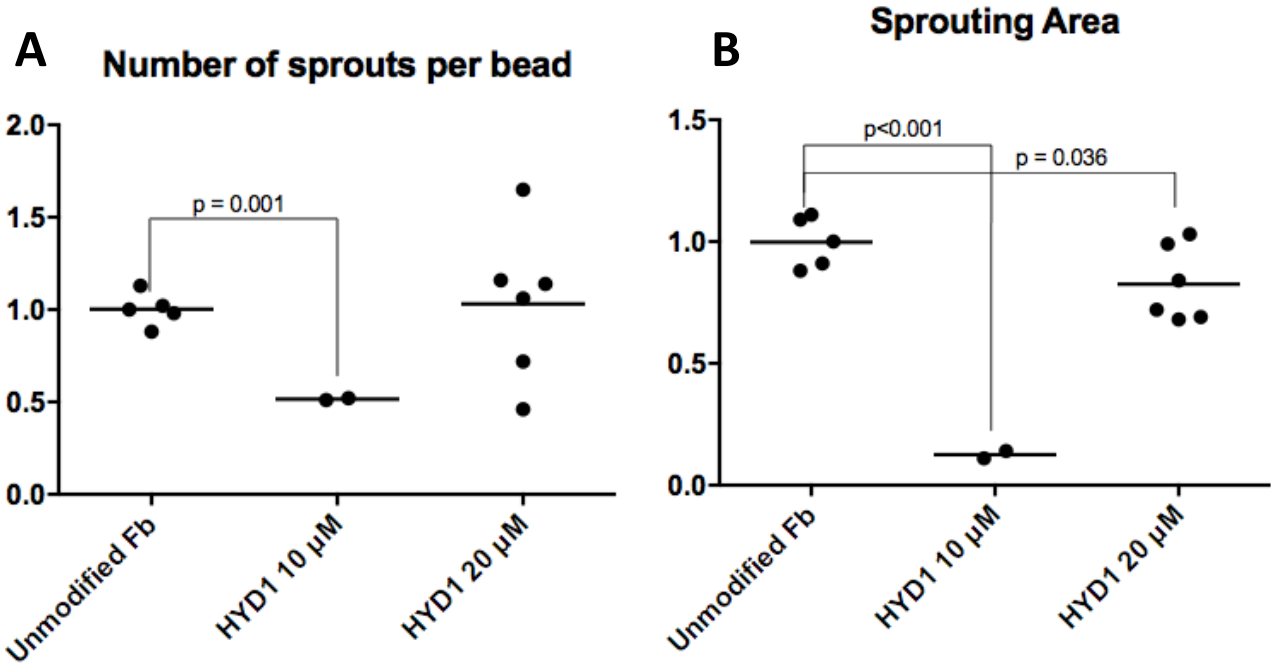

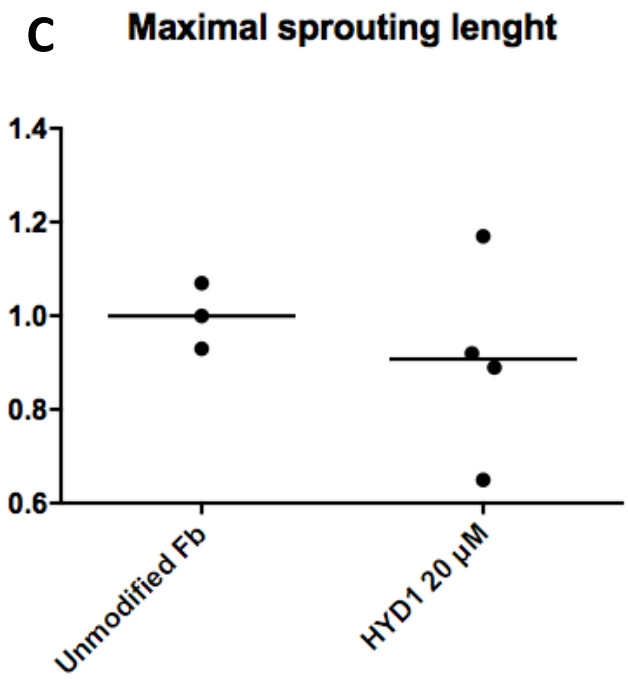

Figure 14 (A-C): EC sprouting of HPMECs in HYD1-functionalized fibrin hydrogels after 3 days of culture, in terms of (A) number of sprouts per bead, (B) sprouting area and (C) maximal sprouting length. The microcarriers embedded in each fibrin gel drop were analyzed and mean values were determined. EC sprouting was normalized to sprouting in unmodified Fb. The percentage of beads with EC sprouts was also determined (Appendix B). Graphs denote results from replicate cultures from two (10 µM) to three independent experiments.

Fibrin functionalization with the T1 bi-domain peptide elicited in average a 1.4-fold increase in all EC sprouting parameters considered, when added at 40 µM in the polymerizing gel, though significant differences were only found in the number of sprouts per microcarrier.

Considering the functionalization with 20 µM of T1 bi-domain peptide, the resulting scenario was fairly different, since a significant inhibition was perceived both in the number of sprouts per bead and sprouting area.

The tethering of HYD1 failed to induce EC sprouting, independently of the EC sprouting parameter considered (**figure 14**). Indeed, the functionalization of fibrin hydrogels with both HYD1 concentrations resulted in a reduction of sprouting area, number of sprouts per bead and maximal sprouting length and some statistically significant differences were found concerning the number of sprouts per bead and the sprouting area.

In **figure 17** some representative images are shown for each of the tested conditions.

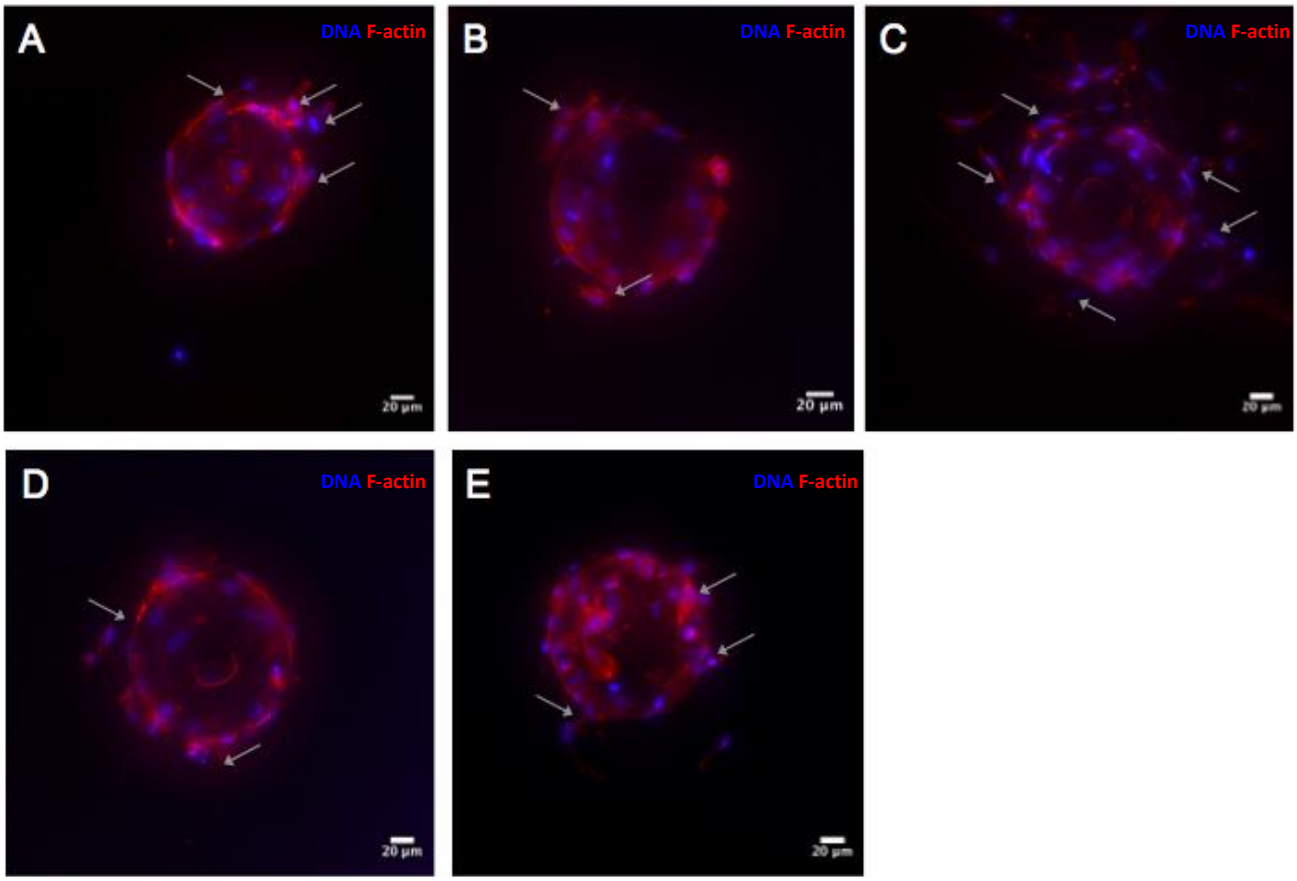

Figure 15 (A-E): IN Cell Analyzer representative images of HPMEC sprouting formation observed for (A) unmodified, (B) T1 20 µM-functionalized, (C) T1 40 µM-functionalized, (D) HYD1 10 µM-functionalized and (E) HYD1 20 µM-functionalized fibrin hydrogels. The samples were processed for F-actin and DNA staining. Grey arrows indicate EC sproutings.

Of note, **Figure 15-C**, is highly representative of what was previously referred regarding the loss of information between z-steps. For such reason, even though 3-D Fiji plugins were used along the image analysis, some sprouting structures were probably underestimated due to situations where the cells appear to be unconnected and their nuclei orientation do not provide any undeniable opposing information.

In addition to the studies already presented, the impact of the addition of VEGF to the culture medium was also evaluated with the goal of understanding if the pro-angiogenic capability of the functionalized hydrogels would be enhanced. It was expected that the addition of this growth factor would increase the observed values for any of the parameters being evaluated and that the trends noticed in the experiments without VEGF would be intensified and not reduced [41]. However, the results indicate the exact same tendencies previously observed, with an inhibition being caused by the functionalization of the hydrogels with the lower concentration of T1 and both concentrations of HYD1 and a slight increase being noticed with the higher T1 concentration, indicating that VEGF was not leading to an effect.

Even though the results are shown in **Figures 43 and 44 (Appendix C),** these findings cannot be considered since we found out later hat the bioactivity of the VEGF was compromised, possibly due to changes in the freezer's temperature when INEB moved to i3S' facilities.

2. EFFECT OF IMMOBILIZED α6β1 LIGANDS ON HCMEC/D3 BEHAVIOR IN 3-D FIBRIN GELS

The human brain microvascular endothelial cell line was derived from human temporal lobe microvessels isolated from tissue that was excised during surgery for control of epilepsy. In their first passage, cells were successively immortalized using the same resources used for the immortalization of the previously referred pulmonary cell line. After the immortalization, limited dilution cloning technique was used to selectively isolate the cells and the clones were very well characterized for brain endothelial phenotype [91].

2.1. hCMEC/D3 sprouting in functionalized fibrin gels

Similarly to the studies performed with the HPMEC-ST1.6R cell line, the formation of capillary-like structures by hCMEC/D3 cells was evaluated using the microcarrier-based angiogenesis assay. Results are shown in **figure 16.**

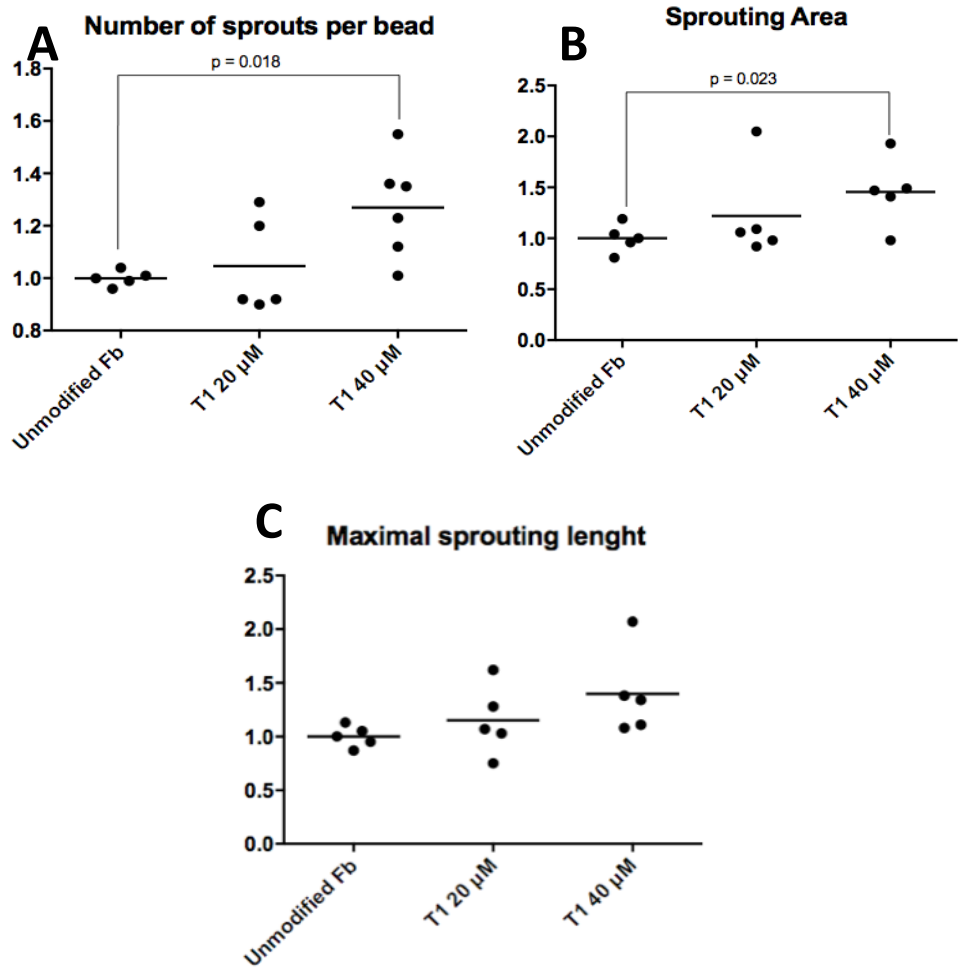

Figure 16 (A-C): EC sprouting of hCMEC/D3 in T1-functionalized fibrin hydrogels after 3 days of culture., in terms of (A) number of sprouts per bead, (B) sprouting area and (C) maximal sprouting length. The microcarriers embedded in each fibrin gel drop were analyzed and mean values were determined. EC sprouting was normalized to sprouting in unmodified Fb. The percentage of beads with EC sprouts was also determined (Appendix B). Graphs denote results from replicate cultures from two to three independent experiments.

At the point when the experiments with hCMEC/D3 were still being performed and analyzed, a High Throughput Confocal Microscope (HCS Confocal CX7, Thermo Fisher Scientific) was in demonstration at i3S. Having the opportunity to try it, we decided to take two samples and get representative images of those conditions: unmodified and T1 40 μM-functionalized fibrin hydrogels, since the most marked effects were being observed for T1-functionalized gels. Images are shown in **figure 17**.

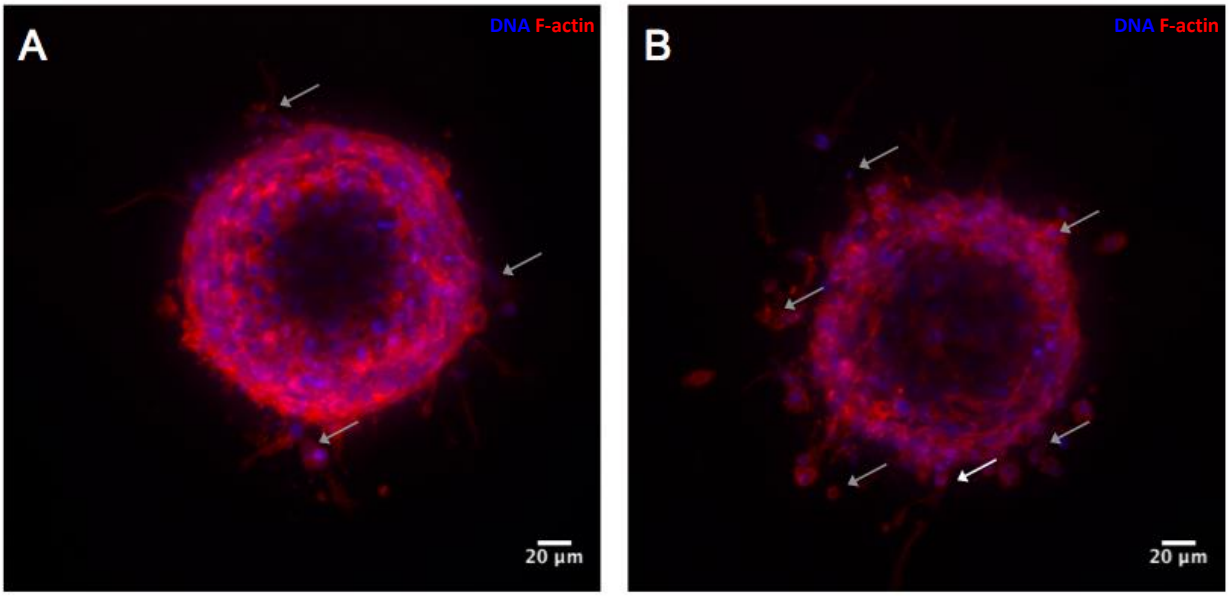

Figure 17 (A-B): HCS Confocal CX7 representative images of the hCMEC/D3 sprouting formation observed for unmodified (A) and T1 40 μM-modified (B) fibrin hydrogels. The samples were processed for DNA and F-actin staining, respectively shown in blue and red. Grey arrows indicate EC sproutings.

Even though the differences between (A) unmodified and (B) T1 40 μM fibrin hydrogels were not quantified using these images, differences between the two conditions were obvious. In line with the results obtained for the total of analyzed hydrogels (**figure 16**), the functionalization of the fibrin hydrogel with a 40-μM concentration of T1 bi-domain peptide resulted on a considerable increase of the angiogenic response in comparison to the control hydrogel.

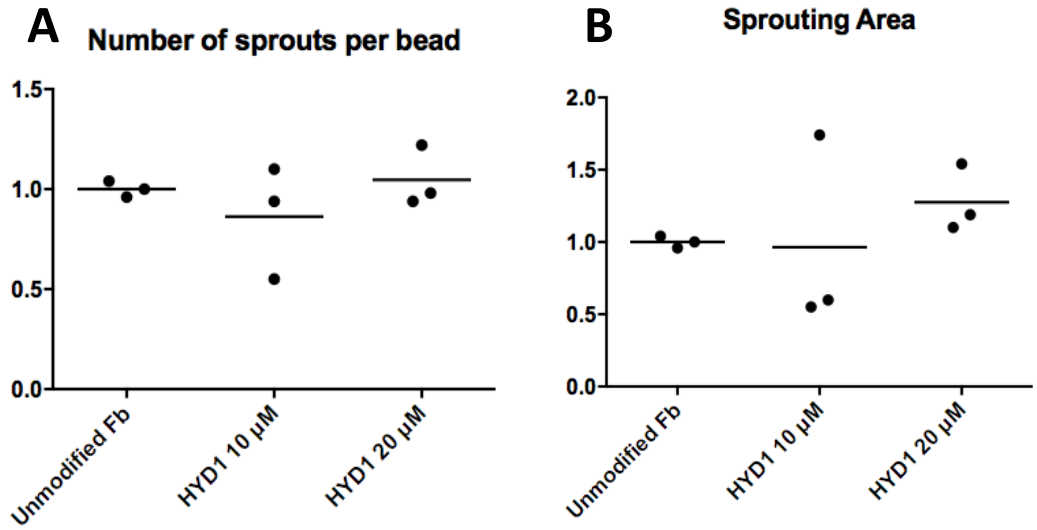

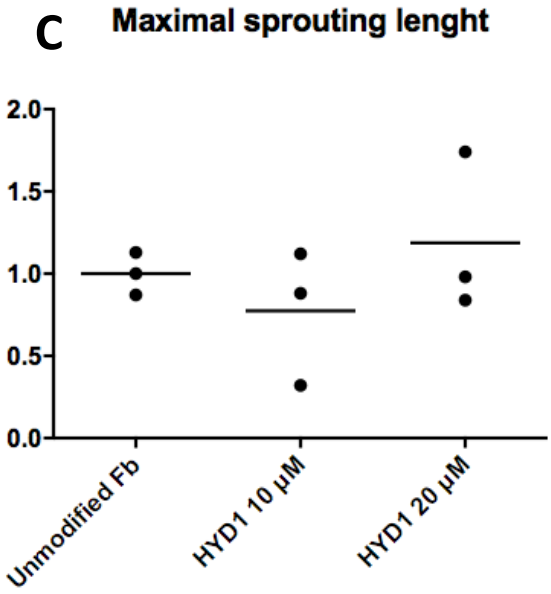

Figure 18 (A-C): EC sprouting of hCMEC/D3 in HYD1-functionalized fibrin hydrogels after 3 days of culture, in terms of (A) number of sprouts per bead, (B) sprouting area and (C) maximal sprouting length. The microcarriers embedded in each fibrin gel drop were analyzed and mean values were determined. EC sprouting was normalized to sprouting in unmodified Fb. The percentage of beads with EC sprouts was also determined (Appendix B). Graphs denote results from replicate cultures from two to three independent experiments

An increasing trend on every EC sprouting parameter was observed for hydrogels functionalized with T1 peptide, this tendency being more striking for the highest concentration tested **(figure 16).** The hydrogels functionalized with 40 µM of T1 peptide led in average to a 1.4-fold increase in every considered parameter, when compared to unmodified fibrin. Statistically significant differences were found for the number of sprouts per bead and the sprouting area. Regarding the lower concentration of T1 peptide tested (20 µM), a slight yet not significant increase was also noticed. In turn, the tethering of fibrin with both tested concentrations of HYD1 peptide failed to promote EC sprouting, as shown in **figure 18**.

2.2. hCMEC/D3 sprouting in T1-functionalized fibrin gels in the presence of VEGF

Tae-Hee Lee *et al* evaluated the effect of the addition of VEGF on integrin expression and activation in human brain microvascular endothelial cells (HBMEC). Their results indicated a direct role of α6 integrin in mediating the angiogenic processes of HBMEC and suggested that α6 integrin expression and activity was induced by VEGF, a positive angiogenic regulator. Additionally, when stimulating the cells with VEGF, HBMEC showed an increased adhesion onto laminin-coated plates, being such effect eliminated after treatment with α6 integrin antibody, showing that α6 integrin is, in these cells, activated by VEGF [41].

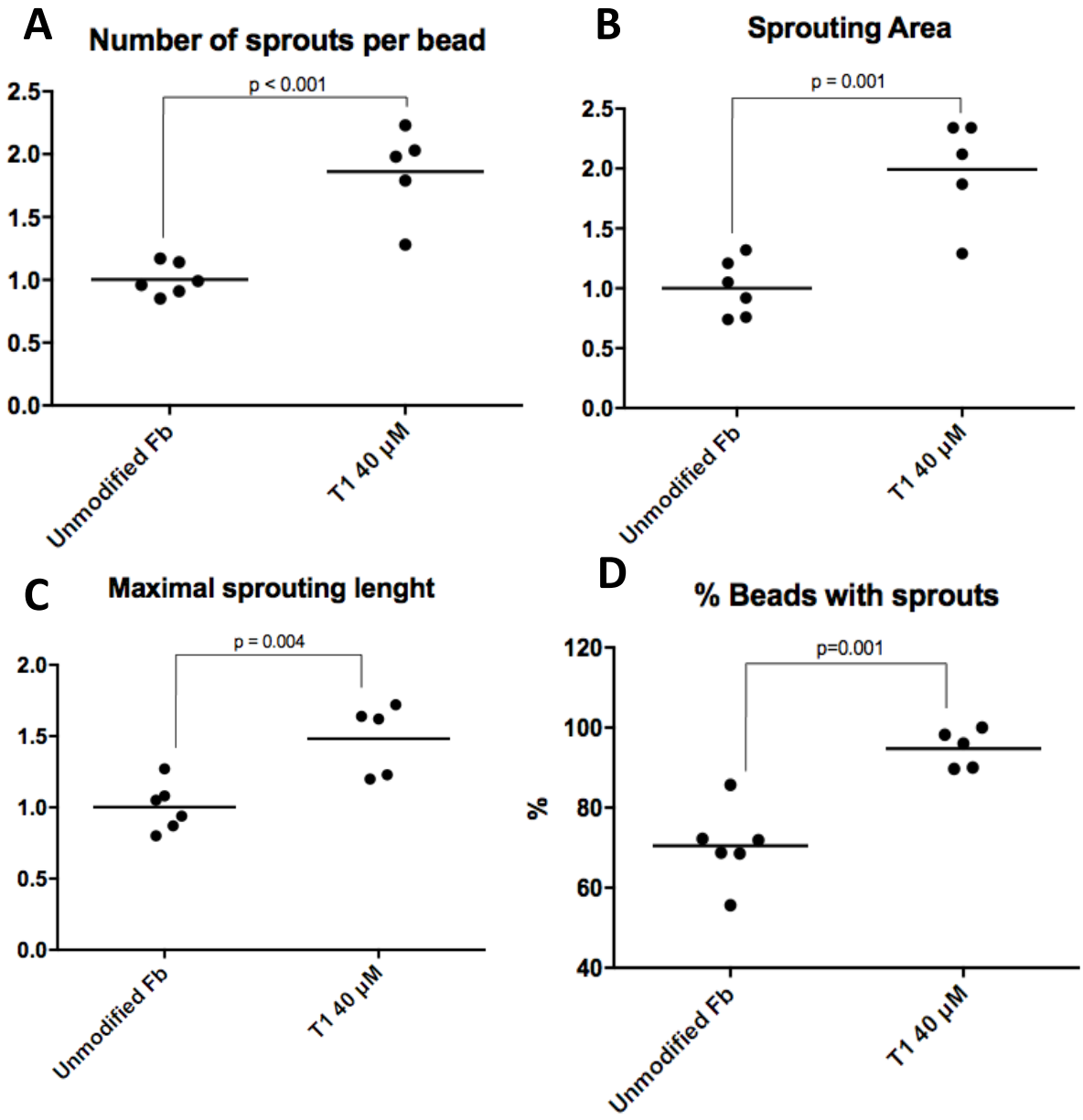

Figure 19 (A-D): EC sprouting of hCMEC/D3 in T1-functionalized fibrin hydrogels after 3 days of culture in the presence of 25 ng/mL of VEGF. (A) Number of sprouts per bead, (B) Sprouting area and (C) Maximal sprouting length. The microcarriers embedded in each fibrin gel drop were analyzed and mean values were determined. The percentage of beads with EC sprouts was also determined (D). EC sprouting was normalized to sprouting in unmodified Fb. Graphs denote results from replicate cultures from two independent experiments.

In the presence of VEGF, hCMEC/D3 cells were therefore expected to express higher levels of α6β1 integrin and lead to a higher cell response to immobilized T1 bi-domain peptide, namely in terms of EC sprouting. In fact, as shown in **Figure 19**, in the presence of VEGF the differences between T1-functionalized fibrin and unmodified gels were more notorious. Statistically significant differences were achieved in all the considered sprouting parameters, with T1-functionalized gels leading to a 1.9-fold increase of the number of sprouts per bead, a 2-fold increase of the sprouting area and a 1.5-fold increase of the maximal sprouting length. Additionally, an increase of about 25% was noticed for the quantification of the percentage of beads with sprouts.

In **figure 20** representative images of the angiogenic response obtained for unmodified and T1 40 μM-modified fibrin hydrogels, after three days of culture in the presence of VEGF, are shown.

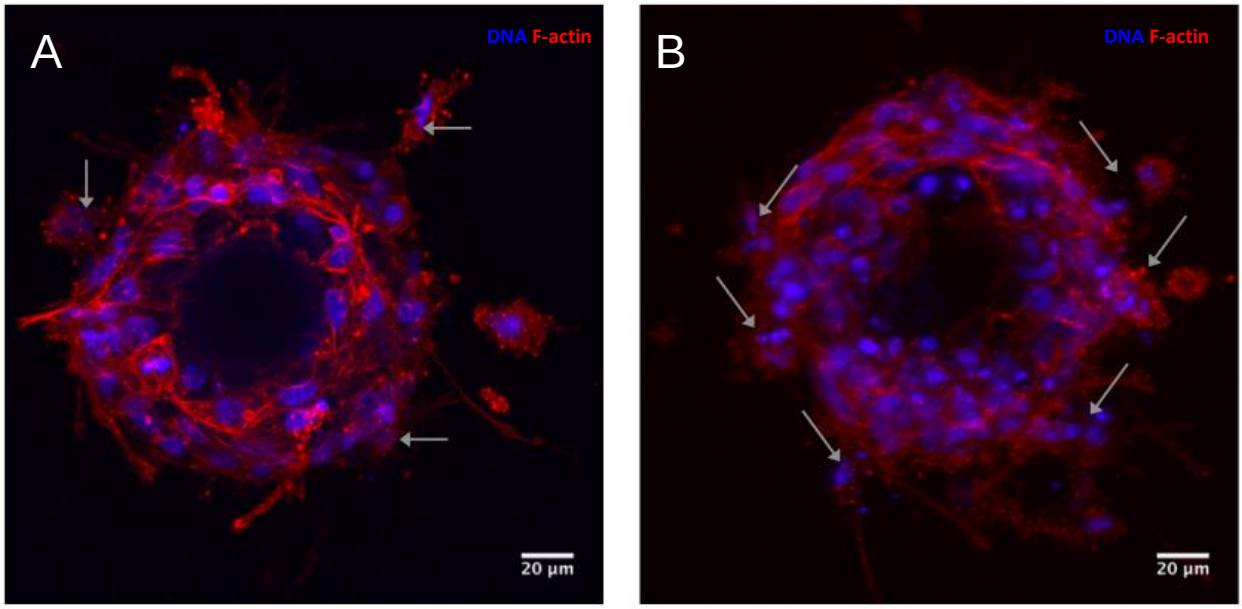

Figure 20 (A-B): Confocal representative images of hCMEC/D3 sprouting in unmodified (A) and T1 40 μM-modified (B) fibrin hydrogels in the presence of 25 ng/mL of VEGF. The samples were processed for F-actin and DNA staining, shown in red and blue, respectively. Grey arrows indicate endothelial cell sproutings.

2.3. Immunocytochemical analysis of α6 integrin expression and Laminin deposition in T1-functionalized fibrin gels

The expression of α6 integrin and laminin deposition by hCMEC/D3 embedded in T1-functionalized fibrin gels was investigated by immunofluorescence staining after 3 days of culture.

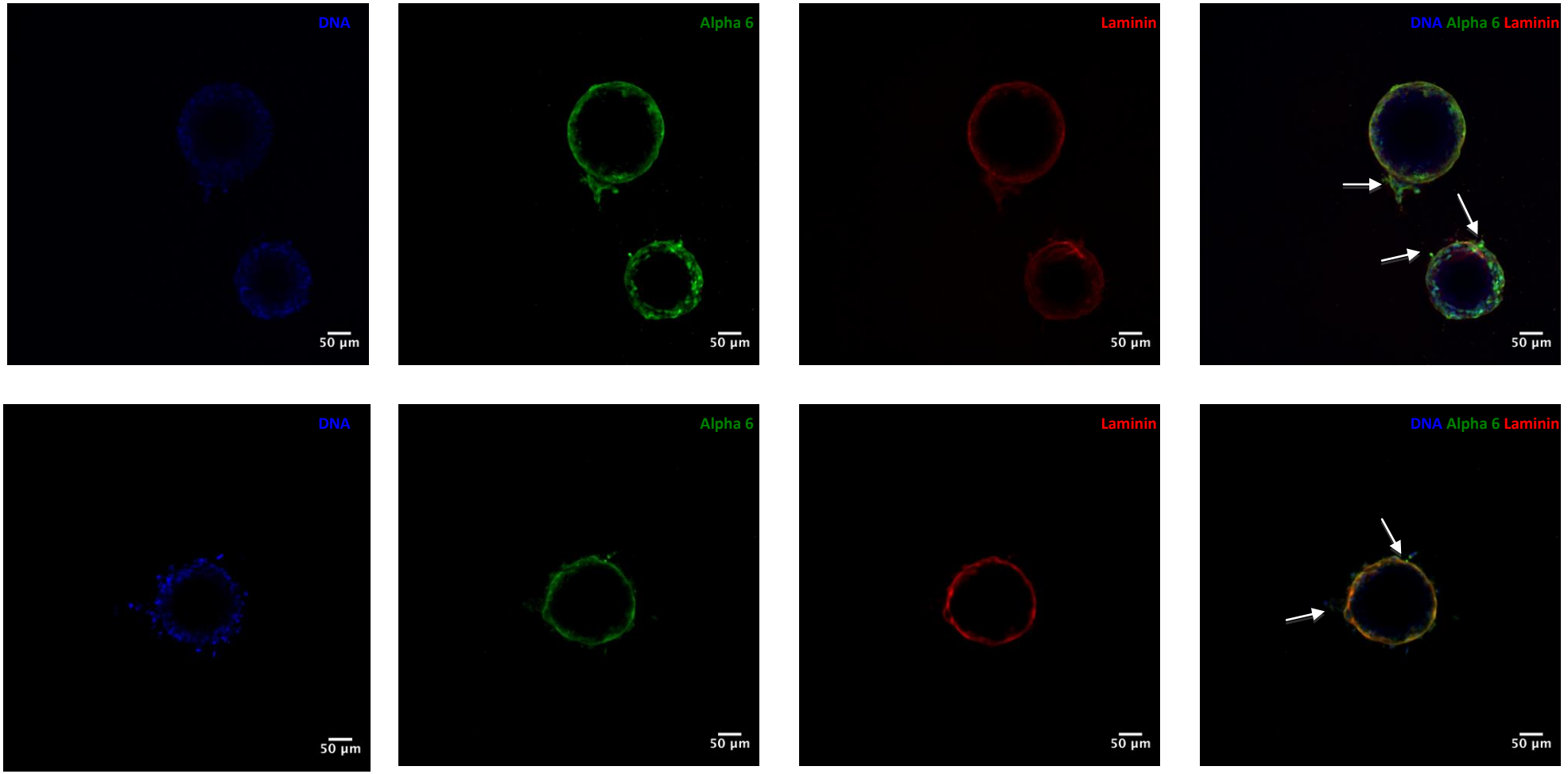

Figure 21: Double immunofluorescence staining of α6 integrin and Laminin in unmodified (upper line) and T1-functionalized (lower line) fibrin hydrogels. Cell/fibrin constructs were cultured for 3 days and subsequently processed for immunofluorescence labeling of α6 integrin subunit (in green) and Laminin (in red). Representative 2-D projections of CLSM z-stack images of cell/fibrin constructs covering a depth of approximately 60 µm are shown. White arrows indicate cellular sproutings. Scale Bar: 50 µm

The α6 integrin subunit is known to mediate a set of biological activities. Stepp and respective co-workers showed that this integrin is involved in the maintenance of the integrity of stratified tissues through mechanical connections between laminin and the filamentous cytoskeleton of the cells [99]. Moreover, studies by Tae-Hee Lee with HBMEC indicated a straight role of α6 integrin in the angiogenic process of those cells [41]. Since it is known that the integrity of tissues is maintained by mechanical connections between the cytoskeleton of cells and laminin, a large non-collageneous glycoprotein from basement membranes [100], double immunostaining of α6 integrin and laminin was performed with hCMEC/D3 in order to evaluate their expression, localization and distribution. Representative 2-D projections of CLSM z-stack images of cell/fibrin constructs are shown in **figure 21**. In fact, the expression of α6 integrin by hCMEC/D3 was observed, along with the deposition of laminin.

Besides the double staining, a single immunofluorescence staining of α6 integrin was also made with the same cells. Representative 2-D projections of CLSM z-stack images of cell/fibrin constructs are presented in **Figure 45 (Appendix D).**

No differences were found between cells embedded in unmodified and T1-functionalized hydrogels.

2.4. Effect of immobilized T1 on EC sprouting within fibrin mediated by α6β1 integrin

After confirming the expression of α6 integrin subunit by hCMEC/D3, similarly to what was previously observed with HBMECs [41], we assessed if EC sprouting within T1-functionalized fibrin hydrogels (40 μM in the polymerizing gel) was mediated through integrin α6β1. For this purpose, functional blocking monoclonal antibodies against α6 (Rat Anti-human CD49f) or β1 integrin subunits (Hamster Anti-rat CD29) were used. Results are shown in **figure 22**.

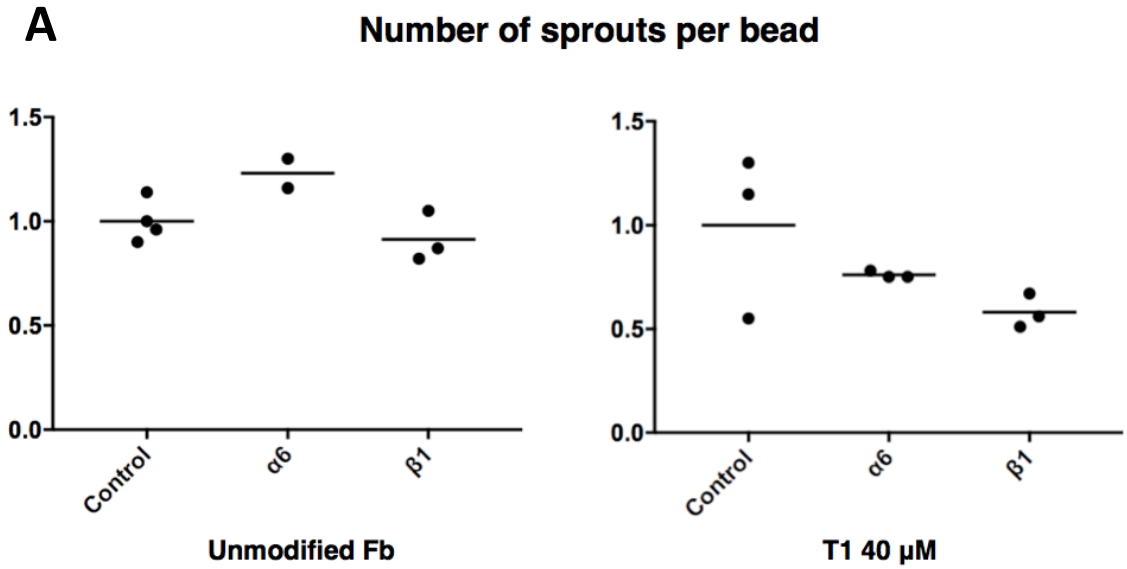

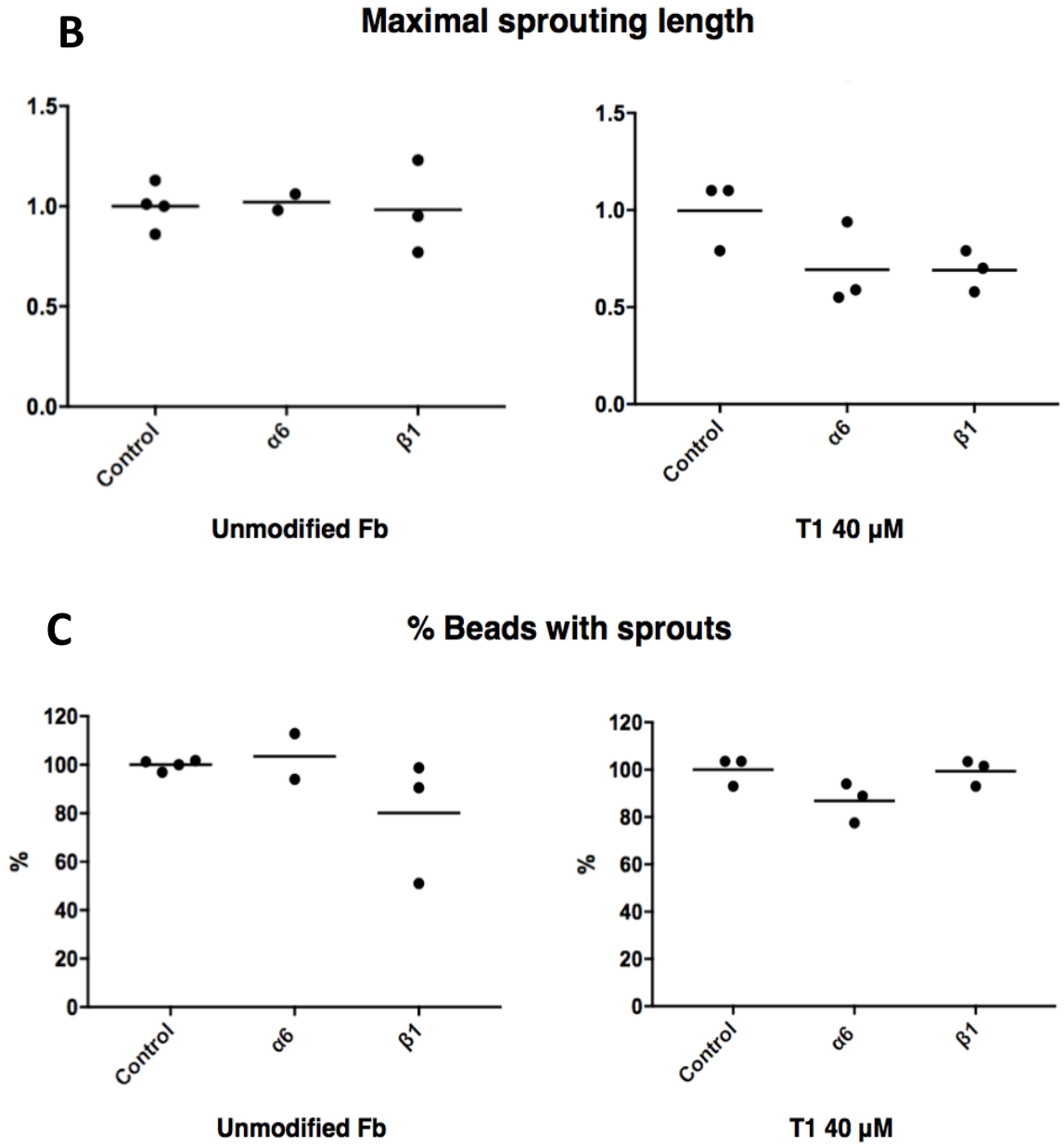

Figure 22 (A-C): Functional blocking assay: EC sprouting of hCMEC/D3 in T1-functionalized fibrin hydrogels (40 µM in the polymerizing gel), after 3 days of culture in the absence (control) or presence of functional blocking monoclonal antibodies against α6 or β1 integrin subunits. Cells were cultured in the presence of 25 ng/mL of VEGF and EC sprouting was determined using the microcarrier-based in vitro angiogenic assay. (A) represents the results of the quantification of the number of sprouts per bead and (B) the results of maximal sprouting length. EC sprouting was normalized to sprouting in unmodified Fb. 10 to 15 microcarriers embedded in each fibrin gel drop were analyzed and mean values determined. The percentage of beads with EC sprouts was also determined (C). Graphs denote results from replicate cultures from one independent experiment.

The results presented in **figure 22** were obtained from only one independent experiment and the number of quantified microcarriers was reduced (10 to 15 beads from each fibrin gel). Nevertheless, the blocking of α6 integrin subunit resulted in EC sprouting inhibition in terms of number of sprouts per bead and maximal sprouting length, even though significant differences were not attained. In line with these results, blocking of β1 integrin subunit elicited a similar effect. As expected, blocking of α6 integrin subunit did not impact EC sprouting in unmodified fibrin gels, as expected from the absence in native fibrin of binding sites for integrin α6β1 [66].

The tendency observed corroborate the results obtained by Tae-Hee Lee on his study regarding the regulation of α6 integrin by VEGF [41] and are a strong endorsement of the role of α6 and β1 integrins on the angiogenic processes of hCMEC/D3. Besides, Shr-Jeng Leu and co-workers also tested the inhibition of α6β1-dependent cell adhesion and CCN1-induced endothelial tubule formation through the addition of soluble T1 peptide, confirming that soluble T1 peptide blocks the interaction between CCN1 and α6β1 integrin, therefore inhibiting the formation of tubule structures [73].

Despite its important and undeniable role, the interaction between α6β1 integrin with T1 peptide is not the only responsible for the promotion of the adhesion of endothelial cells and the formation of tubule structures. Heparan sulfate proteoglycans are also required to act as co-receptors, interacting with heparin binding motifs [101].

It is known from the literature that fibrin presents numerous binding sites for cells, ECM proteins and growth factors, contributing to its considerable ability in modulating important cellular processes. Moreover, it is also known that cells can interact with fibrin through cell-surface receptors binding to heparin-binding domains on fibrinogen molecules [66]. Even though no statistically significant differences were found, the observed tendencies in the functional blocking assays are in line with these findings, since the obtained inhibition rates were always lower than the fold increases described in **section 2.2**, confirming the involvement of other interactions.

2.5. hCMEC/D3 metabolic activity in functionalized fibrin gels

In order to assess the effect of immobilized peptides on cell viability and cell proliferation, hCMEC/D3 cells were firstly seeded as single cells in fibrin gels (50 µL-drops). For this purpose, hCMEC/D3 were initially cultured in unmodified fibrin hydrogels at three different cell-seeding densities (ranging from 1 to 3 × 10^6 cells/mL). The cell seeding density allowing a higher cellular organization without compromise of cell viability was then selected for subsequent studies. Results are presented in **figure 23.** Among the three densities, the intermediate one appeared to be the best concentration for use in the subsequent assays, since it resulted in cells with a spindle-shaped morphology starting to organize into 3-D large round structures, highlighted by the arrows in the figure.

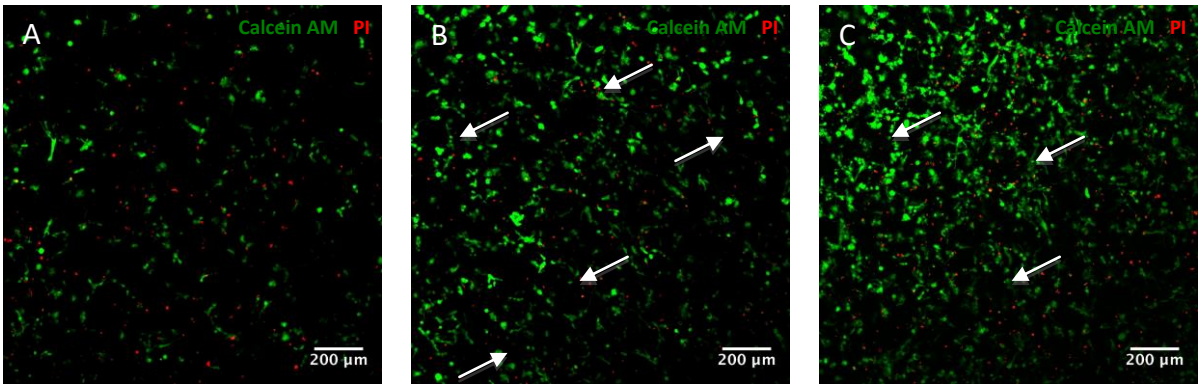

Figure 23 (A-C): Effect of the cell seeding density on the distribution of viable (in green) and dead (in red) hCMEC/D3 cells within 3-D unmodified fibrin gels, after 4 days of cell culture. (A) 1 × 10^6 cells/mL; (B) 2 × 10^6 cells/mL; (C) 3 × 10^6 cells/mL. The cell/fibrin constructs were incubated with Calcein AM and Propidium Iodide for labeling of viable and dead cells, respectively, and imaged by laser confocal scanning microscopy (CLSM).). Representative 2-D projections of CLSM z-stack images of cell/fibrin constructs covering a depth of approximately 50 µm are shown. Scale bar: 200 µm.

Afterwards, the metabolic activity of hCMEC/D3 within functionalized fibrin hydrogels (40 µM in the polymerizing gel) was evaluated through a resazurin-based assay. Such method consists on the reduction of the resazurin dye, which is a blue and non-fluorescent dye, into a pink and fluorescent compound that is called resorufin, being this reduction a responsibility of the reductases existing in the living cells. This said, resorufin fluorescence has been used as an indicator of cell viability and has been correlated with cell proliferation and cytotoxicity phenomena.

The graph in **figure 24** represents the results of the calibration curve obtained at day 0, required to estimate cell numbers at the different time points of culture from fluorescence readings.

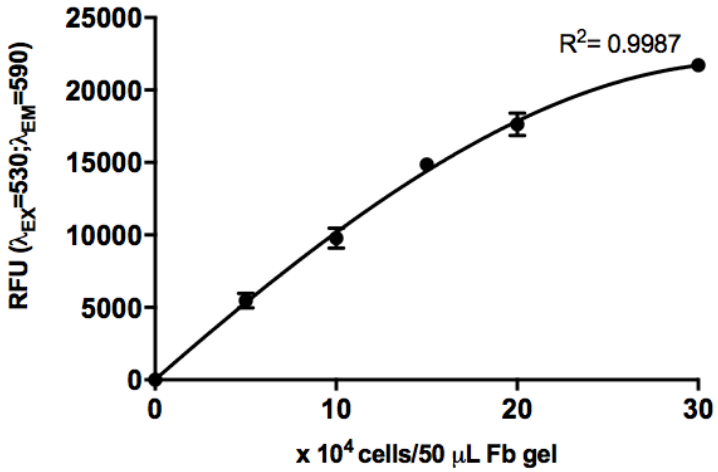

Figure 24: Standard curve of resazurin signal, as a function of cell number. hCMEC/D3 were seeded within unmodified fibrin-gels at cell number ranging from 0 to 30 × 10^4 cells per 50 µL-gel. Results shown correspond to samples incubated for two hours and fifteen minutes in complete medium containing 20% (v/v) of resazurin. Each cell density was evaluated in triplicates (mean ± SD; n=3).

Afterwards, cell proliferation on unmodified and T1-functionalized (40 µM of peptide in the polymerizing gel) fibrin hydrogels was evaluated at day 0 and day 2. Results are presented in **figure 25** and show that the immobilization of T1 peptide did not affect cell proliferation.

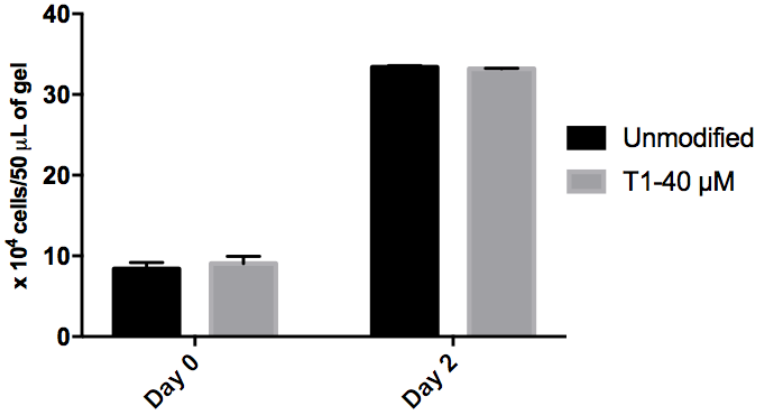

Figure 25: Effect of immobilized T1 peptide on cell proliferation of hCMEC/d3 in fibrin hydrogels. Cell number at day 0 and day 2 of cell culture was estimated from cell metabolic activity, as determined using a resazurin-based assay. The cell number was deduced from a polynomial standard curve, in which fluorescence values were plotted against a known number of cells seeded in parallel within unmodified fibrin gels. (mean ± SD; n=4).

2.6. Cell viability evaluation in functionalized-fibrin gels

Cell viability of hCMEC/D3 cells cultured within unmodified and T1-functionalized fibrin hydrogels (40 µM in the polymerizing gel) was assessed at the end 4 days of cell culture, incubating the cell/fibrin constructs with Calcein AM/PI and Hoechst 33342. Representative 2-D projections of CLSM z-stack images are shown in **Figure 26**.

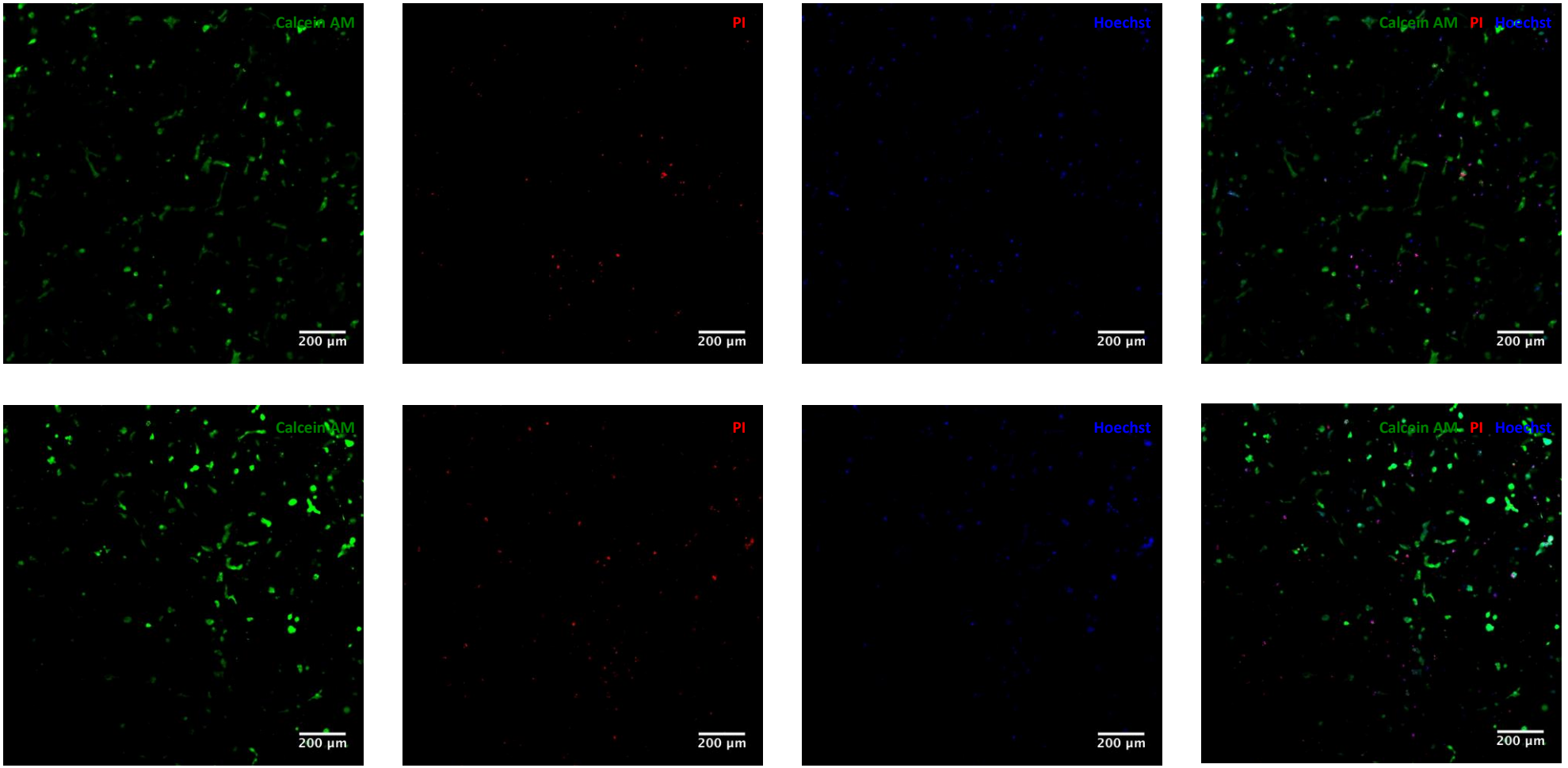

Figure 26: Cell viability of hCMEC/D3 cultured in unmodified (upper line) and T1- functionalized (lower line) fibrin hydrogels. Cell/fibrin constructs were cultured for 4 days and subsequently incubated with Calcein AM, PI and Hoechst 33342, for detection of live (in green), dead (in red), and DNA (in blue), respectively. Representative 2-D projections of CLSM z-stack images of cell/fibrin constructs covering a depth of approximately 50 µm are shown. Scale Bar: 200 µm.

Qualitative analysis of cell viability showed no apparent differences regarding the number of dead cells between the two conditions analyzed.

Afterwards, a quantitative analysis of cell viability was performed by flow cytometry to disclosure the effect of immobilized T1 on cell viability. Results are shown in **figures 27 and 28** and reveal similar percentages of live and dead cells on unmodified and T1-functionalized fibrin hydrogels, thus confirming that T1 immobilization did not compromise cell viability within fibrin hydrogels.

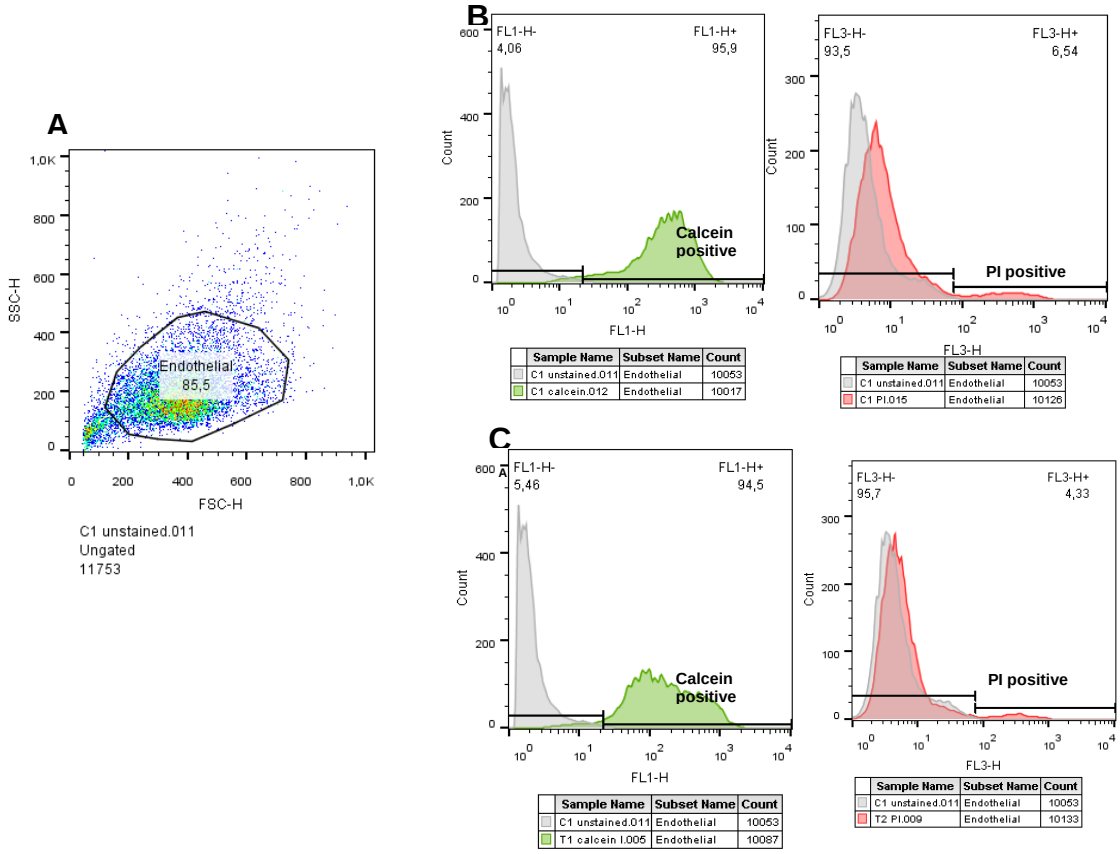

Figure 27: Cell viability flow cytometry analysis of hCMEC/D3 cultured in unmodified and T1-functionalized fibrin hydrogels. Cells were dissociated with StemPro® Accutase®, incubated with calcein AM (for detection of viable cells) or PI (for detection of dead cells), and analyzed by flow cytometry. Debris were excluded by gating on forward and side scatter and fluorescence gates set using unlabeled cells. **(A)** Representative forward and side scatter dot-plot of the unstained population. Representative fluorescence histograms for **(B)** cells isolated from unmodified fibrin hydrogels and **(C)** cells isolated from T1-functionalized fibrin hydrogels**.**

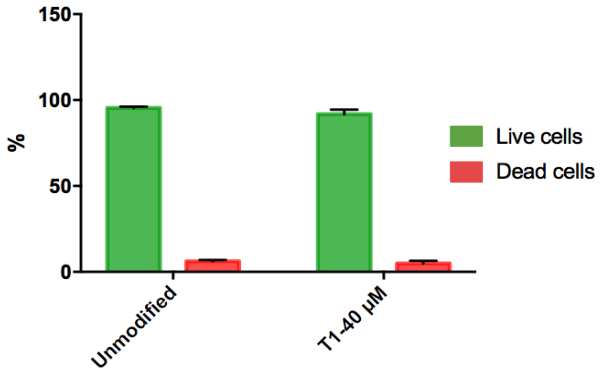

Figure 28: Cell viability flow cytometry analysis of hCMEC/D3 cultured in unmodified and T1-functionalized fibrin hydrogels. Percentage of live and dead hCMEC/d3 isolated from unmodified and T1-functionalized fibrin hydrogels (mean ± SD; n=3, each correspondent to a pool of four Fb drop cultures).

3. EVALUATION OF THE VISCOELASTIC PROPERTIES OF THE FIBRIN GELS

Dynamic shear measurements were used to disclosure if the covalent immobilization of bi-domain peptides affected the stiffness properties (viscoelastic properties) of the gel, which are known to modulate cell behavior.

Oscillatory shear techniques are commonly used to evaluate the rheological behavior of viscoelastic materials. In such method, the relative contributions of both viscous and elastic components of the materials are quantified to characterize their viscoelasticity.

The shear elastic modulus (G') and the shear viscous modulus (G'') are defined as the amplitude ratio of the component of the stress in phase with the strain to the strain amplitude and theirs values are given by the following equations:

$$G' = \frac{\text{stress}}{\text{strain}} \text{ x } \cos\delta \qquad G'' = \frac{\text{stress}}{\text{strain}} \text{ x } \sin\delta$$

Figure 29: Equations for the calculation of the shear elastic and shear viscous modulus (G' and G''). δ represents the contact angle

For a material that is perfectly elastic, the stress and the strain waveforms are in phase, which means that the contact angle and the G'' values are zero and that G' has a finite value. Thus, for a given value of strain amplitude, G' gives a measure of the energy that is elastically stored by the system when exposed to frequency oscillation [102].

In turn, for a completely viscous material, the stress and strain waveforms are totally out of phase, with a value of 90º for the contact angle, 0 for the G' and a finite value for G''. In such situation, G'' represents a measure of the energy that is being dissipated during flow, per cycle of oscillation, for each value of strain amplitude [102].

Thus, the viscoelastic performance of a material consists of a viscous and elastic portion. Complex modulus (G*) is the vector sum of the two and it depicts the gel stiffness properties. Its value is given by the following equation and the toughness of the material increases with the increase of this modulus [102].

$$|G'| = \sqrt{(G')^2 + (G'')^2}$$

Figure 30: Equation for the calculation of the complex modulus (G*)

In the present study, dynamic shear strain amplitude sweep tests were initially performed, in which the samples were subjected to different shear stress values at a constant frequency to determine the linear viscoelastic region of the fibrin hydrogel. The G* was monitored as a function of the strain values and the range in which the G* values remained more or less constant was denoted as the linear viscoelastic region of the gel at the known frequency and temperature values. Subsequently, dynamic frequency sweep tests were performed, during which the samples were exposed to different frequency values at a constant stress and temperature. The storage (G') and loss (G'') modulus were recorded as a function of frequency and the dominant modulus at a particular frequency indicated whether the material was elastic or viscous.

Results are presented in **Figure 31**. These reveal that both the unmodified and modified fibrin gels presented a mostly-elastic behavior, as their shear elastic modulus showed to be considerably higher than the shear viscous one. The obtained complex moduli (G*) are close to those reported for mammalian (rat) brain (ranging from 400 to 1000 Pa) [103]. Such result could also be confirmed by the vector sum of viscous and elastic components, given by complex modulus (G*). Although the values found for G' and G'' moduli were lower than those reported in the literature for the same concentration of fibrinogen (6 mg/mL) [104] [96], the ratio between the G' and G'' moduli is in agreement with previous studies. Both native and functionalized hydrogels present a noteworthy elastic behavior, which is fundamental for the natural function of fibrin in blood clots [105]. Most importantly, it can be inferred that the T1-modification of the hydrogel did not significantly affect its mechanical properties, which is in agreement with previous findings reporting minor disruption of fibrin structure when small peptides were immobilized into fibrin using the same immobilization approach [70].

In fact, this strategy allows the covalent incorporation of peptides into fibrin with retention of biological activity, to specific sites in fibrin(ogen) α chain that are not used for fibrinogen intermolecular crosslinking [106].

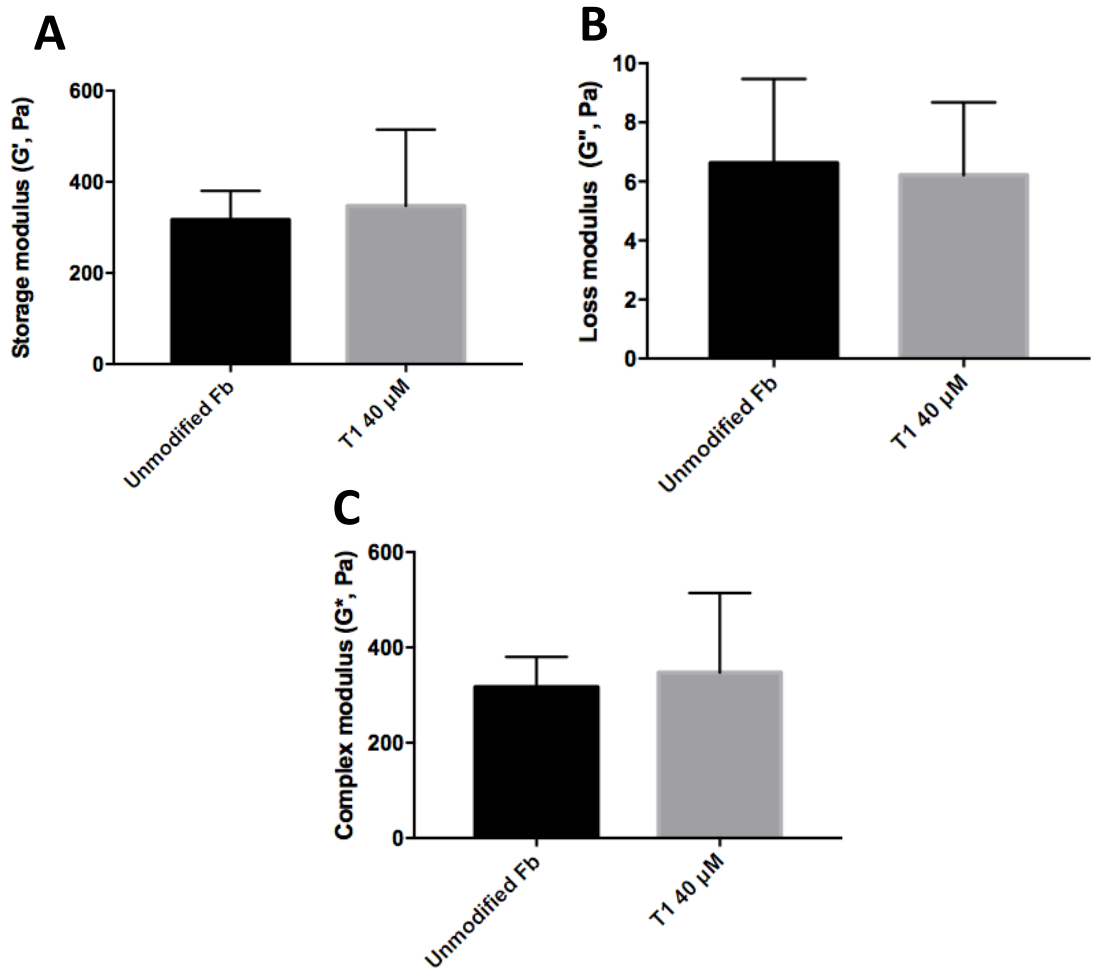

Figure 31 (A-C): Effect of T1 bi-domain peptide immobilization on fibrin stiffness. Storage modulus (G'), loss modulus (G''), and complex modulus (G*) of unmodified and T1-functionalized fibrin hydrogels (40 µM in the polymerizing solution) are shown, as assessed by rheological analysis (mean ± SD; n = 6 independent measurements).

These results were important since changes in fibrin properties at the viscoelasticity level could also impact cellular behavior. Our results therefore suggest that the EC sprouting enhancement observed in T1-functionalized gel was not associated to changes in fibrin network structure.

4. EFFECT OF IMMOBILIZED α6β1 LIGANDS ON OEC BEHAVIOR IN T1-FUNCTIONALIZED FIBRIN GELS

4.1. EC sprouting of OECs in T1-functionalized fibrin gels

To disclosure if T1-functionalized fibrin hydrogels were effective in promoting EC sprouting of a clinically relevant source of endothelial cells, the microcarrier-based angiogenic assay was performed using outgrowth endothelial cells (OECs) derived from human umbilical cord blood. The reported phenotype characterization of these cells reveal that they uniformly express endothelial markers such as CD34, CD36 and VE-Cadherin [107]. Moreover, OECs are uniformly negative for hematopoietic cell-specific surface antigens, such as CD45 or CD14 [108].

As OECs are routinely expanded in culture medium with VEGF, supplementary VEGF was not added to the culture during in vitro angiogenic experiments.

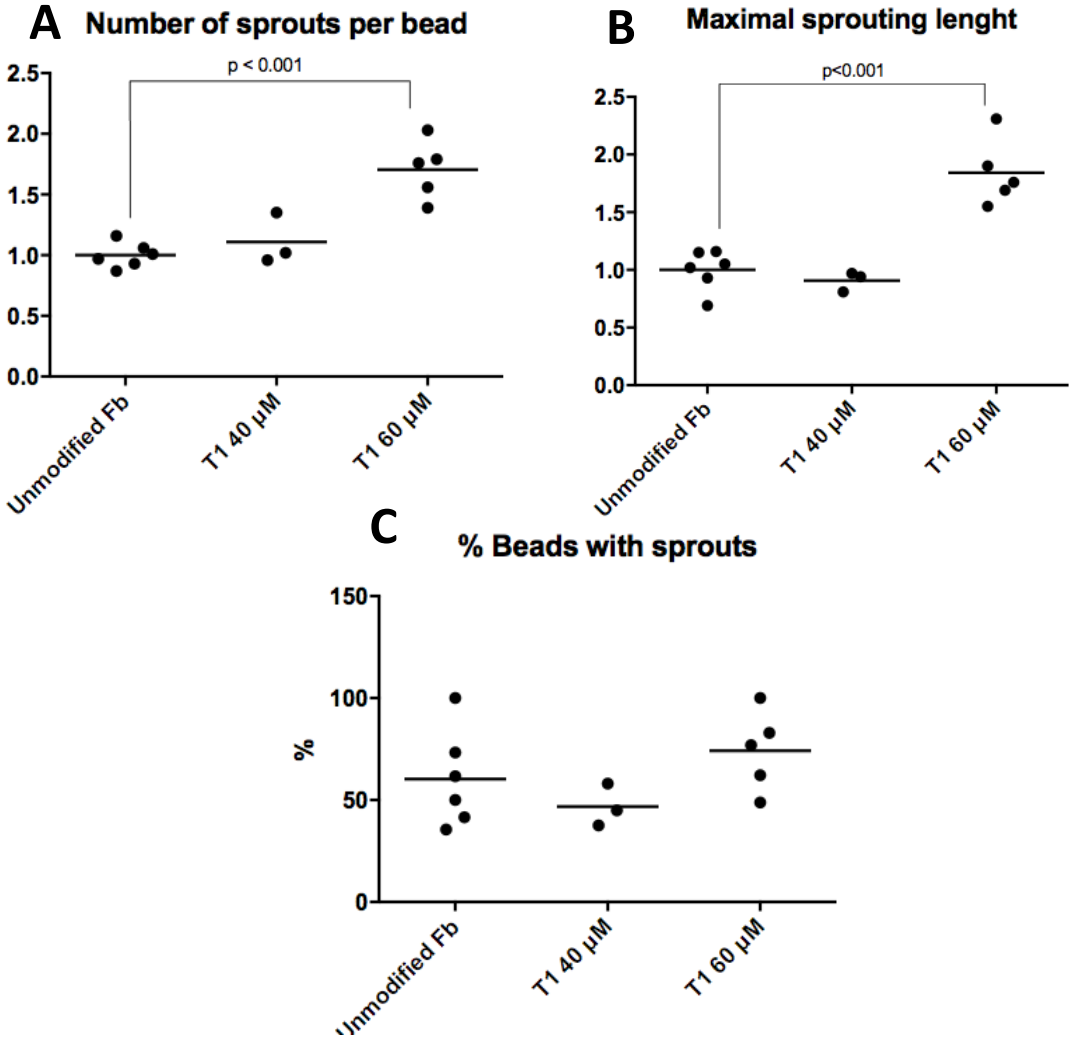

Figure 32 (A-C): EC sprouting of OECs seeded in T1-functionalized fibrin hydrogels after 3 days of culture, in terms of (A) Number of sprouts per bead and (B) maximal sprouting length. The microcarriers embedded in each fibrin gel drop were analyzed and mean values were determined. The percentage of beads with EC sprouts was also determined (C). EC sprouting was normalized to sprouting in unmodified Fb. Graphs denote results from replicate cultures from two independent experiments.

.

As shown in **Figure 32,** the functionalization of the hydrogels with 40 μM of T1 bi-domain peptide did not result in a significant increase in relation to unmodified fibrin, in contrast to its effect on HPMEC-ST1.6R and hCMEC/D3. However, the rising of the input concentration of T1 peptide to 60 μM led to a statistically significant increase in EC sprouting in terms of maximal sprouting length (1.8-fold increase) and the number of sprouts per bead (1.7-fold increase). In what concerns to the percentage of beads with sprouts, the differences were not so evident. Nevertheless, a slight increase could be noticed when functionalizing the fibrin with 60 μM of T1 peptide, while a mild decrease was observed with the lower T1 peptide concentration.

Additionally, statistically significant differences were obtained when increasing the concentration of T1 peptide from 40 μM to 60 μM, with p-values of 0.002 and 0.013 being obtained for maximal sprouting length and number of sprouts per bead, respectively.

In **figure 33** representative images of the three tested conditions are presented. The image chosen to represent the lowest concentration of T1 peptide does not have any sprouts, since the quantification of the percentage of beads with sprouting structures, presented in **figure 32-C**, indicated that less than 50% of the beads presented sprouts. Considering the global results in terms of number of sprouts and maximal sprouting length, the results between unmodified and T1-40 μM modified fibrin gels were really similar and significantly lower than the T1-60 μM functionalized gels, as confirmed by the images. These findings suggest that the ligand concentration required for EC sprouting improvement in fibrin is cell type dependent, and possibly associated with integrin expression levels.

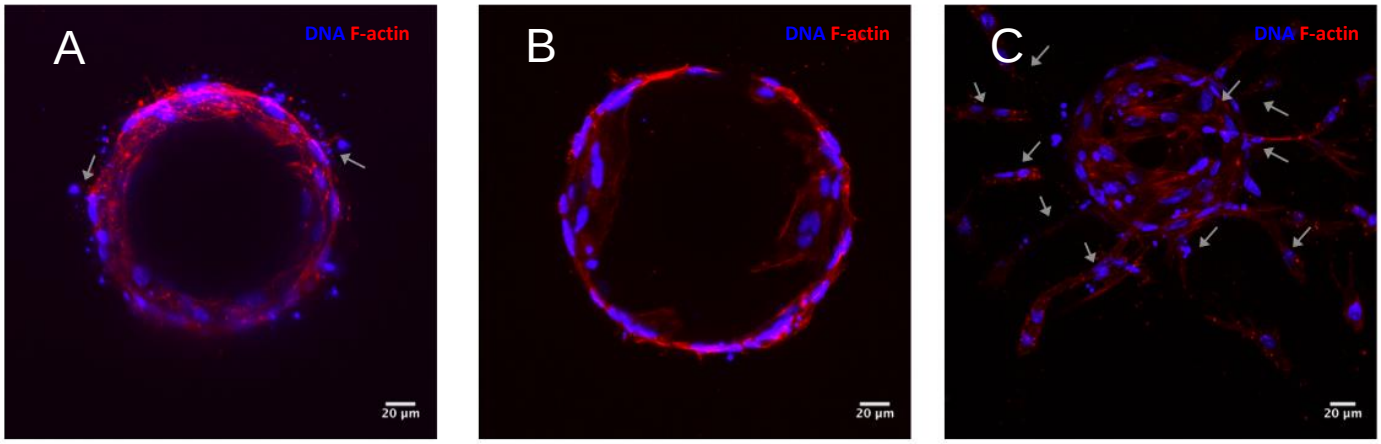

Figure 33 (A-C): Confocal representative images of EC sprouting of OECs cultured in (A) unmodified, (B) T1 40 μM-functionalized and (C) T1 60 μM-functionalized fibrin hydrogels. The samples were processed for DNA and F-actin staining, shown in blue and red respectively. Grey arrows indicate EC sproutings.

5. *IN VIVO* CAM ASSAY

As demonstrated by the previously described results, the functionalization of the fibrin hydrogels with the T1 peptide, obtained by the cleavage of the CCN1 angiogenic protein, has been shown to have the ability to promote endothelial cell migration and proliferation, as well as the formation of capillary-like structures *in vitro*. Such positive results encouraged the progression to *in vivo* studies. The CAM assay was the chosen method since it is a complete *in vivo* environment, immuno-incompetent until birth, with no relevant ethical issues associated. Further, it allows a non-invasive observation of the impact of the test substances placed onto the CAM [109] [110].

Three days after the implantation of the hydrogels on the top of the CAM, the tissue (CAM inoculation site) was excised and the gross evaluations and morphologies of CAM tissue responses to the implanted scaffolds are shown, in a macro perspective, in **figure 34.**

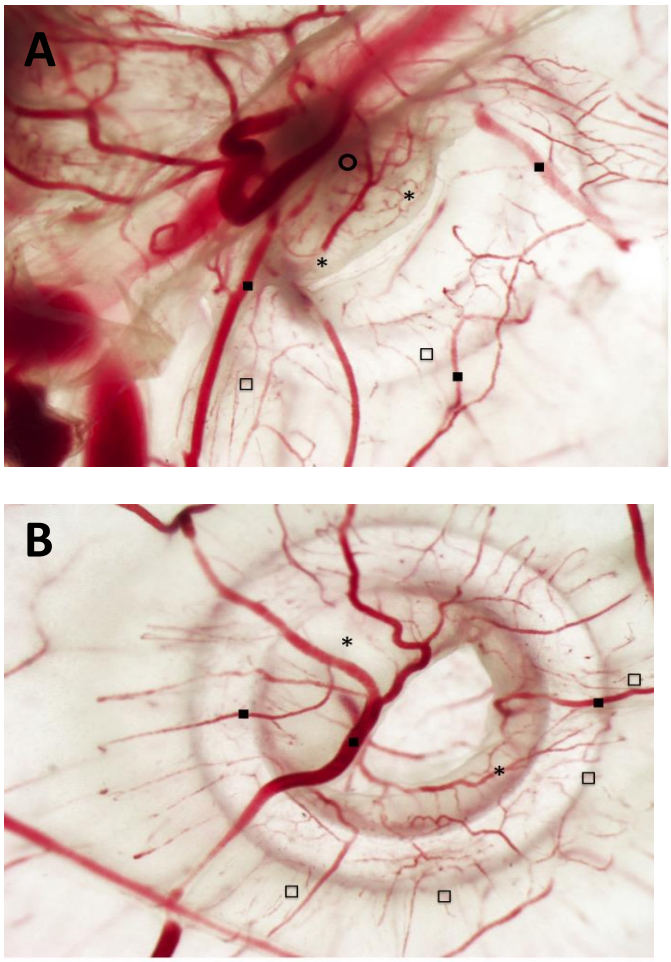

Figure 34 (A-B): StereoMicroscope images representative of the two tested conditions: (A) unmodified and (B) T1-functionalized fibrin gels in the CAM's inoculation site. In both cases it was possible to observe some remains of the gel (*) and to distinguish the pre-existing vessels (■) from the newly formed ones (< 20 μm diameter) (□). In addition to the angiogenic response, an inflammatory reaction was observed, mainly in CAMs with unmodified fibrin gels (O). Magnification: 20×.

Moreover, a quantitative vascular density assay was made, showing that T1-functionalized hydrogels induced a significantly higher angiogenic response than the unmodified gel, as displayed in **figure 35**. **Figure 35-A** displays, individually, the results from the three independent experiments, showing that the increased angiogenic response induced by the functionalized fibrin hydrogels was a reproducible result. In turn, in **figure 35-B**, a summary of all the evaluated pairs is shown, revealing the statistically significant increase of the number of newly-formed vessels by CAM's inoculation with T1-functionalized hydrogels, corresponding to an average increase of 20%.

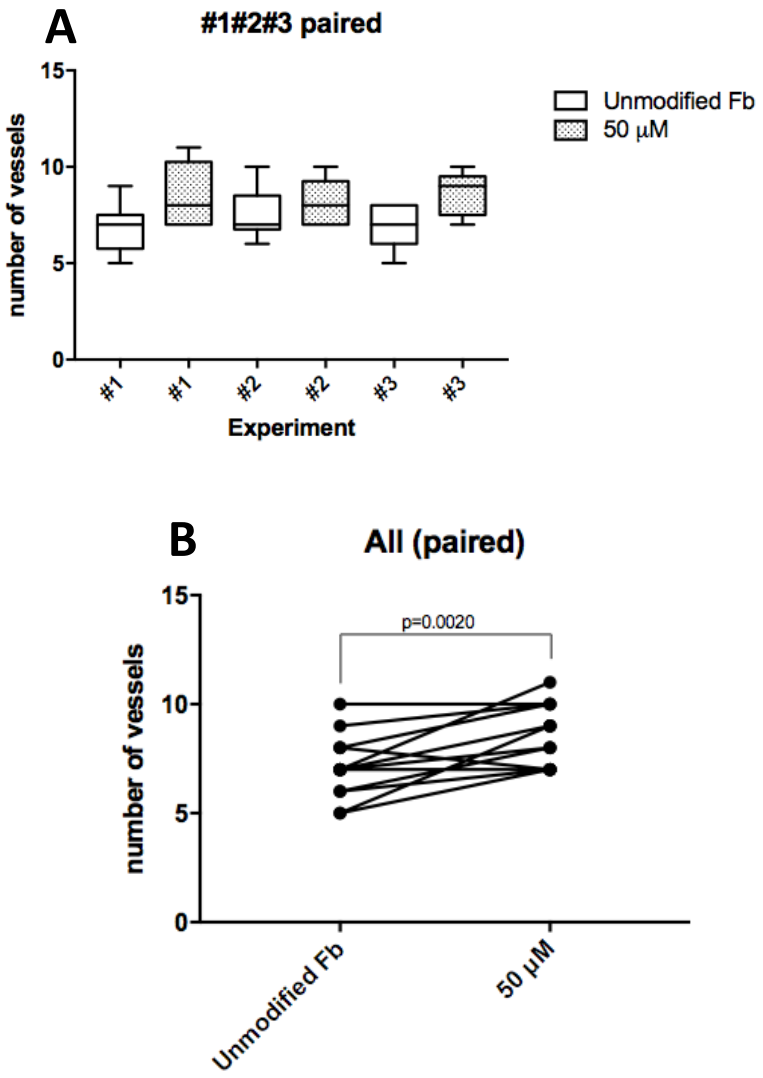

Figures 35 (A-B): Quantitative studies of the number of newly formed vessels in each of the conditions tested. Graph A represents the results of the pairs obtained in each of the three independent experiments and Graph B shows a comparison between the two conditions based on all the pairs.

Further, CAM tissue was also processed for histological analysis. Below, two representative examples of CAMs exposed to unmodified (**Figure 36-A and C**) and T-1 modified (**Figure 36-B and D**) fibrin hydrogels. Histological analysis validated previous results, obtained by optical analysis of the entire inoculation site. Specifically in what concerns the inflammatory reaction and the presence of fibrin residues.

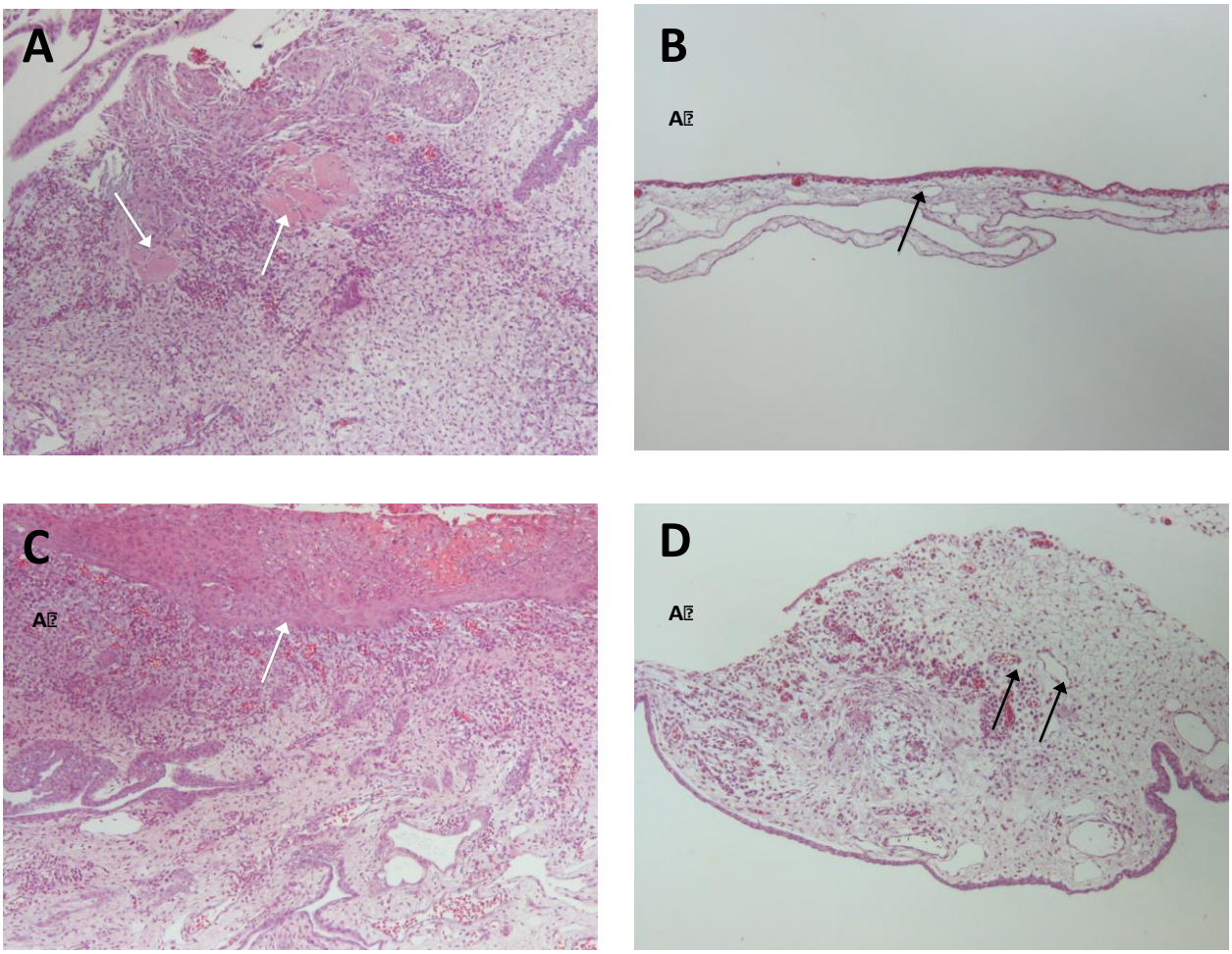

Figure 36 (A-D): Hematoxylin-eosin (H&E) staining of CAM with control unmodified (A and C) and T1-functionalized (B and D) fibrin hydrogels, 3 days after inoculation. White arrows indicate fibrin hydrogel remains that were not degraded by the invading cells and black arrows represent blood vessels. Moreover, the recruitment of immune precursor cells is also observable, mainly in the control situations. Magnification: 100×.

In the first example, the tissue in contact with the control hydrogel (**figure 36-A**), is extensively more dilated than the membrane in contact with the modified hydrogel (**figure 36-B**), most likely as a consequence of the inflammatory process (note the recruitment of immune precursor cells - the little and rounded ones that stain purple by the H&E staining).

Moreover, it is still possible to observe fibrin hydrogel remains in **figure 36-A**, contrarily to the opposite image (**figure 36-B**). This is in accordance with the counting of the newly formed vessels, as the cells were not able to fully degrade the hydrogel and, thus, were not able to proliferate and migrate more and, consequently, less vascular structures were formed.

In the second example, the membrane in contact with the modified hydrogel (**figure 36-D**) shows some level of dilation and inflammation but it is still a mild response in comparison to the control condition (**figure 36-D**). Fibrin residues are again noticeable in the control but not in the presence of T1 peptide.

The inflammatory response was quantified using a semi-quantitative score analysis (score 1: whenever inflammation was higher than in the counterpart area; score 0: whenever inflammation was lower than in the counterpart area), both in the macroscopic images of the excised tissues and the H&E stained slides. Inflammatory response was identified by the

presence of denser and darker zones at the inoculation site or, in the H&E staining, by dilation of the CAM and recruitment of immune precursor cells.

The graph bellow (**figure 37**) summarizes our results, showing that CAMs in contact with unmodified gels presented a significantly higher inflammatory response than the tissues that were in contact with the functionalized ones. Results are consistent both for the macro images and the H&E slides.

In addition, a quantitative evaluation of the reaction area was made, through measurements of the referred dense and dark areas and the results are depicted in **figure 38**.

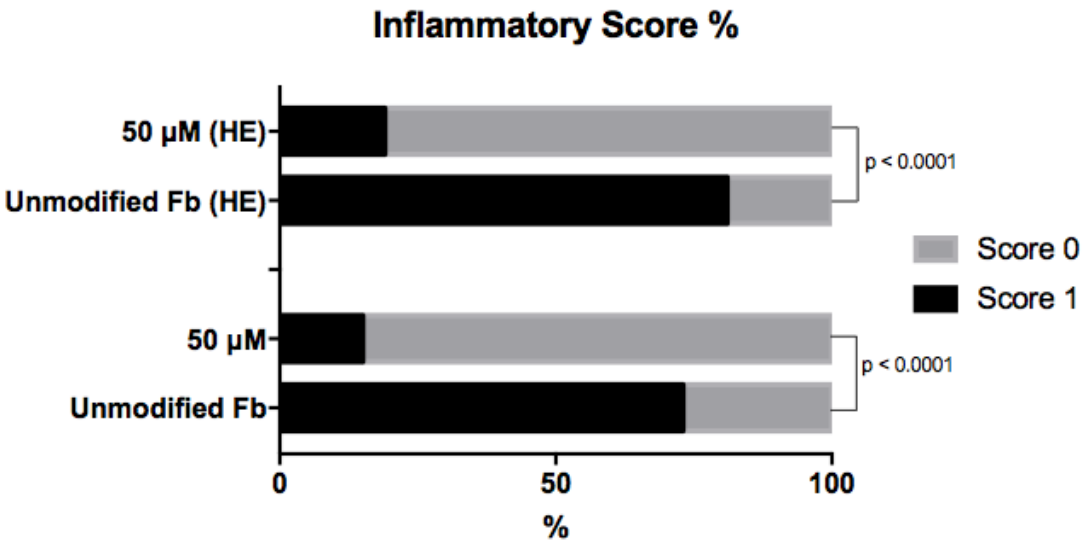

Figure 37: Inflammatory score of the inoculated pairs. Upper bars represent the results from H&E slides evaluation, while the lower bars represent the results from the macro evaluation. Score 1: more inflammation than in the counterpart ring; Score 0: less inflammation than in the counterpart ring.

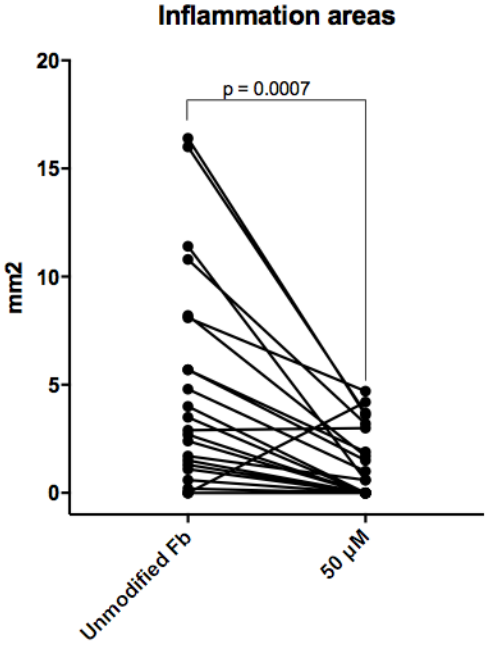

Image 38: Quantification of inflammatory areas of the inoculated pairs.

As summarized in the upper bars of **figure 37**, the histological sections were also used to score inflammation, as a way of confirming the inflammatory scores that were noticed in the macroscopic images. Illustrative images of the inflammatory reaction are shown in **figure 39**. **Figure 39-A** is highly representative of the huge inflammatory reaction that could be seen in almost every control tissue, while **Figure 39-B** illustrates the counterpart area, in which the CAM in contact with the T1-functionalized hydrogel also presented some inflammation.

The number of inflammatory cells is clearly superior on the implantation site of unmodified gels. In turn, the inoculation with T1-functionalized hydrogels also originated, for some cases, an inflammatory response in the CAM, but it was significantly lower in most of the cases.

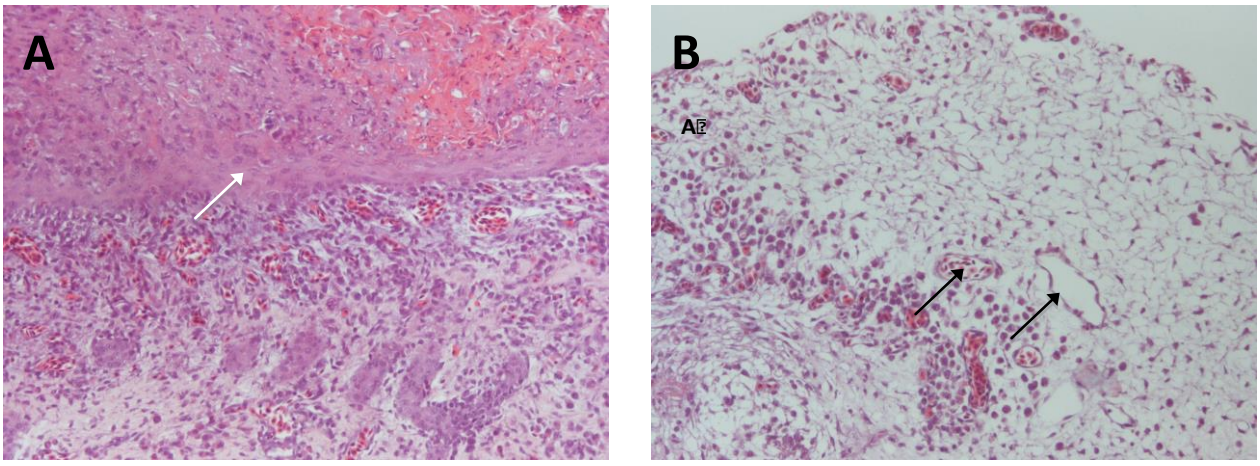

Figures 39 (A-B): H&E staining of CAM at day 3 after implantation. Representative images of the inflammatory reaction observed for unmodified (A) and T1-functionalized (B) fibrin hydrogels. White arrows indicate the presence of fibrin residues and black arrows represent blood vessels. Magnification: 200×.

It is important to highlight that the example depicted on **figure 39-B** was not common, since most of the tissues that were in contact with modified gels did not present any considerable inflammatory reaction. Therefore, this figure is being presented only as a comparison tool, as the extent of the inflammation is very different from one situation to another.

Together with the studies of the inflammatory reaction, a semi-quantitative scoring evaluation was made, in the basis of the H&E slides, regarding the presence of fibrin residues in either case. The results revealed that 50% of the control cases still presented fibrin remains at the time of the tissue excision, against only 2% of the T1-functionalized gels.

It was expected some kind of immune reaction to happen, since a foreign body was being placed upon the membrane, but the enormous inflammation observed for the control gels, as well as its almost inexistence for the modified ones, was not predictable.

This reduction of the inflammatory reaction observed for the T1-functionalized gels was, as already mentioned, accompanied by an increase of fibrin degradation. These two findings can be related, since a higher rate of biomaterial degradation would reduce the contact time between the tissue and the material and, as a consequence, the inflammatory reaction is expected to be less aggressive. Moreover, T1 peptide might have an inductor role for the secretion of anti-inflammatory cytokines, causing the global anti-inflammatory effect of the functionalized fibrin.

As far as we know, the anti-inflammatory effect of T1-functionalized fibrin hydrogels, suggested by the previously reported data, is yet to be investigated. If proven right, the combination of pro-angiogenic and anti-inflammatory properties of such hydrogels would have an important impact in research and clinical applications, namely in what respects neurodegenerative disorders.

CHAPTER 4
FINAL REMARKS
FUTURE PERSPECTIVES

FINAL REMARKS

The objective of the herein reported work consisted in the development of fibrin-based hydrogels able to foster the neovascularization of bioengineered tissues, in particular for application in the injured central nervous system. For this purpose, fibrin hydrogels were functionalized with the integrin α6β1 binding sequence of the angiogenic inducer CYR61 (T1 peptide), due to its reported pro-angiogenic activity. . The immobilization of T1 peptide to a biomaterial as a strategy to enhance its angiogenic properties is novel. In addition, we explored the binding of another integrin α6β1 ligand – the synthetic peptide HYD1 – previously shown by our group to promote cell migration and neurite extension of embryonic stem cell-derived neural stem/progenitor cells cultured within 3-D fibrin gels. Fibrin functionalization was expected to enhance fibrin ability to promote neovascularization, namely by promoting proliferation, migration and capillary-like structure formation, *in vitro*, as well as angiogenesis, *in vivo*.

For the preliminary assessment of the angiogenic ability of T1/HYD1-functionalized fibrin gels, a cell line of human pulmonary microvascular endothelial cells (HPMEC-ST1.6R) and the *in vitro* microcarrier-based assay were used. For the highest input concentration tested of T1 peptide (40 μM), already a trend for a 1.4-fold increase in average was detected in all the evaluated EC sprouting parameters, though significant differences were only observed in the number of sprouts per microcarrier. Immobilization of HYD1, however, failed to induce EC sprouting, regardless of the input concentration tested.

The bioactivity of functionalized gels was then assessed using a cell line of human brain microvascular endothelial cells (hCMEC/D3). Further supporting the previous results, functionalization of fibrin gels with 40 μM of T1 peptide resulted, in average, in a 1.4-fold increase of hCMEC/D3 sprouting in all the parameters analyzed, and statistically significant differences were found, this time, in the number of sprouts per bead and also in the sprouting area. However, and also in line with the previous results, HYD1 showed no angiogenic effect. The effect of T1 peptide was enhanced in the presence of VEGF, a soluble angiogenic inducer described to induce integrin α6β1 activation and expression [41]. Specifically, fibrin gels functionalized with 40 μM of T1 bi-domain peptide elicited a statistically significant increase in all EC sprouting parameters, namely to a 1.9-fold increase of the number of sprouts per bead, a 2-fold increase of the sprouting area, and a 1.5-fold increase in the maximal sprouting length. Additionally, a 25% increase in the percentage of beads presenting sprouting structures was observed. Incubation with functional blocking monoclonal antibodies against α6 and β1integrin subunits, partially inhibited the number of sprouts per bead and the maximal sprouting length in T1-functionalized gels, but not in unmodified gels. Although the differences observed were not significant, these results suggest that the EC sprouting elicited by immobilized T1 peptide was partially mediated by integrin α6β1.

Immobilized T1 peptide did not affect cell viability or proliferation of hCMEC/d3, as shown by flow cytometry analysis of LIVE/DEAD cells and cell metabolic activity, respectively.

Further characterization of T1-functionalized gels in terms of mechanical properties showed no significant changes in fibrin viscoelastic properties after covalent binding of T1 peptide, pointing out that the EC sprouting enhancement observed in T1-functionalized gel was not associated to changes in fibrin network structure.

The testing of T1-functionalized fibrin gels with OECs from human umbilical cord blood provided relevant evidence of the bioactivity of T1-functionalized fibrin. In brief, 60 μM of T1 in the polymerizing gel gave rise to a statistically significant increase of EC sprouting, leading to a 1.7-fold increase of the number of sprouts per bead and to a 1.8-fold increase of the maximal sprouting length, when comparing to unmodified fibrin gels. In turn, functionalization with 40 μM of T1 did not instigate any differences in comparison to the unmodified control. These findings suggest that the ligand concentration required for EC sprouting improvement in fibrin is cell-type dependent, and possibly associated with integrin expression levels.

Finally, to evaluate the in vivo angiogenic potential of T1-functionalized fibrin, a CAM assay was performed using fibrin gels functionalized with an intermediate concentration of T1 (50μM) and unmodified fibrin gels as control. The results were reproducible between the three independent experiments performed and statistically significant differences were found, with an increase of about 20% in what concerns the number of newly formed vessels, therefore pointing out the pro-angiogenic potential of T1-functionalized fibrin gels. CAMs receiving T1-functionalized fibrin gels displayed a significant decrease of the inflammatory reaction when compared to that caused by unmodified fibrin, which may be related to the faster degradation observed for these gels as compared to unmodified gels, associated to the increased formation of new vessels by invasive vasculature. The possible anti-inflammatory effect of T1-functionalized fibrin combined with its angiogenic properties makes it potential interesting for application in the injured CNS as well as in neurodegenerative disorders.

FUTURE PERSPECTIVES

Taking into consideration the obtained results along the development of this master thesis, future studies are required in order to increase the robustness of the results.

First and foremost, it is important to increase the number of MCs analyzed in certain experiments, such as that of the function-blocking assay, so that the robustness of the work is increased. Due to time constraints, this was not possible until the delivery of this report.

Moreover, although some significant differences were already obtained, it is necessary to increase the number of experiments to confirm the effect of the addition of VEGF to the culture medium of hCMEC/D3 cells, since only two independent experiments were performed.

Furthermore, regarding OECs, even tough statistically significant differences were already observed, there is a need of investing some more time and repeat the experiment, as only two independent assays (with three replicates) were made with the highest concentration of T1 peptide.

In what concerns the rheological study carried out, since it is a quite time-consuming procedure, the characterization of all the fibrin gels developed was not possible. It may be interesting to characterize HYD1-modified hydrogels, as well as fibrin gels functionalized with 60 μM of T1 peptide, in order to assess if such modifications affect the viscoelasticity properties of the hydrogel, even though it is not expected to happen.

Moreover, since the increase of the bi-domain peptides concentration, specially in what regards the T1 peptide, seemed to result in a rise of the number of sprouts and their extension, it would be interesting to investigate the effect of higher concentrations of T1 peptide on cell behavior. Besides, a quantification of the number of cells per sprout should be performed, in order to better define the concept of capillary-like structure.

Concerning the CAM assay, some interesting results were obtained considering a potential anti-inflammatory effect of the T1-modified hydrogels. To our knowledge, such effect is yet to be explored and the investment on the consolidation of these results seems to be appealing and easily justifiable, due to the range of possible applications of a hydrogel that is simultaneously pro-angiogenic and anti-inflammatory. To get insight into the pro-angiogenic ability of T1-functionalized fibrin gels *in vivo*, other animal models, such as a subcutaneous one or a rat model of spinal cord injury - such as the contusion model – should be used.

The until-now obtained results indicate that fibrin gels functionalized with the T1 peptide are interesting for endothelial cell culture in a 3-D environment and potentially promising for the development of prevascularized tissues and their *in vivo* application. Together with previous findings regarding their capability of promoting neural stem cell migration and neuronal extension, these results seem very promising in what concerns the applicability of these hydrogels within the CNS.

REFERENCES

1. Europe, C.o. *European Day for Organ Donation and Transplantation (EODD)*. 2016.
2. Hirschi, K.K., et al., *Vascular Assembly in Natural and Engineered Tissues.* New York Academy of Sciences, 2002. **961**: p. 223-242.
3. Lovett, M., et al., *Vascularization Strategies for Tissue Engineering.* Tissue Engineering Part B, 2009. **15**(3): p. 353-370.
4. Kaully, T., et al., *Vascularization - the conduit to viable engineered tissues.* Tissue Engineering Part B: Reviews, 2009. **15**(2): p. 159-169.
5. Jain, R.K., et al., *Engineering vascularized tissue.* Nature Biotechnology, 2005. **23**(7): p. 821-823.
6. Moon, J.J. and J.L. West, *Vascularization of engineered tissues: approaches to promote angio-genesis in biomaterials.* Current topics in medicinal chemistry, 2008. **8**(4): p. 300-310.
7. Nomi, M., et al., *Principals of neovascularization for tissue engineering.* Molecular aspects of medicine, 2002. **23**(6): p. 463-483.
8. Walchli, T., et al., *Quantitative assessment of angiogenesis, perfused blood vessels and endothelial tip cells in the postnatal mouse brain.* Nature Protocols, 2015. **10**(1): p. 53-74.
9. Eilken, H.M. and R.H. Adams, *Dynamics of endothelial cell behavior in sprouting angiogenesis.* Current opinion in cell biology, 2010. **22**(5): p. 617-625.
10. Khoo, C.P., K. Micklem, and S.M. Watt, *A comparison of methods for quantifying angiogenesis in the Matrigel assay in vitro.* Tissue Engineering Part C Methods, 2011. **17**(9): p. 895-906.
11. Yoo, S.Y. and S.M. Kwon, *Angiogenesis and Its Therapeutic Opportunities.* Mediators of Inflammation, 2013. **2013**: p. 1-11.
12. Grant, D.S., et al., *Interaction of Endothelial Cells with Laminin A Chain Peptide (SIKVAV) in Vitro and Induction of Angiogenic Behavior in Vivo.* Journal of Cellular Physiology, 1992. **153**: p. 614-625.
13. Robinet, A., et al., *Elastin-derived peptides enhance angiogenesis by promoting endothelial cell migration and tubulogenesis through upregulation of MT1-MMP.* Journal of cell science, 2005. **118**(2): p. 343-356.
14. Hall, H., T. Baechi, and J.A. Hubbell, *Molecular properties of fibrin-based matrices for promotion of angiogenesis in vitro.* Microvascular Research, 2001. **62**(3): p. 315-326.
15. Vallon, M., et al., *Developmental and pathological angiogenesis in the central nervous system.* Cellular and molecular life sciences, 2014. **71**(18): p. 3489-3506.
16. Tam, S.J. and R.J. Watts, *Connecting vascular and nervous system development: angiogenesis and the blood-brain barrier.* Annual review of neuroscience, 2010. **33**: p. 379-408.
17. Wilhelm, I., et al., *Role of the blood-brain barrier in the formation of brain metastases.* International journal of molecular sciences, 2013. **14**(1): p. 1383-1411.
18. Lee, H.S., et al., *Brain angiogenesis in developmental and pathological processes: regulation, molecular and cellular communication at the neurovascular interface.* FEBS Journal, 2009. **276**(17): p. 4622-4635.
19. Acar, G., G. Tanriover, and R. Demir, *Angiogenesis in neurological disorders: a review.* Neurological Research, 2012. **34**(7): p. 627-635.
20. Bartanusz, V., et al., *The blood-spinal cord barrier: morphology and clinical implications.* Annals of neurology, 2011. **70**(2): p. 194-206.
21. Loy, D.N., et al., *Temporal progression of angiogenesis and basal lamina deposition after contusive spinal cord injury in the adult rat.* Journal of Comparative Neurology, 2002. **445**(4): p. 308-324.
22. Mautes, A.E.M., et al., *Vascular Events After Spinal Cord Injury: Contribution to Secondary Pathogenesis.* Physical Therapy, 2000. **80**(7): p. 673-687.
23. Ohab, J.J., et al., *A neurovascular niche for neurogenesis after stroke.* The Journal of Neuroscience, 2006. **26**(50): p. 13007-13016.

24. Rauch, M.F., et al., *Engineering angiogenesis following spinal cord injury: a coculture of neural progenitor and endothelial cells in a degradable polymer implant leads to an increase in vessel density and formation of the blood-spinal cord barrier.* European Journal of Neuroscience, 2009. **29**(1): p. 132-145.
25. Arai, K., et al., *Brain angiogenesis in developmental and pathological processes: neurovascular injury and angiogenic recovery after stroke.* FEBS Journal, 2009. **276**(17): p. 4644-4652.
26. Ford, M.C., et al., *A macroporous hydrogel for the coculture of neural progenitor and endothelial cells to form funcional vascular networks in vivo.* 2006.
27. Laschke, M.W. and M.D. Menger, *Vascularization in tissue engineering: angiogenesis versus inosculation.* European Surgical Research, 2012. **48**(2): p. 85-92.
28. Seliktar, D., et al., *MMP-2 sensitive, VEGF-bearing bioactive hydrogels for promotion of vascular healing.* Journal of Biomedical Materials Research Part A, , 2004. **68**(4): p. 704-716.
29. Richardson, T.P., et al., *Polymeric system for dual growth factor delivery.* Nature biotechnology, 2001. **19**(11): p. 1029-1034.
30. Hendel, R.C., et al., *Effect of Intracoronary Recombinant Human Vascular Endothelial Growth Factor on Myocardial Perfusion.* Circulation, 2000. **101**(2): p. 118-121.
31. Simons, M., et al., *Pharmacological Treatment of Coronary Artery Disease With Recombinant Fibroblast Growth Factor-2: Double-Blind, Randomized, Controlled Clinical Trial.* Circulation, 2002. **105**(7): p. 788-793.
32. Li, J., Y.P. Zhang, and R.S. Kirsner, *Angiogenesis in wound repair: angiogenic growth factors and the extracellular matrix.* Microscopy Research and Technique, 2003. **60**(1): p. 107-114.
33. Gonçalves, L.M., S.E. Epstein, and J.J. Piek, *Controlling collateral development: the difficult task of mimicking mother nature.* Cardiovascular Research, 2001. **49**: p. 495-496.
34. Mazué, G., et al., *Preclinical and Clinical Studies with recombinant human basic fibroblast growth factor.* Annals New York Academy of Sciences, 1991: p. 329-340.
35. Bianco, P. and P.G. Robey, *Stem cells in tissue engineering.* Nature, 2001. **414**(6859): p. 118-121.
36. Henry, T.D., et al., *The VIVA Trial: Vascular Endothelial Growth Factor in Ischemia for Vascular Angiogenesis.* Circulation, 2003. **107**(10): p. 1359-1365.
37. Zisch, A.H., M.P. Lutolf, and J.A. Hubbell, *Biopolymeric delivery matrices for angiogenic growth factors.* Cardiovascular Pathology, 2003. **12**(6): p. 295-310.
38. Naderi, H., M.M. Matin, and A.R. Bahrami, *Review paper: critical issues in tissue engineering: biomaterials, cell sources, angiogenesis, and drug delivery systems.* Journal of Biomaterials Applications, 2011. **26**(4): p. 383-417.
39. Chen, R.R. and D.J. Mooney, *Polymeric growth factor delivery strategies for tissue engineering.* Pharmaceutical Research, 2003. **20**(8): p. 1103-1112.
40. Mikos, A.G., et al., *Engineering Complex Tissues.* Tissue Engineering, 2006. **12**(12): p. 3307-3339.
41. Lee, T.H., et al., *Integrin regulation by vascular endothelial growth factor in human brain microvascular endothelial cells: role of alpha6beta1 integrin in angiogenesis.* Journal of Biological Chemistry, 2006. **281**(52): p. 40450-40460.
42. Avraamides, C.J., B. Garmy-Susini, and J.A. Varner, *Integrins in angiogenesis and lymphangiogenesis.* Nature Reviews Cancer, 2008. **8**(8): p. 604-617.
43. Jaffe, E.A., et al., *Culture of Human Endothelial Cells derived from Umbilical Veins.* The Journal of Clinical Investigation, 1973. **52**: p. 2745-2756.
44. Morin, K.T. and R.T. Tranquillo, *In vitro models of angiogenesis and vasculogenesis in fibrin gel.* Experimental Cell Research, 2013. **319**(16): p. 2409-2417.
45. Wenger, A., et al., *Modulation of In Vitro Angiogenesis in a Three-Dimensional Spheroidal Coculture Model for Bone Tissue Engineering.* Tissue engineering, 2004. **10**(9-10): p. 1536-1547.
46. Wenger, A., et al., *Development and characterization of a spheroidal coculture model of endothelial cells and fibroblasts for improving angiogenesis in tissue engineering.* Cells Tissues Organs, 2005. **181**(2): p. 80-88.

47. Borges, J., et al., *Engineered Adipose Tissue Supplied by Functional Microvessels.* Tissue Engineering, 2003. **9**(6): p. 1263-1270.
48. Griffith, C.K., et al., *Diffusion Limits of an in vitro thick prevascularized tissue.* Tissue Engineering, 2005. **11**(1-2): p. 257-266.
49. Sung, H.J., et al., *The effect of scaffold degradation rate on three-dimensional cell growth and angiogenesis.* Biomaterials, 2004. **25**(26): p. 5735-5742.
50. Mehdizadeh, H., et al., *Three-dimensional modeling of angiogenesis in porous biomaterial scaffolds.* Biomaterials, 2013. **34**(12): p. 2875-2887.
51. Brandl, F., F. Sommer, and A. Goepferich, *Rational design of hydrogels for tissue engineering: impact of physical factors on cell behavior.* Biomaterials, 2007. **28**(2): p. 134-146.
52. Sweeney, T.M., et al., *Basement membrane and the SIKVAV laminin-derived peptide promote tumor growth and metastases.* Cancer and Metastasis Reviews, 1991. **10**(3): p. 245-254.
53. Kibbey, M.C., D.S. Grant, and H.K. Kleinman, *Role of the SIKVAV Site of Laminin in Promotion of Angiogenesis and Tumor Growth: An In Vivo Matrigel Model.* Journal of the National Cancer Institute, 1992. **84**(21): p. 1633-1638.
54. Moon, J.J., S.H. Lee, and J.L. West, *Synthetic Biomimetic Hydrogels Incorporated with Ephrin-A1 for Therapeutic Angiogenesis.* Biomacromolecules, 2007. **8**: p. 29-42.
55. Browning, M.B., et al., *Endothelial cell response to chemical, biological, and physical cues in bioactive hydrogels.* Tissue Engineering Part A, 2014. **20**(23-24): p. 3130-3141.
56. D'Andrea, L.D., et al., *Targeting angiogenesis: structural characterization and biological properties of a de novo engineered VEGF mimicking peptide.* PNAS: Proceedings of the national academy of sciences of the United States of America, 2005. **102**(40): p. 14215-14220.
57. Leslie-Barbick, J.E., et al., *The promotion of microvasculature formation in poly(ethylene glycol) diacrylate hydrogels by an immobilized VEGF-mimetic peptide.* Biomaterials, 2011. **32**(25): p. 5782-5789.
58. Cai, L., C.B. Dinh, and S.C. Heilshorn, *One-pot Synthesis of Elastin-like Polypeptide Hydrogels with Grafted VEGF-Mimetic Peptides.* Biomaterials Science, 2014. **2**(5): p. 757-765.
59. Guo, L., et al., *Promotion of microvasculature formation in alginate composite hydrogels by an immobilized peptide GYIGSRG.* Science China Chemistry, 2012. **55**(9): p. 1781-1787.
60. Grant, D.S., et al., *The Role of Basement Membrane in Angiogenesis and Tumor Growth.* Pathology - Research and Practice, 1994. **190**(9-10): p. 854-863.
61. Fittkau, M.H., et al., *The selective modulation of endothelial cell mobility on RGD peptide containing surfaces by YIGSR peptides.* Biomaterials, 2005. **26**(2): p. 167-174.
62. Steffens, G.C.M., et al., *Modulation of Angiogenic Potential of Collagen Matrices by Covalent Incorporation of Heparin and Loading with Vascular Endothelial Growth Factor.* Tissue engineering, 2004. **10**(9-10): p. 1502-1509.
63. Kuratomi, Y., et al., *Identification of Metastasis-Promoting Sequences in the Mouse Laminin alpha1 Chain.* Experimental Cell Research, 1999. **249**: p. 386-395.
64. Luhmann, T., et al., *The induction of cell alignment by covalently immobilized gradients of the 6th Ig-like domain of cell adhesion molecule L1 in 3D-fibrin matrices.* Biomaterials, 2009. **30**(27): p. 4503-4512.
65. Guarnieri, D., et al., *Covalently immobilized RGD gradient on PEG hydrogel scaffold influences cell migration parameters.* Acta Biomaterialia, 2010. **6**(7): p. 2532-2539.
66. Brown, A.C. and T.H. Barker, *Fibrin-based biomaterials: modulation of macroscopic properties through rational design at the molecular level.* Acta Biomaterialia, 2014. **10**(4): p. 1502-1514.
67. Lawrie, A.S., et al., *Prothrombin time derived fibrinogen determination on Sysmex CA-6000 TM.* Journal of clinical pathology, 1998.
68. Duong, H., B. Wu, and B. Tawil, *Modulation of 3D Fibrin Matrix Stiffness by Intrinsic Fibrinogen-Thrombin Compositions and by Extrinsic Cellular Activity.* Tissue Engineering part A, 2009. **15**(7): p. 1865-1876.
69. Janmey, P.A., J.P. Winer, and J.W. Weisel, *Fibrin gels and their clinical and bioengineering applications.* Journal of the Royal Society Interface, 2009. **6**(30): p. 1-10.

70. Schense, J.C. and J.A. Hubbell, *Cross-linking exogenous bifunctional peptides into fibrin gels with factor XIIIa.* Bioconjugate chemistry, 1999. **10**(1): p. 75-81.
71. Schense, J.C., et al., *Enzymatic incorporation of bioactive peptides into fibrin matrices enhances neurite extension.* Nature biotechnology, 2000. **18**(4): p. 415-419.
72. Sakata, Y. and N. Aoki, *Cross-linking of alpha2-plasmin inhibitor to fibrin by fibrin-stabilizing factor.* Journal of Clinical Investigation, 1980. **65**(2): p. 290-297.
73. Leu, S.J., et al., *Identification of a novel integrin alpha 6 beta 1 binding site in the angiogenic inducer CCN1 (CYR61).* The Journal of Biological Chemistry, 2003. **278**(36): p. 33801-33808.
74. Silva, J.N., et al., *Development of fibrin hydrogels functionalized with covalently bound alpha6beta1 ligands for neural stem cell (NSC) based transplantation therapies.* Journal of Tissue Engineering and Regenerative Medicine, 2014. **8 (S1)**: p. 39-40.
75. Kirkpatrick, C.J., et al., *Experimental approaches to study vascularization in tissue engineering and biomaterial applications.* Journal of Materials Science: Materials in Medicine, 2003. **14**(8): p. 677-681.
76. Khan, G.J., et al., *Assessment Methods of Angiogenesis and Present Approaches for Its Quantification.* Cancer Research Journal, 2014. **2**(3).
77. Jain, R.K., et al., *Quantitative angiogenesis assays: progress and problems.* Nature Medicine, 1997. **3**(11): p. 1203-1208.
78. Park, M.J., et al., *Nerve growth factor induces endothelial cell invasion and cord formation by promoting matrix metalloproteinase-2 expression through the phosphatidylinositol 3-kinase/Akt signaling pathway and AP-2 transcription factor.* Journal of Biological Chemistry, 2007. **282**(42): p. 30485-30496.
79. Staton, C.A., M.W. Reed, and N.J. Brown, *A critical analysis of current in vitro and in vivo angiogenesis assays.* International Journal of Experimental Pathology, 2009. **90**(3): p. 195-221.
80. Koolwijk, P., et al., *Cooperative effect of TNFalpha, bFGF, and VEGF on the formation of tubular structures of human microvascular endothelial cells in a fibrin matrix. Role of urokinase activity.* The Journal of Cell Biology, 1996. **132**(6): p. 1177-1185.
81. Nehls, V. and D. Drenckhahn, *A novel, microcarrier-based in vitro assay for rapid and reliable quantification of three-dimensional cell migration and angiogenesis.* Microvascular Research, 1995. **50**: p. 311-322.
82. Young, E.W., *Advances in microfluidic cell culture systems for studying angiogenesis.* Journal of laboratory automation, 2013. **18**(6): p. 427-436.
83. Bellacen, K. and E.C. Lewis, *Aortic ring assay.* JoVE (Journal of Visualized Experiments), 2009(33): p. e1564.
84. Plunkett, M.L. and J. Hailey, *An in vivo quantitative angiogenesis model using tumor cells entrapped in alginate.* Laboratory investigation, 1990. **62**(4): p. 510-517.
85. Dellian, M., et al., *Quantitation and physiological characterization of angiogenic vessels in mice: effect of basic fibroblast growth factor, vascular endothelial growth factor/vascular permeability factor and host microenvironment.* American Journal of Pathology, 1996. **149**(1): p. 59-71.
86. Rubinstein, A.L., *Zebrafish: from disease modeling to drug discovery.* Current Opinion in Drug Discovery and Development, 2003. **6**(2): p. 218-223.
87. Wilting, J., et al., *In vivo effects of vascular endothelial growth factor on the chicken chorioallantoic membrane.* Cell and Tissue Research, 1993. **274**(1): p. 163-172.
88. Yonezawa, S., T. Asai, and N. Oku, *Angiogenesis assays: a critical appraisal of current techniques - dorsal air sac model*, ed. J.W. Sons. 2007.
89. Krump-Konvalinkova, V., et al., *Generation of Human Pulmonary Microvascular Endothelial Cell Lines.* Laboratory Investigation, 2001. **81**(12): p. 1717-1727.
90. Amaral, I.F., et al., *Fibronectin-mediated endothelialization of chitosan porous matrices.* Biomaterials, 2009. **30**: p. 5465-5475.
91. Weksler, B.B., et al., *Blood-brain barrier-specific properties of a human adult brain endothelial cell line.* FASEB Journal, 2005. **19**(13): p. 1872-1874.

92. Weksler, B.B., I.A. Romero, and P.O. Couraud, *The hCMEC/D3 cell line as a model of the human blood brain barrier.* Fluids and Barriers of the CNS, 2013. **10**(1): p. 1-10.
93. Ingram, D.A., et al., *Identification of a novel hierarchy of endothelial progenitor cells using human peripheral and umbilical cord blood.* Blood, 2004. **104**(9): p. 2752-2760.
94. Nehls, V. and D. Drenckhahn, *A microcarrier-based cocultivation system for the investigation of factors and cells involved in angiogenesis in three-dimensional fibrin matrices in vitro.* Histochemistry and Cell Biology, 1995. **104**(6): p. 459-466.
95. Mihalyi, E., *Physicochemical studies of bovine fibrinogen. IV. Ultraviolet absorption and its relation to the structure of the molecule.* Biochemistry, 1968. **7**(1): p. 208-223.
96. Bento, A.R., et al., *Three-dimensional culture of single embryonic stem-derived neural/stem progenitor cells in fibrin hydrogels: neuronal network formation and matrix remodelling.* Journal of Tissue Engineering and Regenerative Medicine (In press).
97. Ferreira, A.R., et al., *The endothelial cell neural stem cell cross talk in the context of the development of spinal cord tissue engineering strategies.* Journal of Tissue Engineering and Regenerative Medicine, 2014. **8 (S1)**: p. 367-368.
98. Grasseli, F., et al., *Angiogenic activity of porcine granulosa cells co-cultured with endothelial cells in a microcarrier-based three-dimensional fibrin gel.* Journal of Physiology and Pharmacology, 2003. **54**(3): p. 361-370.
99. Stepp, M.A., et al., *alpha6beta4 integrin heterodimer is a component of hemidesmosomes.* Proceedings of the National Academy of Sciences, 1990. **87**(22): p. 8970-8974.
100. Timpl, R. and H. Rohde, *Laminin - A glycoprotein from basement membranes.* The journal of Biological Chemistry, 1979. **254**(19): p. 9933-9937.
101. Chen, N., C.C. Chen, and L.F. Lau, *Adhesion of human skin fibroblasts to Cyr61 is mediated through integrin alpha 6beta 1 and cell surface heparan sulfate proteoglycans.* The Journal of Biological Chemistry, 2000. **275**(32): p. 24953-24961.
102. Khyati, D., *Characterization of Rheological Properties and Degradation of Genipin Crosslinked Fribin Hydrogel for Annulus Repair.* CUNY Academic Works, 2012: p. 1-64.
103. Elkin, B.S., A.I. Ilankovan, and B. Morrison, *A detailed viscoelastic characterization of the P17 and adult rat brain.* Journal of Neurotrauma, 2011. **28**: p. 2235-2244.
104. Ryan, E.A., et al., *Structural Origins of Fibrin Clot Rheology.* Biophysical journal, 1999. **77**: p. 2813-2826.
105. Piechocka, I.K., et al., *Structural hierarchy governs fibrin gel mechanics.* Biophysical Journal, 2010. **98**(10): p. 2281-2289.
106. Kimura, S. and N. Aoki, *Cross-linking site in fibrinogen for alpha2-plasmin inhibitor.* The Journal of Biological Chemistry, 1986. **261**(33): p. 15891-15895.
107. Lin, Y., et al., *Origins of circulating endothelial cells and endothelial outgrowth from blood.* The Journal of Clinical Investigation, 2000. **105**(1): p. 71-77.
108. Ingram, D.A., N.M. Caplice, and M.C. Yoder, *Unresolved questions, changing definitions, and novel paradigms for defining endothelial progenitor cells.* Blood, 2005. **106**(5): p. 1525-1531.
109. Almeida, M.I., et al., *miR-195 in human primary mesenchymal stromal/stem cells regulates proliferation, osteogenesis and paracrine effect on angiogenesis.* Oncotarget, 2015. **7**(1): p. 7-22.
110. Ribatti, D., *Chapter 5: Chick Embryo Chorioallantoic Membrane as a Useful Tool to Study Angiogenesis.* International Review of Cell and Molecular Biology, 2008. **270**: p. 181-224.

SUPPLEMENTARY DATA

APPENDIX A

Optimization of the *in vitro* microcarrier-based assay to assess the angiogenic properties of functionalized fibrin gels.

To attain a homogeneous colonization of the MCs by EC cells, two stirring process were investigated. The stirring process should allow the homogeneous colonization of a high number of MCs while assuring the retention of MC integrity and preventing MC aggregation. The two different strategies applied are illustrated in **figure 40: (A)** the use of Petri dishes containing 2 mL of MC/cell suspension placed an orbital shaker and **(B)** the use of spinner flasks containing 8 mL of MC/cell suspension placed on a magnetic stirrer. In both stirring processes, the orbital speed was set to 60 r.p.m..

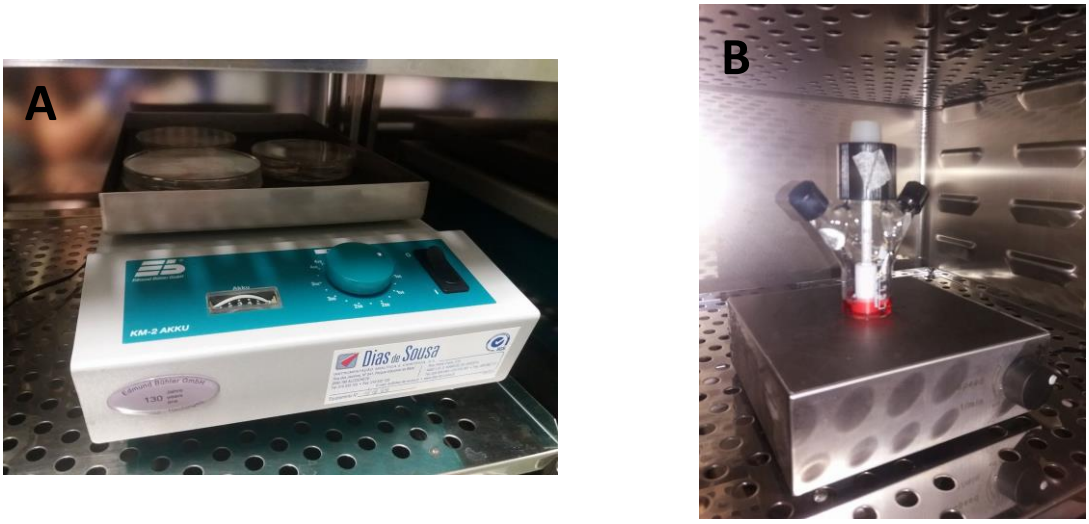

Figure 40 (A-B): Strategies used along the optimization the colonization of the microcarriers by hCMEC/D3 cells. (A) shows Petri dishes containing the cell/MC suspension on an orbital shaker. (B) shows the cell/MC suspension in a spinner flask placed on top of a magnetic stirrer.

Secondly, the effect of the stirring time was investigated: 1.5 days and 2 days. After several experiments, the use of Petri dishes on an orbital shaker and the lower stirring time (1.5 days) turned to be more satisfactory, in terms of preservation of MC integrity, MC aggregation, and efficiency of MC coating.

Finally, the cell seeding density required to obtain a homogeneous and reproducible colonization of the microcarriers was established for each cell type. A cell seeding density of 1.5×10^6 cells/mL was used to the two cell lines (HPMEC-ST1.6R and hCMEC/D3), while a higher cell density was required for OECs (3×10^6 cells/mL; **figure 41 (A-D).**

As the use of this cell density with OECs led to a poor and heterogeneous colonization of the MCs, a higher density was also tested (3×10^6 cells/mL). As shown in **figure 41 (C and**

D), the higher density resulted in a homogenous coating of the MCs and was therefore selected for the assay.

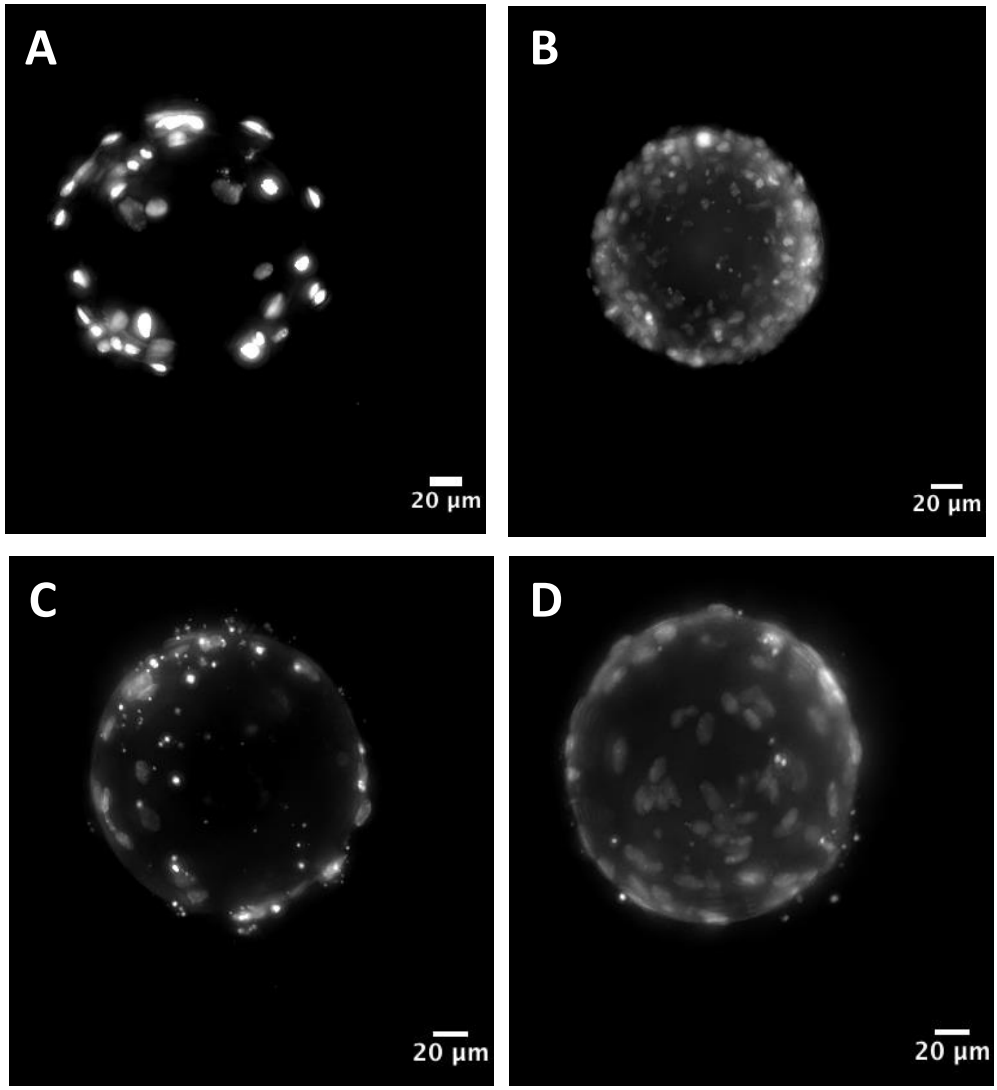

Figure 41 (A-D): Optimization of the cell density required for microcarrier colonization by HPMECs, hCMEC/d3 and OECs. (A) Colonization with 1.5 × 10^6 HPMEC/mL, (B) Colonization with 1.5 × 10^6 hCMEC/D3/mL. (C) Colonization with 1.5 × 10^6 OEC/mL. (D) Colonization with 3 × 10^6 OEC/mL. Cells were cultured for 1.5 days under dynamic cell culture provided by an orbital shaker, and subsequently processed for DNA staining (Hoechst). Representative 2-D projections of IN Cell Analyzer z-stack images of the microcarriers covering a depth of approximately 100 µm are shown. Scale bar: 20 µm
A 1.5 × 10^6 cell seeding density resulted in a poor and heterogeneous colonization of the MCs by OEC, while a higher density (3 × 10^6 cells/mL) successfully promoted a homogeneous and reproducible colonization of the MCs.

APPENDIX B

Percentage of beads with sprouts

– **HPMEC**

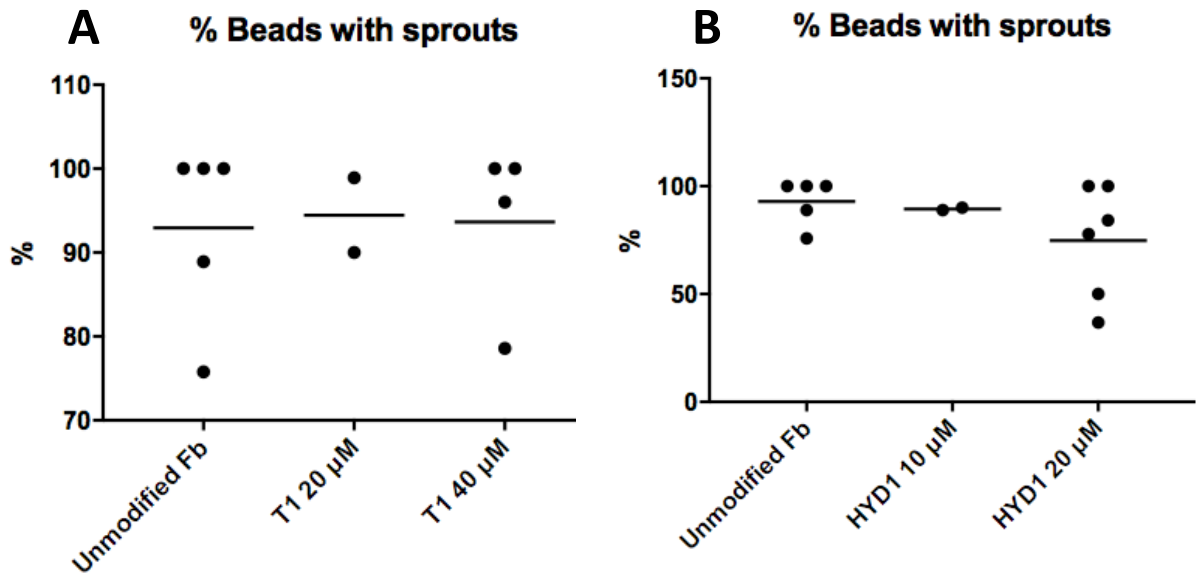

– **hCMEC/D3 without VEGF**

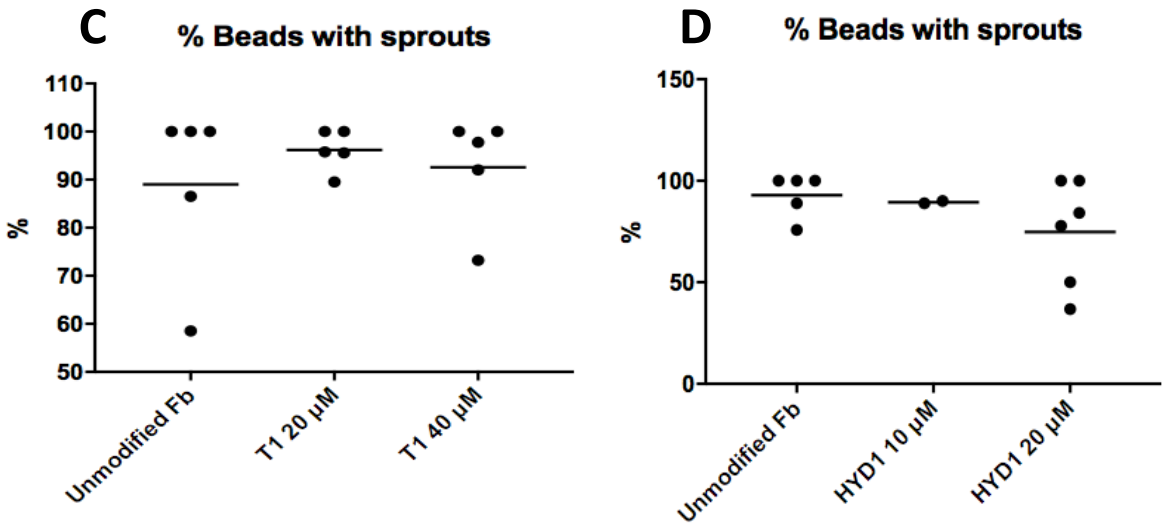

Figure 42 (A-D): EC sprouting into T1-functionalized and HYD1-functionalized fibrin hydrogels in terms of percentage of beads with sprouts. (A and B) HPMEC cells and (C and D) hCMEC/D3 cells.. Graphs denote results from replicate cultures from two to three independent experiments.

APPENDIX C

Effect of the addition of VEGF to the culture medium

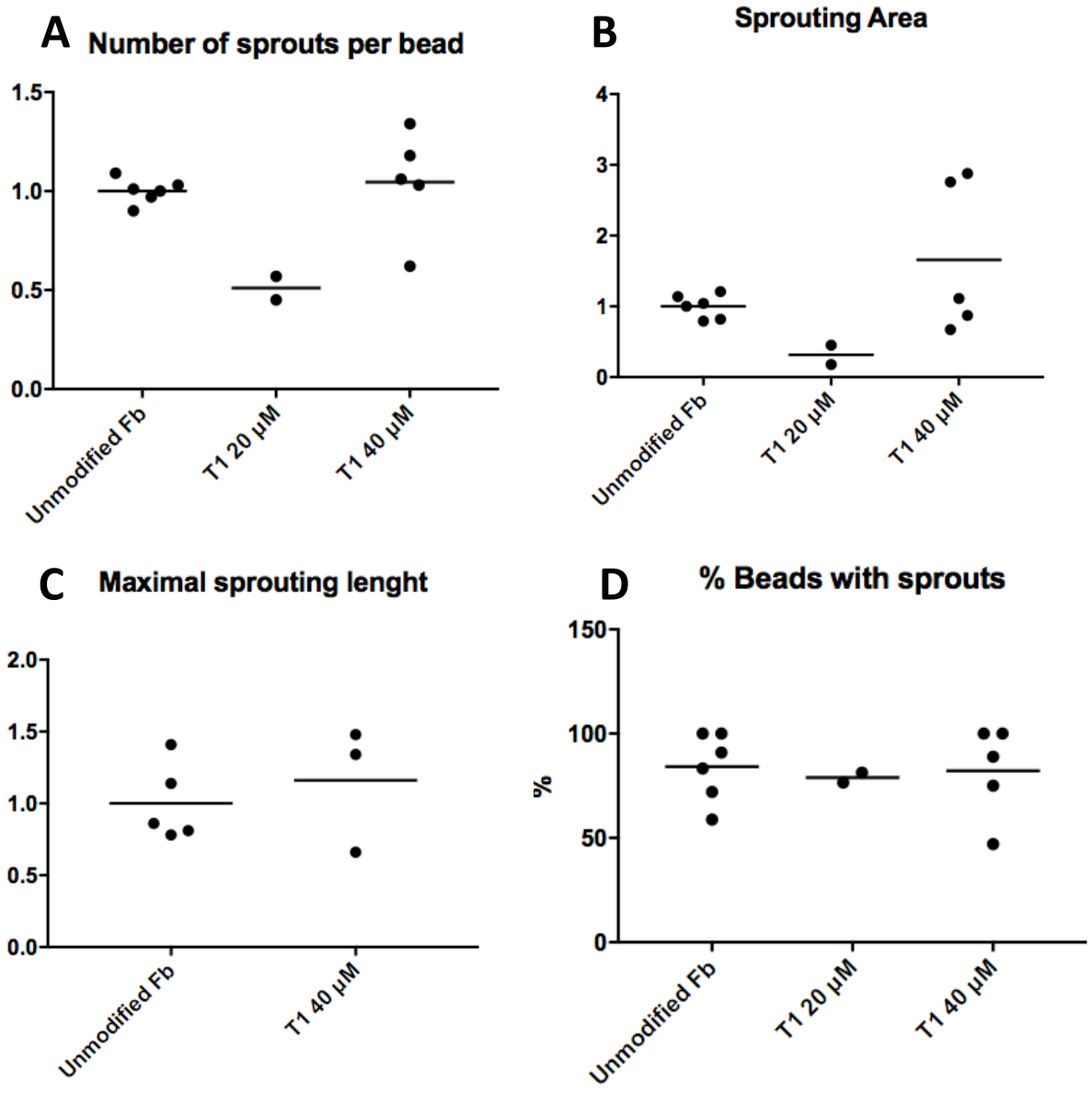

Figure 43 (A-D): EC sprouting of HPMECs into T1-functionalized fibrin hydrogels after 3 days of culture in the presence of 25 ng/mL of VEGF. (A) Number of sprouts per bead, (B) sprouting area and (C) maximal sprouting length,. The microcarriers embedded in each fibrin gel drop were analyzed and mean values were determined. The percentage of beads with EC sprouts was also determined (D). Graphs denote results from replicate cultures from two (20 µM) to three independent experiments.

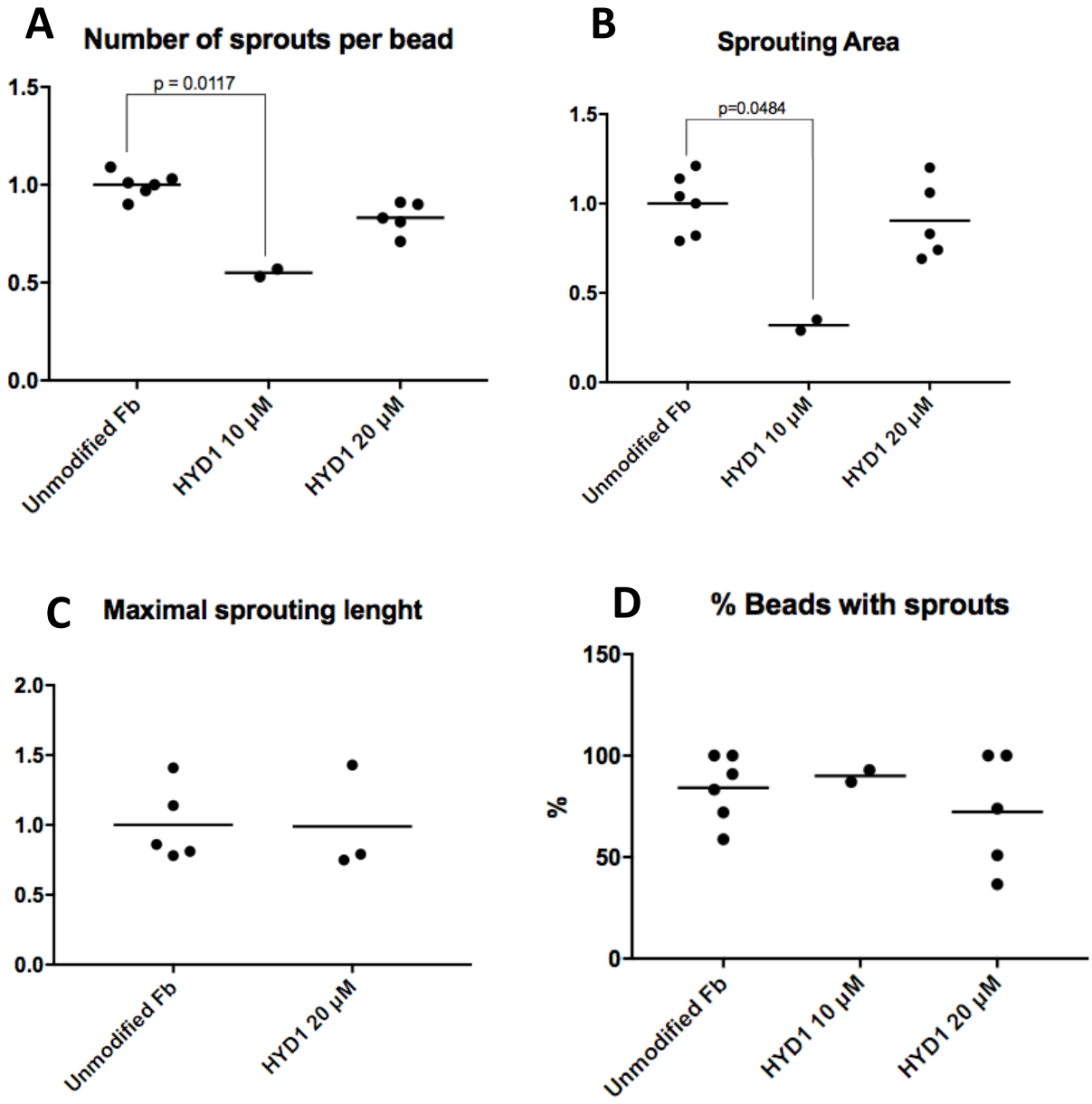

Figure 44 (A-D): EC sprouting of HPMECs into HYD1-functionalized fibrin hydrogels after 3 days of culture in the presence of 25 ng/mL of VEGF. (A) Number of sprouts per bead, (B) sprouting area and (C) maximal sprouting length,. The microcarriers embedded in each fibrin gel drop were analyzed and mean values were determined. The percentage of beads with EC sprouts was also determined (D). Graphs denote results from replicate cultures from two (10 µM) to three independent experiments.

.

APPENDIX D

α6 integrin single immunofluorescence staining

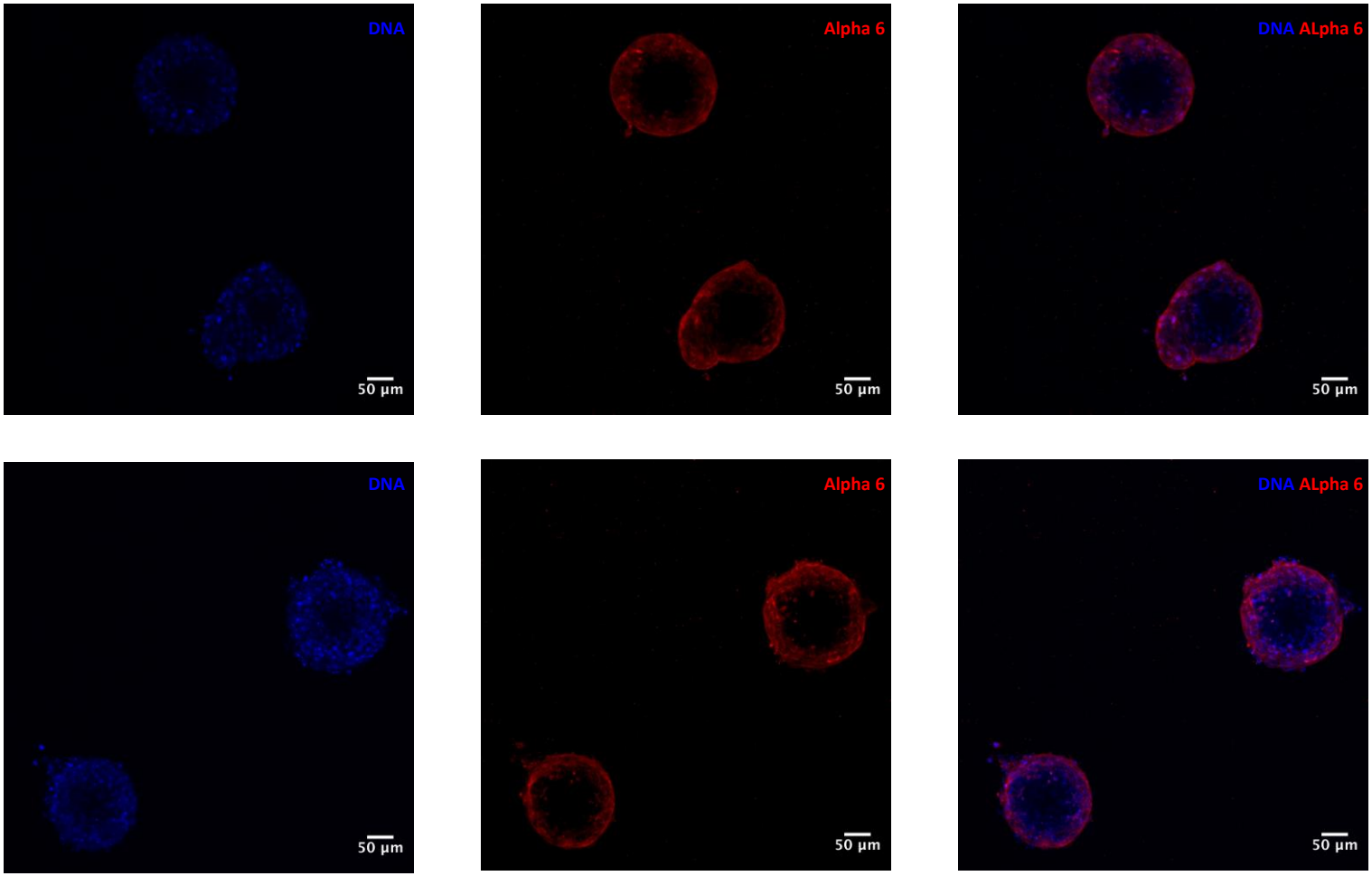

Figure 45: Immunofluorescence staining of α6 integrin in unmodified (upper images) and T1-functionalized (lower images) fibrin hydrogels. Cell/fibrin constructs were cultured for 3 days and subsequently processed for immunofluorescent labeling of α6 integrin (in red). Representative 2-D projections of CLSM z-stack images of cell/fibrin constructs covering a depth of approximately 60 µm are shown. White arrows indicate cellular sprouting. Scale Bar: 50 µm.